DEPARTMENT OF TRANSPORTATION

Optimizing Asphalt Mixtures for Low-volume Roads in Minnesota

Manik Barman, Principal Investigator
Civil Engineering
University of Minnesota Duluth

AUGUST 2023

Research Report
Final Report 2023-34

LRRB
LOCAL ROAD RESEARCH BOARD

To request this document in an alternative format, such as braille or large print, call 651-366-4718 or 1-800-657-3774 (Greater Minnesota) or email your request to ADArequest.dot@state.mn.us. Please request at least one week in advance.

Technical Report Documentation Page

1. Report No. MN 2023-34	2.	3. Recipients Accession No.	
4. Title and Subtitle Optimizing Asphalt Mixtures for Low-volume Roads in Minnesota		5. Report Date August 2023 6.	
7. Author(s) Manik Barman, Heena Dhasmana, Vishruthi Manickavasagan, Mihai Marasteanu		8. Performing Organization Report No.	
9. Performing Organization Name and Address University of Minnesota Duluth Department of Civil Engineering 1405 Univ. Drive, Duluth, MN 55812		10. Project/Task/Work Unit No. CTS #2020008 11. Contract (C) or Grant (G) No. (c) 1003325 (wo) 104	
12. Sponsoring Organization Name and Address Minnesota Department of Transportation Office of Research & Innovation 395 John Ireland Boulevard, MS 330 St. Paul, Minnesota 55155-1899		13. Type of Report and Period Covered Final Report 14. Sponsoring Agency Code	
15. Supplementary Notes http://mdl.mndot.gov/			

16. Abstract (Limit: 250 words)

Minnesota has a large number of low-volume asphalt roads. These roads typically fail because of environmental factors, such as frigid temperatures, freeze-thaw cycles, and seasonal and daily temperature variations. The goal of this study was to suggest modifications to asphalt mixture designs currently used for low-volume roads in Minnesota to improve the resistance of the mixes against the environmentally driven distresses. The study was conducted by accomplishing multiple tasks, such as a literature review, online survey, fieldwork studying the cause of the asphalt pavement distresses, laboratory work comparing asphalt mixtures designed with Superpave-4, Superpave-5, and regressed air voids methods, and studying the field compaction of Superpave-5 mixes. The mechanical performance of the asphalt mixes was studied by conducting Disc-Shaped Compact Tension (DCT), Indirect Tensile Strength (ITS), and Dynamic Modulus (DM) tests. The study included both laboratory- and plant-produced mixes. The study found that asphalt layers for the low-volume roads did not get enough densification, which augments environmentally driven distresses, such as thermal cracks, and longitudinal joint cracks. The Superpave-5 method holds considerable promise for the design of asphalt mixtures for low-volume roads in Minnesota, which may likely increase the asphalt layer densification and mitigate some of the common distresses.

17. Document Analysis/Descriptors Low volume roads, Pavement layers, Density, Asphalt mixtures, Pavement distress, Superpave, Low temperature, Pavement cracking, Fracture mechanics		18. Availability Statement No restrictions. Document available from: National Technical Information Services, Alexandria, Virginia 22312	
19. Security Class (this report) Unclassified	20. Security Class (this page) Unclassified	21. No. of Pages 152	22. Price

Optimizing Asphalt Mixtures for Low-volume Roads (LVRs) in Minnesota

FINAL REPORT

Prepared by:

Manik Barman, Ph.D.
Heena Dhasmana, Ph.D.
Vishruthi Manickavasagan
Department of Civil Engineering
University of Minnesota, Duluth

Mihai Marasteanu, Ph.D.
University of Minnesota, Twin Cities

August 2023

Published by:

Minnesota Department of Transportation
Office of Research & Innovation
395 John Ireland Boulevard, MS 330
St. Paul, Minnesota 55155-1899

Acknowledgments

The authors of this report gratefully acknowledge the financial support of the Minnesota Department of Transportation and Local Road Research Board (LRRB) for carrying out this research. The research team is grateful to the Technical Advisory Panel (TAP) members (listed below), including Technical Liaison, Mr. Joel Ulring, for providing valuable suggestions and guidance. The contribution of Mr. Ron Bumann, a former State-aid technician, who helped with field core data, is highly appreciated. The contributions of the Beltrami, Koochiching, Pope, and St. Louis counties towards conducting the fieldwork (core collection and distress survey) are sincerely acknowledged. We also thank Northland Constructors for providing us with the materials (aggregates and binders) for this research. Special thanks go to the Project Coordinators Brent Rusco and colleagues from the Center for Transportation Studies for their time and administrative support. The research team sincerely acknowledges the contribution of several graduate (especially Giselle Irankunda and Daniel Begin) and undergraduate students, faculty members, and staff of the University of Minnesota Duluth and Twin Cities campus, who helped the research team at different phases of this project.

TAP Members

1. Joel Ulring, Pavement Preservation Engineer, MnDOT (Technical Liaison)
2. Mike Flaagan, County Engineer at Pennington County Highway Department
3. John Garrity, Bituminous Engineer, MnDOT
4. Greg Johnson, Assistant Bituminous Engineer, MnDOT
5. Tim Donaghue, District State Aid Engineer, District 2 - Bemidji
6. Paul W. Nolan, Materials and Road Research Engineering Specialist, MnDOT
7. Jerry Geib, Research Operations Engineer, MnDOT
8. Julie Swiler, Information Officer, MnDOT
9. Jim Foldesi, Public Works Director/Highway Engineer, St. Louis County
10. Dan Staebell, Northcentral Regional Director, Asphalt Pavement Alliance

Table of Contents

List of Figures

List of Tables

Executive Summary

Low-volume roads occupy 70 percent of the total road miles in the United States and have a significant influence on the economy of the country. These roads typically carry less than 400 vehicles per day. The lion's share of these roads has been built with an asphalt surface. As they carry less traffic, their service life is dictated more by environmental factors, such as seasonal and daily temperature variations, rainfall, snowfall, frigid temperature, freeze-thaw cycle, etc., than wheel-load repetitions. The asphalt mixture for the low-volume roads thus shall be designed based on environmentally driven distresses, not wheel-load-related distresses. While there have been improvements and changes to the structural design procedures for low-volume roads, the asphalt mixtures for these roads are still designed using the same procedure that was developed for the high-volume roads, which typically fail by load-related distresses, such as fatigue cracking and rutting.

The goal of this project was to explore opportunities to minimize environmentally driven distresses by improving the asphalt mixture design and suggesting modifications to the current asphalt mixture design practices in Minnesota for low-volume roads. The study was conducted by accomplishing multiple tasks, such as a literature review, online survey, fieldwork studying the common distresses and asphalt layer densification, laboratory work comparing asphalt mixtures designed with different methods, and field compaction study. The research compared the performance of asphalt mixes designed using three different methods: conventional Superpave-4, Superpave-5, and regressed air voids. The mechanical performance of plant-produced mixes designed using the Superpave-5 method was also investigated.

The literature review and online survey formed the foundational part of the study, providing valuable context and understanding of low-volume road distresses and the current practice of asphalt mixture designs followed in Minnesota. It was found that the distresses of low-volume roads were predominantly caused by environmental factors rather than load-related causes, where transverse cracking was the most common distress in a wet-freeze climate like Minnesota. The study found that the majority of asphalt layer densification occurred during the initial three years of service life. Beyond this period, the field air void percentage typically did not decrease and rarely fell below the design air voids (e.g., 4%). The use of regressed air void design and Superpave-5 mixture design methods were identified as promising for improving the densification and mechanical performance of the asphalt mixtures. The literature review highlighted the benefits of the polymer-modified binder in mitigating transverse cracking.

The study included an analysis of the asphalt field cores collected from a total of 34 road sections located in 10 different counties of Minnesota. The volumetric analysis of the cores revealed that the initial air voids percentage in the asphalt layer, immediately after construction, typically ranged between 5.3% and 7.2%. While traffic volume was found to play a role in the densification of the asphalt layer, the air voids percentage did not decrease to the design air voids (e.g., 3% and 4%), which was in agreement with the relevant literature reviewed in this study. The field study identified three major

distresses of Minnesota's low-volume roads, namely, longitudinal cracking, longitudinal joint cracking, and transverse cracking, all of which are caused by environmental factors.

In the laboratory study, seven different asphalt mixes were designed: three mix designs each for conventional Superpave-4 and Superpave-5 methods, and one mix design for the regressed air voids method. In addition, the laboratory study included plant-produced Superpave-5 mixes from three field projects located in Minnesota. This comprehensive study approach facilitated a good comparison of the mechanical properties of the various asphalt mixes, providing valuable insights into the relative efficacy of different mix design methods, especially for low-volume roads. Disc-shaped Compact Tension (DCT), Indirect Tensile Strength (ITS), and Dynamic Modulus tests were performed to study the fracture toughness and resilience of the mix samples across a spectrum of temperatures. The performance of asphalt mixes was influenced by the aggregate gradation differences between Superpave-4 and Superpave-5. It was found that a 5% air void mix with 30 numbers of gyration exhibited superior performance under low-temperature conditions than its counterpart, conventional Superpave-4 asphalt mix. The fracture performance of the Superpave-5 further improved when an additional 0.5% binder was added. The flexibility index results showed that Superpave-5 mixes were more stable and balanced compared to their Superpave-4 counterparts; they also had better indirect tensile strength. The dynamic modulus results of the mixes indicated that the overall performance of Superpave-5 mixes matched or even surpassed Superpave-4 mixes, suggesting their rutting behavior would not be inferior. The performance of the regressed air void mix was not superior to the Superpave-5 mixes.

The study also compared three field-produced Superpave-5 mixes with seven lab-produced Superpave-4, Superpave-5, and regressed air voids mixes. Field mix with polymer-modified binder and less RAP(Recycled Aggregate Pavement) percentage (17% and 20%) performed better than the two other field mixes that were prepared with unmodified binder and higher RAP percentage (30%). Overall, a slight superiority in the performance of lab-produced Superpave-5 asphalt mixes was observed when all the mixes were compared.

The study concludes that the Superpave-5 method holds considerable promise for the design of asphalt mixtures for low-volume roads in Minnesota, demonstrating enhanced fracture resistance, indirect tensile strength, and overall performance compared to the current Superpave-4 method in use in Minnesota. However, the study recommends field verification before the implementation of the Superpave-5 method for low-volume roads. Moreover, the study recommends an increase of 0.5% in binder content, which could enhance the fracture energy of mixes, potentially improving road performance and longevity. Lastly, the research supports the use of the polymer-modified binder (e.g., PG58H-34) in the surface layer to help reduce transverse cracking, the most common distress on low-volume roads in Minnesota.

Chapter 1: Introduction

Low-volume roads occupy 70 percent of the total road miles in the United States (Apronti, 2016; FHWA, 2009). According to MN MUTCD (2018) and Skok et al. (2003), roads with less than 400 average daily traffic (ADT) are referred to as low-volume roads. The 20-year design equivalent single-axle load (ESAL) of such roads is usually below one million and falls under the "traffic level 2" category per MnDOT's *Standard Specification for Construction* (MnDOT, 2018). According to Centerline and Lane Mileage Reports of MnDOT (MnDOT, 2019a), the vast majority of the County, Township and City paved roadways are below 1,000 AADT and most are asphalt roads. These roads experience low traffic volume and thus their mode of failure differs from high-volume roads. They fail mainly due to environmental factors, such as seasonal and daily temperature variations, oxidation of asphalt, freeze-thaw cycles, etc., rather than the wheel-load repetitions, which is the reason for the failure of high-volume roads. Therefore, the asphalt mixtures for low-volume roads shall be designed based on the environmentally driven distresses, not the wheel-load-driven distresses. While there have been improvements and changes to the structural design procedures for low-volume roads, the asphalt mixtures for low-volume roads are still designed using the same procedure that was developed for high-volume roads, which fail by load-related distresses, such as fatigue cracking and rutting.

1.1 Need for Current Study

A separate mix design procedure that focuses on material selections and mix designs is not available for low-volume asphalt roads in Minnesota, as they have not been researched as extensively as for high-volume roads. Additionally, researchers have focused more on the structural and geometric designs of low-volume roads than their mixture designs. According to a study conducted in Iowa (Engle, 2004), low-volume roads differ from their high-volume counterparts in three principal areas: (i) mix design performance requirements, (ii) project budget scenario, and (iii) aggregate requirements and availability. The mixture design requirements for low-volume roads are usually less limiting and performance-related (Engle,2004). The budgets for projects on low-volume roads are relatively low.

Assuming that the performance requirement of the low-volume roads is less limiting compared to the high-volume roads, many important factors that create premature distresses are overlooked. One issue is the less densification of the asphalt layers over time. The initial compacted air voids percentage for asphalt layer is usually above 6%. In high-volume roads, the air voids decrease with time because of the high traffic load repetitions. In low-volume roads, the air voids do not decrease much because of fewer wheel-load repetitions. The higher air voids can create a weak asphalt layer that can experience thermal cracking, moisture damage and freeze-thaw-related durability issues, especially in the wet-freeze climate areas like Minnesota.

In summary, it is important to recognize that the asphalt mixture failure mechanisms of low-volume roads are different than the high-volume roads, and asphalt mixtures for low-volume roads shall be

designed based on the environmentally driven distresses. Mixtures shall be designed in such a way that the percentage of air voids in the mixtures is less during the service period.

1.2 Research Scope and Objectives

The study first focused on understanding the current practices of asphalt mixture designs for low-volume roads. Field studies were performed to determine the volumetrics of the asphalt layers and to identify the common distresses that occur in low-volume asphalt roads of Minnesota. Then a laboratory study was conducted to determine the needed improvement in the asphalt mixture design. Several asphalt mixtures designed with the conventional Superpave, Superpave-5 (high-density asphalt mix), and regressed air voids methods were compared. The study also included testing of plant-produced asphalt mixtures and field cores designed with the Superpave-5 method. The key objectives of this study were:

1. To study the current practices of low-volume road asphalt mixture designs for cold climate areas like Minnesota through a comprehensive literature review and online survey.
2. To understand the common distresses of the low-volume asphalt roads through a literature survey and a distress survey.
3. To understand the asphalt layer mixture volumetrics and densification by collecting and analyzing field cores.
4. To conduct an experimental study to determine the needed improvement of the asphalt mixtures. This task included a comparative study of the asphalt mixes designed with the conventional Superpave method, Superpave-5 method (high-density asphalt mix), and regressed air voids method.
5. To study the field compaction of the Superpave-5 mixes.
6. To provide recommendations on improvement of the asphalt mixes for the low-volume roads of Minnesota.

Chapter 2: Literature Review

2.1 Introduction

The study began with a comprehensive literature review. Distresses of low-volume asphalt pavements, current asphalt mixture design practices, and findings from several relevant research works conducted for low-volume roads and asphalt mixtures were included in the literature review. Research reports published by state DOTs and various journal and conference articles were reviewed.

2.2 Common Distresses in Minnesota's Low-volume Roads

Various distresses observed in asphalt pavements are transverse cracking, longitudinal cracking, multiple block cracking, rutting, raveling, potholes, etc. As the pavement ages and experiences traffic load repetitions, pavement distresses begin to accumulate. While some distresses are either traffic load-related or environmental factors-related, sometimes two or more distresses can compound and turn into a more severe distress. For example, water infiltration through cracks can lead to the development of stripping and pothole. This chapter briefly discusses different distresses observed in Minnesota's asphalt pavements, with an emphasis on the low-volume road.

2.2.1 Transverse Cracking

Transverse cracks are predominantly perpendicular to the centerline of the pavement. These cracks are caused by shrinkage of the asphalt layer or because of the reflection of cracks that exist in the underlying layer. These cracks do not initiate from the traffic load but deteriorate with the traffic load repetitions. This distress is the most prevailing distress of Minnesota's asphalt roads and very common in low-volume roads. Photographs of the transverse cracks and other distresses discussed in this chapter are provided in the Appendix.

2.2.2 Longitudinal Cracking

Longitudinal cracking can be load-related and non-load-related and is predominantly parallel to the centerline of the pavement. Load-related longitudinal cracks are usually top-down fatigue cracks. The non-load-related longitudinal cracks can be caused by poorly constructed lane joints, shrinkage of the asphalt layer, cracks reflecting up from an underlying layer, and longitudinal segregation due to improper paver operation. While the fatigue-related longitudinal cracking is less in Minnesota's low-volume roads, the non-load-related cracking, especially the centerline joint longitudinal cracks, are quite common and often leads to potholes at the intersection of the longitudinal crack and transverse crack.

2.2.3 Multiple (Block) cracking

Multiple (block) cracking is a pattern of cracks dividing pavement into large rectangular or polygonal blocks. The size of the blocks usually ranges from 6 inches to approximately 3 feet across. Block cracking is typically caused by shrinkage of the asphalt pavement due to daily temperature cycles.

2.2.4 Fatigue/Alligator Cracking

Alligator or bottom-up fatigue cracking is a series of interconnected cracks caused by fatigue failure of the asphalt surface under repeated traffic loading. These cracks initiate at the bottom of the lower-most bound layer along the wheel path. If the asphalt surface is placed on the stabilized base, the crack can initiate at the bottom of the base layer, otherwise at the bottom of the asphalt surface layer. As the number and magnitude of loads becomes excessive, these cracks begin to form along the wheel path. After repeated loading, these cracks connect forming many-sided sharp-angled panels that develop into a pattern resembling the back of an alligator. The leading causes of this distress are usually inadequate structural support for the design traffic, poor asphalt mixture, and excess load repetition, etc. This type of distress is commonly found in high-volume roads. Minnesota's low-volume roads do not primarily fail by this distress, except for some very old low-volume road pavements, which did not undergo any major rehabilitation work for a long time.

2.2.5 Rutting

Rutting is a longitudinal surface depression along the wheel path and is caused by deformation or consolidation of the pavement layers or subgrade. It can be caused by insufficient pavement thickness, lack of compaction, and unstable asphalt mixtures. This distress is more prevalent on high-volume roads and not usually found on low-volume roads unless the roads are used by heavily loaded trucks.

2.2.6 Raveling

Raveling is the dislodging of aggregate particles from the asphalt surface because of the loss of binder or weathering of the asphalt mixtures. Dust coating on the aggregates during mixture preparation, aggregate segregation and inadequate compaction can result in raveling. This distress occurs in low-volume asphalt roads.

2.2.7 Potholes

Potholes are mostly the end result of any pavement distress. Potholes vary in size and severities based on the distress mechanism, pavement material quality, and construction procedures. Potholes are very common distress found on low-volume roads. In Minnesota, which is in the cold and wet-freeze climate zone (Figure 2-1), potholes aggravate during the spring season when the ice accumulated inside cracks thaws. Recently, it was found that the increased number of freeze-thaw cycles is a major cause for the potholes in Minnesota. Segregation of asphalt mixtures, poor patching, poor compaction during construction can also lead to localized potholes (Walker, 2019).

Climate Zone	Annual Rainfall	Freezing Index (°F-Days)
Wet Non-Freeze	> 28"	< 100
Wet Freeze	> 28"	> 100
Dry Non-Freeze	< 28"	< 100
Dry Freeze	< 28"	> 100

Figure 2-1 Different Climates Zones of the USA (You et al., 2018)

2.3 Low-volume Road Asphalt Mixture

This section discusses the materials used in Minnesota's low-volume road asphalt mixtures. Different consensus properties of the aggregates and binders and mixture requirements are briefly discussed.

2.3.1 MnDOT Specification for Materials

2.3.1.1 Aggregates

MnDOT Specification 3139, Graded Aggregate for Bituminous Mixtures, classifies aggregates as class A through E aggregates, steel slag, taconite tailings, recycled asphalt shingles (RAS), crushed concrete, salvage aggregate and reclaimed asphalt pavement (RAP), etc. The different consensus properties considered for aggregate selection, as specified by MnDOT (2018), are gradation, angularity, specific gravity, durability, soundness, stripping potential, sand equivalent value, etc. Table 2.1 presents different aggregate consensus properties as a function of 20-year design ESALs. Low-volume roads usually have lower than 1 million 20-year design ESALs. Four different aggregate gradations are used, as shown in Table 2.2. The aggregate gradation "A", with the maximum aggregate size of ½ inch, is preferred for the final lift in low-volume roads.

Table 2.1 Consensus Properties of Aggregates for Asphalt Mixture (MnDOT, 2018)

Aggregate Blend Property	Traffic Level 2	Traffic Level 3	Traffic Level 4	Traffic Level 5
20-year Design ESAL's	<1 million	1 - 3 million	3 - 10 million	10 - 30 million
Min. Coarse Aggregate Angularity (ASTM D5821) (one face / two face), %- Wear (one face / two face), %- non-Wear	 30/- 30/-	 55/- 55/-	 85/80 60/-	 95/90 80/75
Min. Fine Aggregate Angularity (FAA) (AASHTO T304, Method A) % Wear % non-wear	 40 40	 42 40	 44 40	 45 40
Flat and Elongated Particles, max % by weight, (ASTM D 4791)	-	10 (5:1 ratio)	10 (5:1 ratio)	10 (5:1 ratio)
Min. Sand Equivalent (AASHTO T 176)	-	-	45	45
Max. Total Spall in fraction retained on the #4 sieve Wear non-Wear	 5.0 5.0	 2.5 5.0	 1.0 2.5	 1.0 2.5
Maximum Spall Content in Total Sample Wear non-Wear	 5.0 5.0	 5.0 5.0	 1.0 2.5	 1.0 2.5
Maximum Percent Lumps in fraction retained on the #4 sieve	0.5	0.5	0.5	0.5
Class B Carbonate Restrictions				
Maximum% -#4 Final Lift/All other Lifts	 100/100	 100/100	 80/80	 50/80
Maximum% +#4 Final Lift/All other Lifts	 100/100	 100/100	 50/100	 0/100
Max. allowable scrap shingles-MWSS Wear/Non-Wear	 5/5	 5/5	 5/5	 5/5
Max. allowable scrap shingles -TOSS Final Lift/All other Lifts	 5/5	 5/5	 0/5	 0/0

Table 2.2 Aggregate Gradation Broad Bands (percentage passing of total washed gradation) (MnDOT, 2018)

Sieve size	A	B	C	D
1 in	-	-	100	-
3/4 in	-	100*	85 100	-
1/2 in	100*	85 100	45 90	-
1/2 in	85-100	35-90	-	100
No. 4	60-90	30-80	30-75	65-95
No. 8	45-70	25-65	25-60	45-80
No. 200	2.0-7.0	2.0-7.0	2.0-7.0	3.0-8.0
*The contractor may reduce the gradation broadband for the maximum aggregate size to 97 percent passing for mixtures containing RAP, if the oversize material originates from the RAP source. Ensure the virgin material meets the requirement of 100 percent passing the maximum aggregate sieve size.				

2.3.1.2 Asphalt Binder

The state of Minnesota uses different performance grades of asphalt binder, as shown in Table 2.3. PG 58S – 28 (grade B) and PG 58H – 34 (grade C) are preferred for the low-volume roads. Binder selection is based on whether the binder is used in an overlay or new pavement. For overlays, the binder grade B (58S -28) is recommended and for new pavements, polymerized binder grade C (58H -34) is recommended in the top three inches of the pavement. The asphalt binder content is primarily decided based on the percentage of air voids (e.g., 3%, 4%) and adjusted asphalt film thickness (AFT) (e.g., min. 8.5 microns).

Table 2.3 Binder Grades used in Minnesota (MnDOT, 2018)

Letter	MSCR PG Grade	Equivalent PG Grade
A	PG 52S-34	
B	PG 58S-28	PG 58-28
C	PG 58H-34	PG 58-34, PG 58-34(PMB)
E	PG 58H-28	PG 64-28, PG 64-28(PMB)
F	PG 58V-34	PG 64-34, PG 64-34(PMB)
H	PG 58V-28	PG 70-28, PG 70-28(PMB)
I	PG 58E-34	PG 70-34
L	PG 64S-22	
M	PG 49S-34	

2.3.1.3 Reclaimed Asphalt Pavement (RAP)

The use of RAP helps in reducing pavement construction costs, and it provides a sustainable solution to the usage of waste materials. The state of Minnesota allows usage of RAP in asphalt mixes; however, different cities and counties have different restrictions on the maximum allowable percentage. MnDOT limits the percentage of RAP based on the percentage of new to existing asphalt binder in the mix. Some Minnesota counties additionally restrict or prohibit the use of RAP for pavement surface layers or wearing courses. Figure 2-1 shows wet-freeze climate states that allow 20 or more percentage of RAP in their asphalt layers.

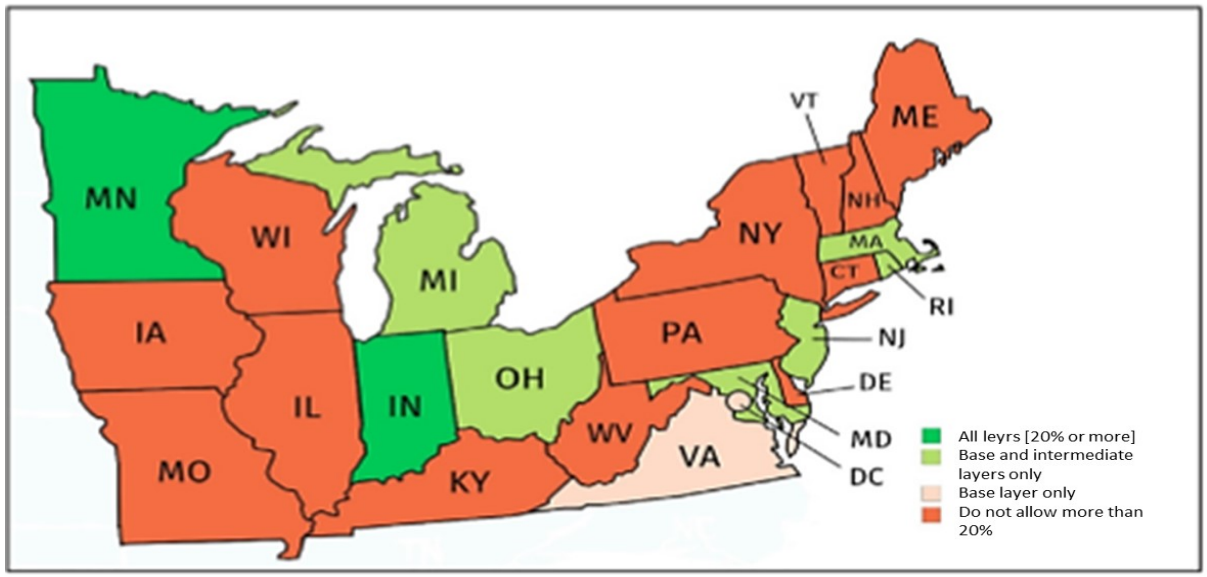

Figure 2-2 Wet-freeze States that use 20 or more Percent of RAP in Asphalt Layer (Chen et al., 2019)

2.3.2 MnDOT Asphalt Mixture Design

Minnesota uses the Superpave method for asphalt mixture design (AASHTO R 35, 2017), which is referred to in the MnDOT's, Plant Mixed Asphalt Pavement Specification (MnDOT 2360). MnDOT 2360. MnDOT designates asphalt mixture designs with suitable mixture designation codes, for example: SPWEB440E. The code identifies factors like mixture design type (e.g., Superpave) course designation (wearing, non-wearing), maximum aggregate size (12.5 mm, 19 mm, 25 mm, etc.) traffic level (<1 million ESAL, 1 to 3 million ESAL, etc.), design air voids (5%, 4%), and asphalt binder grade (PG 58S-28, PG 58H-34, etc.). The following list shows design variables and their notations.

1) The first two letters indicate the mixture design type:
   SP = Gyratory Mixture Design
2) The third and fourth letters indicate the course:
   WE = Wearing and shoulder wearing course
   NW = Non-wearing Course
3) The fifth letter indicates the maximum aggregate size:
   A = ½ in [12.5mm], SP 9.5
   B = ¾ in [19.0mm], SP 12.5
   C = 1 in [25.0mm], SP 19.0
   D = ⅜ in [9.5mm], SP 4.75
4) The first digit in the mix designation code indicates the Traffic Level (ESAL's × 10^6) in accordance with Table 2360-1, "Traffic Levels" (Table 2.4).

Table 2.4 Traffic level and respective 20-Year Design ESAL

Table 2360-1 Traffic Levels	
Traffic Level	**20 Year Design ESALs**
2 *	< 1
3 ‖	1 – < 3
4	1 – < 10
5	10 – ≤ 30
NOTE: The requirements for gyratory mixtures in this specification are based on the 20 year design traffic level of the project, expressed in Equivalent Single Axle Loads (ESAL's) 1 × 10^6 ESALs * AADT < 2,300 ‖ AADT > 2,300 to < 6,000	

5) The last two digits indicate the air void requirement:
   50 = 5.0 percent for wear mixtures,
   40 = 4.0 percent for wear mixtures, and
   30 = 3.0 percent for non-wear and shoulder.
6) The letter at the end of the mixture designation identifies the asphalt binder grade in accordance with Table 2360-2, "Asphalt Grades" (Table 2.3).

For example- a Gyratory Design Mix for a wearing course with a maximum aggregate size of ¾ inches, 10-30 million ESALs traffic, 4% air content, and PG 58 – 28 asphalt binder will be labeled 'SPWEB540B'.

The mix design report should include a job-mix formula (JMF) listing the information on aggregate sources, types, proportions, composite gradation, and asphalt binder content as a percentage of the total mixture (MnDOT, 2019b). Design air voids, aggregate bulk specific gravity values and adjusted asphalt film thickness (AFT), etc., are indicated in the asphalt mixture design report. The AFT ensures an adequate binder coating of the aggregates. Table 2.5 provides various target parameters for the asphalt mixtures based on the 20-year design ESALs (MnDOT, 2018).

Table 2.5 Various Target Parameters for the Asphalt Mixture Design According to MnDOT (2018)

Traffic Level	2	3	4	5
20-year design ESALs	< 1 million	1 - 3 million	3 - 10 million	10 - 30 million
Gyratory mixture requirement:				
Gyrations for N Design	40	60	90	100
% Air voids al N design, wear	4.0	4.0	4.0	4.0
% Air voids at N design non-wear and all shoulder	3.0	3.0	3.0	3.0
Adjusted Asphalt film thickness, minimum m	8.5	8.5	8.5	8.5
Ratio of Added New Asphalt Binder to Total Asphalt Binder, (1). min%	70.0	70.0	70.0	70.0
TSR*, minimum %	75||	75||	80[]	80[]
Fines/Effective asphalt	0.6 - 1.2	0.6 - 1.2	0.6 - 1.2	0.6 - 1.2

* Use 6 in [150 mm) specimens in accordance with 2360.2.I,"Field Tensile Strength Ratio (TSR)"
|| Mn/DOT minimum = 65
[] Mn/DOT minimum = 70
(1)The ratio of added new asphalt binder to total asphalt binder needs to be 70% or greater ((added binder/total binder) x 100≥70) in both mixtures that contain RAP and in mixtures that include shingles as part of the allowable RAP percentage.

2.3.3 Superpave-5 Mixture Design

One of the limitations of the current Superpave asphalt mixture design method is its inability to compact the asphalt mixture in the field with the design air void percentage. The mixture is usually designed with 3 or 4% air voids; however, the newly compacted asphalt typically exhibits 6 to 8% air voids. The air voids percentage decreases with traffic, but it does not go down significantly, especially on low-volume roads. The higher air voids in the asphalt mixtures lead to durability issues in the pavement. To this end, Hekmatfar et al. (2015) and Huber et al. (2016) conducted studies to investigate the feasibility of

achieving lower field air voids during compaction. They proposed a procedure in which the mixture is designed with 5% air voids in the lab and compacted in the field at similar air voids percentage. This mixture design procedure is referred to as the Superpave-5. Their study included asphalt mixtures for three different traffic levels (3 to 30 million ESALs). The major findings of that study are provided below:

I. The study suggested that it is possible to design the asphalt mixture with 5% air voids without lowering the effective binder content and by varying the aggregate gradation.
II. The number of gyrations in the Superpave-5 procedure is lower than the original Superpave mixture design method.
III. The study suggested 30 numbers of gyrations for asphalt mixtures for low-volume roads.
IV. The mechanical properties of the mixtures (dynamic modulus, SCB test results, etc.) designed with Superpave-5 method were comparable or even slightly better than the mixture design with Superpave method.

Under the scope of that study, asphalt mixture designed with original Superpave and Superpave-5 mixture designs were placed in two field sections to verify whether a 5% field air voids could be achieved. Table 2.6 presents the field air voids in one of the two field sections. The asphalt mat which was compacted using the Superpave-5 (N30) mixture achieved around 5% air voids compared to 6% for the mixtures that were designed using the original Superpave mixture design.

Table 2.6 Comparison of Field Air Voids between the Mixtures Designed using the Original Superpave (N100) and Superpave-5 (N30) (Hekmatfar et al. (2015)).

N I00				N30			
Cores No.	G_{mb}	G_{mm}	AV%	Cores No.	G_{mb}	G_{mm}	AV%
N I00-1	2.37S	2.509	5.2	N30-41	2.3Y3	2.502	4.4
N I00-2	2.352		6.3	N30-42	2.40 1		4.0
N I00-3	2.347		6.5	N30-43	2.40 1		4.0
N I00-4	2.161		5.8	N30-44	2..196		4.2
N I00-5	2.369		5.6	N30-45	2.371		5.2
N I00-6	2.359		6.0	N30-46	2.382		4.8
N I00-7	2.152		6.3	N30-47	2.368		5.4
N I00-8	2.360		5.9	N30-48	2.365		5.5
N I00-9	2.362		5.8	N30-49	2.380		4.9
N I00-10	2.317		7.7	N30-50	2.369		5.3
N I00-11	2.316		7.7	N30-51	2.369		5.3
N I00-12	2.141		6.6	N30-52	2..17R		4.9
N I00-13	2.36S		5.6	N30-53	2.388		4.5
N I00-14	2.40S		7.0	N30-54	2.382		4.5
N I00-15	2.379		5.2	N30-55	2.376		5.0
N I00-16	2.417		3.1	N30-56	2.382		4.5
N I00-17	2.345		6.5	N30-57	2.383		4.8
N I00-18	2.329		7.2	N30-58	2.377		5.0
N I00-19	2.325		7.3	N30-59	2.368		5.1
N I00-20	2.358		6.0	N30-60	2.387		4.6
Average AV%			6.0	Average AV%			4.8
SD AV%			1.05	SD AV%			0.44

2.3.4 Relevant Research Studies on Asphalt Mixes

2.3.4.1 Effect of mix design and fracture energy on transverse cracking

Dave et al. (2016) studied the effect of mix design and fracture energy on transverse cracking performance of asphalt pavements. The field performance of asphalt pavement was studied with various cracking measures and compared with mix design parameters such as asphalt binder content, binder grade, and amount of recycling. A total of 26 pavements sections were considered in that study, out of which 10 consisted of non-wearing course materials and the rest were wearing course mixes. DCT test was conducted on the filed cores to study the fracture energy.

The transverse cracking performance was studied in terms of total transverse cracking (TC Total), which is the area under the 'percentage of cracking' versus 'years in service' curve, normalized by total years in

service. Even though a reasonable correlation was not achieved, it was found that the increased asphalt binder content can reduce the transverse cracks, as shown in Figure 2-3. The study also considered several sections with recycled asphalt pavement (RAP) mixes; however, no trend could be established on the influence of the RAP on the cracking performance. The influence of VMA and AFT is shown in Figure 2-4 and Figure 2-5. Unfortunately, a clear trend could not be achieved for these two mixture parameters as well.

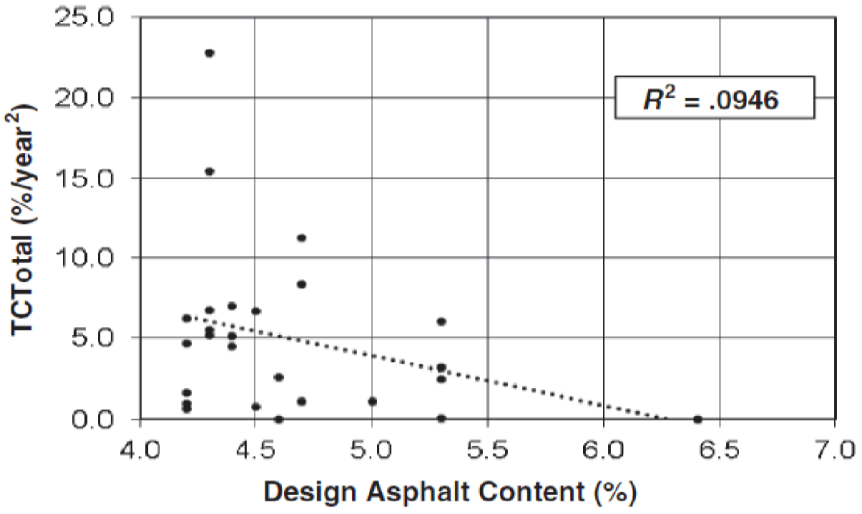

Figure 2-3 Effect of Binder Content on the Transverse Cracking Performance (Dave et al., 2016); Note- TC Total = Total transverse crack percentage per year

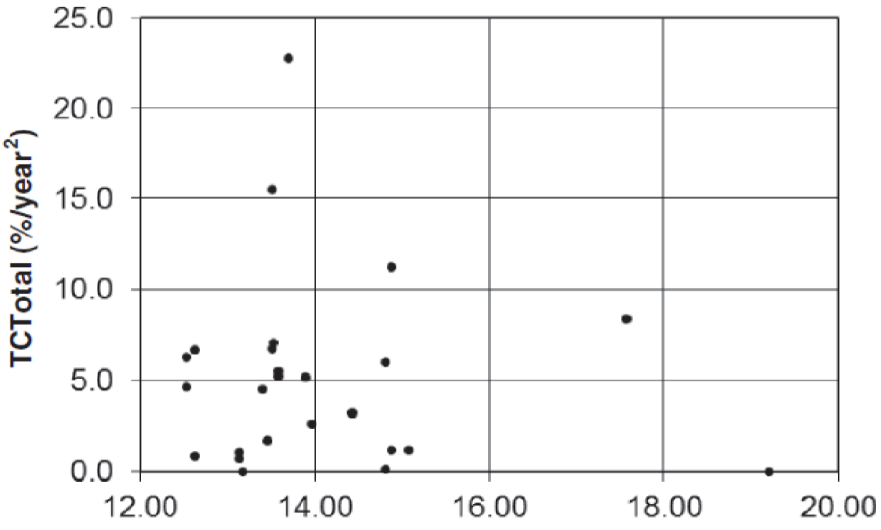

Figure 2-4 Effect of VMA on the Transverse Cracking Performance (Dave et al., 2016)

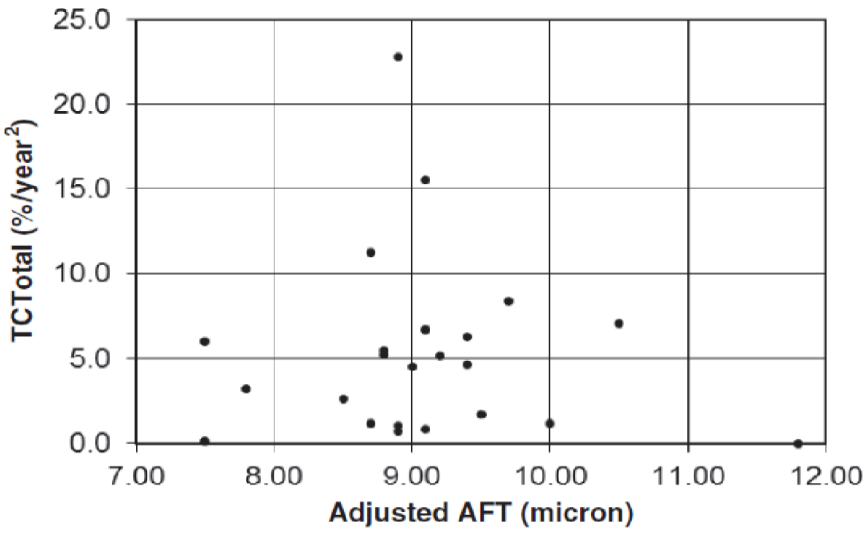

Figure 2-5 Effect of AFT on the Transverse Cracking Performance (Dave et al., 2016)

The researchers found that the pavements with -34°C low-temperature binder grade exhibited superior performance in Minnesota, as shown in Figure 2-6. Although a clear trend could not be achieved on the relationship between the fracture energy and transverse cracking percentage, the mixes with the lowest fracture energy (182 J/m^2) experienced 83% crack versus no cracking for the mixes with the highest fracture energy (1,080 J/m^2) (Figure 2-7).

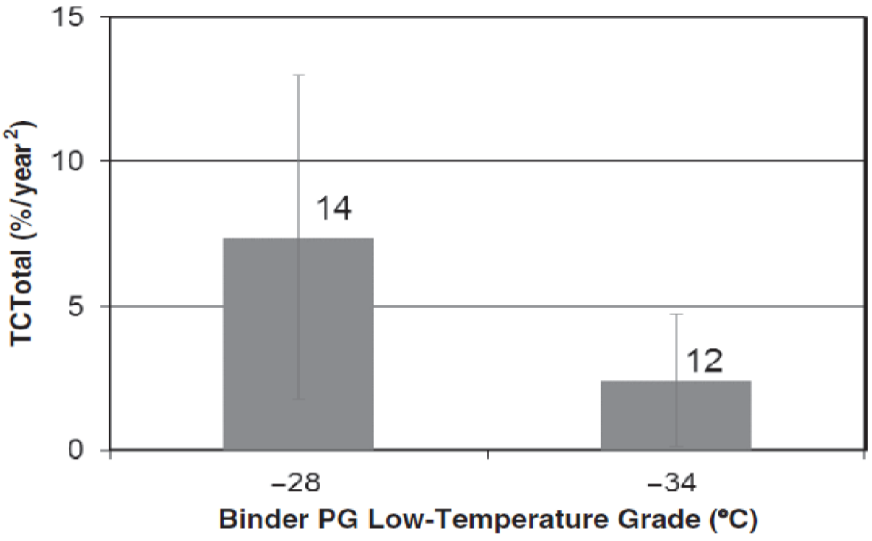

Figure 2-6 Effect of Binder Low-Temperature Grade on the Transverse Cracking Performance (Dave et al., 2016)

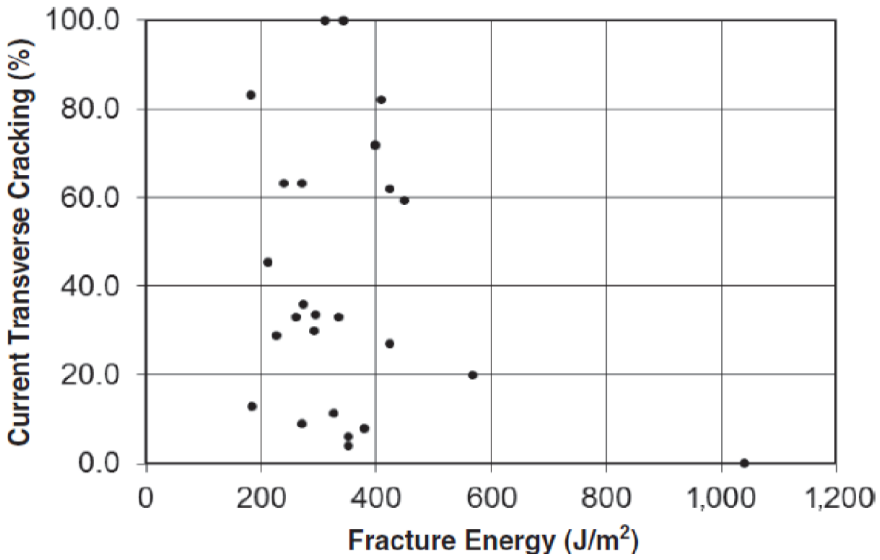

Figure 2-7 Effect of Fracture Energy on the Transverse Cracking Performance (Dave et al., 2016)

A study conducted by Marasteanu et al. (2012), showed that there is a strong correlation between the asphalt mixture fracture toughness and transverse cracking. The study revealed that asphalt pavements perform well against thermal cracking when the asphalt mixes used for the construction exhibit 400 J/m^2 DCT test measured (Figure 2-8) or 350 J/m^2 semi-circular bend (SCB) (Figure 2-9) test measured fracture energy.

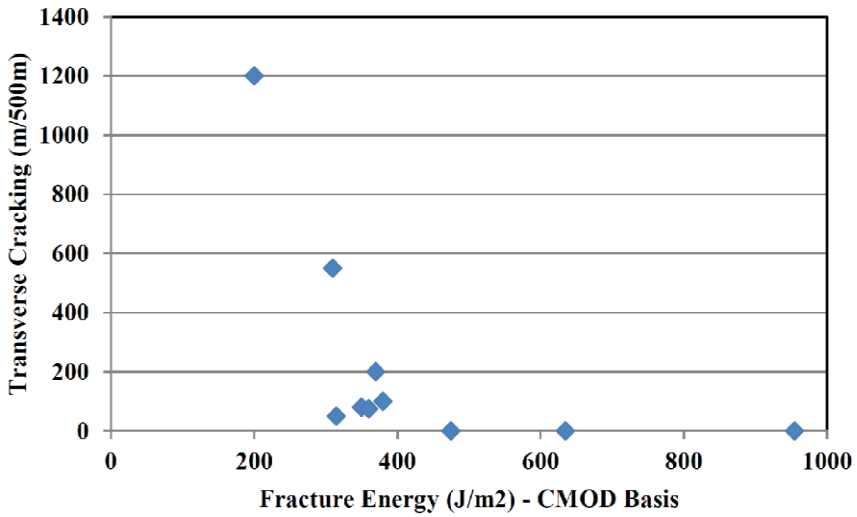

Figure 2-8 Correlation Between DCT Measured Fractured Energy and Transverse Cracking (Marasteanu et al., 2012)

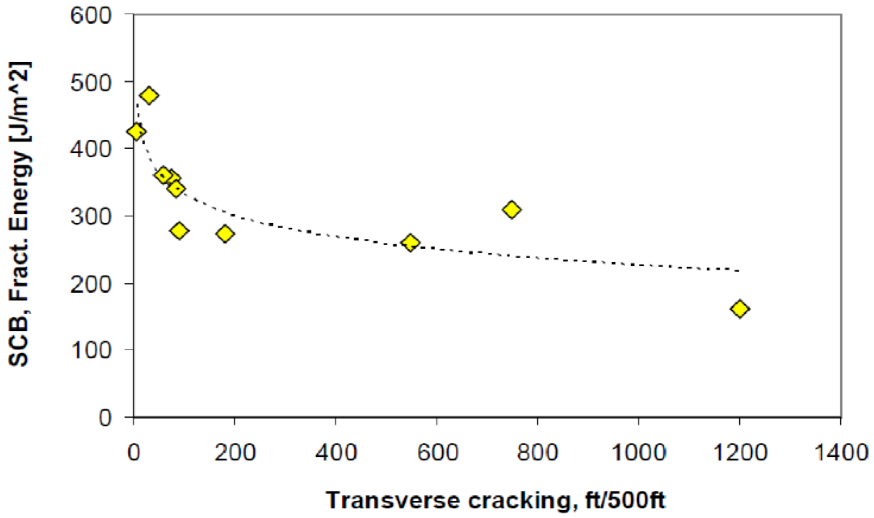

Figure 2-9 Correlation Between SCB Measured Fractured Energy and Transverse Cracking (Marasteanu et al., 2012)

2.3.4.2 Improved pavement performance with the balanced mix design approach

Newcomb and Zhou (2018) emphasized the importance of Balanced Mix Design (BMD) for enhancing the performance of asphalt pavements. The study, however, focused on the high-volume road asphalt mixtures. As depicted in Figure 2-10, in a balanced mix design approach, the maximum and the minimum percentages of asphalt binders are decided based on the rutting and cracking criteria, respectively. The study developed a framework for the balanced mix design for the Minnesota Department of Transportation, as shown in Figure 2-11. The flow chart in Figure 2-11 summarizes the procedure for the mixture design as per the BMD framework. This framework was established through a laboratory study using four different asphalt mixtures typically used in Minnesota. Test results indicated a lower optimal binder content than what was achieved using the Superpave procedure; however, the researchers cautioned that this may not happen in all other cases. The study suggested that the cracking and rutting performance criteria need to be refined based on the climate, lift thickness, traffic level, and placement within the pavement structure and the DCT test could be a part of the mix design procedure.

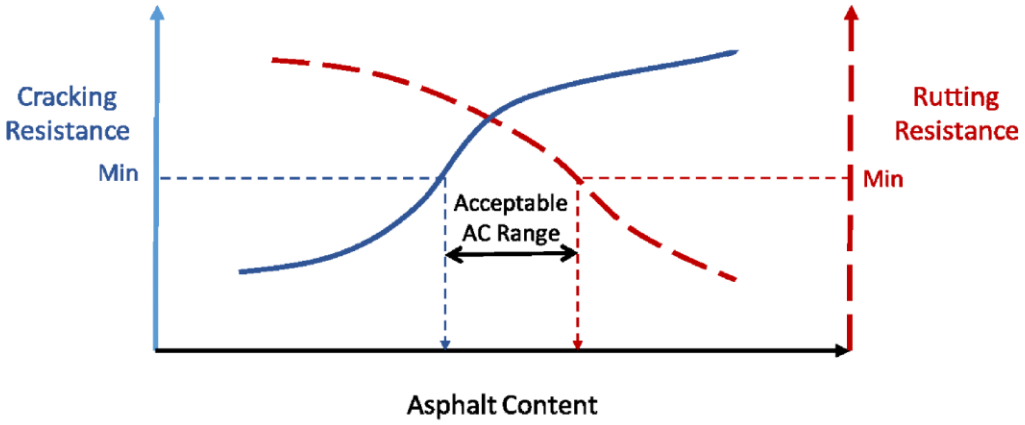

Figure 2-10 Concept of Balanced Mix Design (Newcomb and Zhou, 2018)

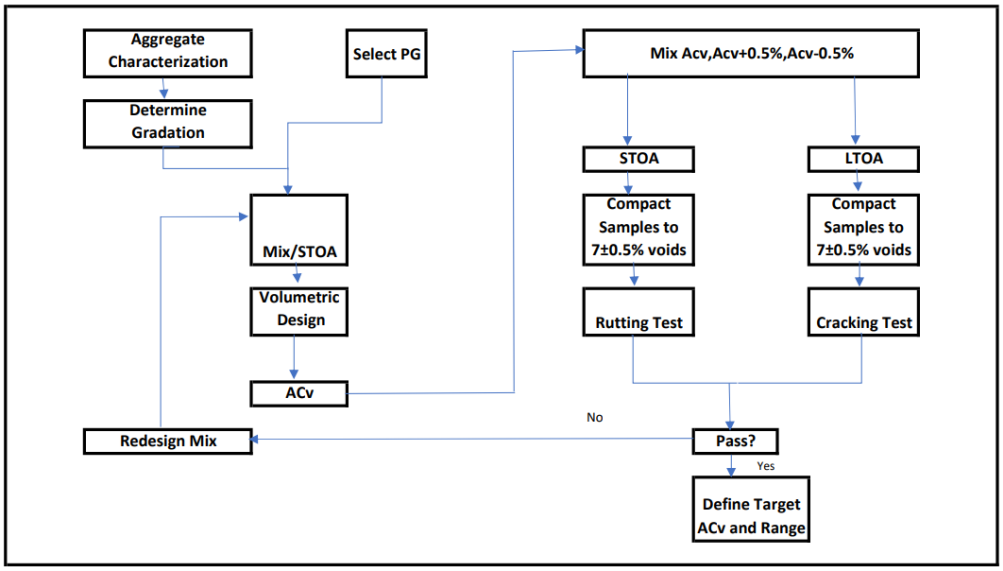

Figure 2-11 Flow Chart of the BMD Approach (Newcomb and Zhou, 2018)

2.3.4.3 Materials for low-volume asphalt roads in wet-freeze climate

Chen et al. (2019) studied the material selection criteria for asphalt pavements in wet-freeze climate zones of the United States and Canada. They believed that the use of a polymer-modified binder is beneficial in wet-freeze areas with respect to controlling low-temperature cracking. The use of performance-enhancing polymers such as (i) styrene-butadiene rubber (SBR), (ii) styrene-butadiene-styrene (SBS), (iii) styrene-ethylene-butylene-styrene copolymer (SEBS), (iv) crumb rubber modifiers (CRM), and (vi) epoxy terminated ethylene terpolymer (Elvaloy® AM or EAM) was suggested. The observation indicated that the addition of polyphosphoric acid (PPA) might enhance low-temperature performance to reduce the occurrence of low-temperature cracks, and PPA could constitute up to 1% of the mixture (D'Angelo, 2009).

Chen et al. (2019) noted that if warm mix asphalt (WMA) is used in the pavement, then the chemical additive could give good results in wet freeze areas. The use of the anti-stripping agent was proposed to benefit in resisting the moisture damage of asphalt mixes. Michigan DOT also uses crumb rubber primarily from recycled tires. Recycled asphalt shingles have been used by the Illinois department of transportation to combat the effect of wet-freeze action.

2.3.4.4 Influence of binder type, aggregate, and mixture composition

The effect of binder type, aggregate and mixture composition on the fracture energy was investigated by Braham et al. (2007). In that study, 28 types of asphalt mixtures for cold climates were designed and tested for fracture energy. The disc-shaped compact tension (DCT) test was conducted to determine the fracture energy. The fracture energy can characterize the resistance of asphalt mix against the low temperature induced thermal cracking, a critical problem for Minnesota's asphalt roads. Two types of aggregates (granite and limestone), ten different asphalt binder types (PG 58S-28 was one of them), two asphalt contents (optimum and optimum plus 0.5%), and two air voids (4% and 7%) were the test variables. Samples were tested at three temperatures: low (2°C below the low-temperature grade), medium (10°C above the low-temperature grade), and high (22°C above the low-temperature grade).

Figure 2-12 shows that the fracture energy remained very low for the mixes that were tested at low temperature, irrespective of the binder type, indicating a brittle behavior and the vulnerability of the asphalt mixtures to cracking during the winter season. As shown in Figure 2-13, it was found that the mixture with granite showed higher fracture energy compared to the limestone.

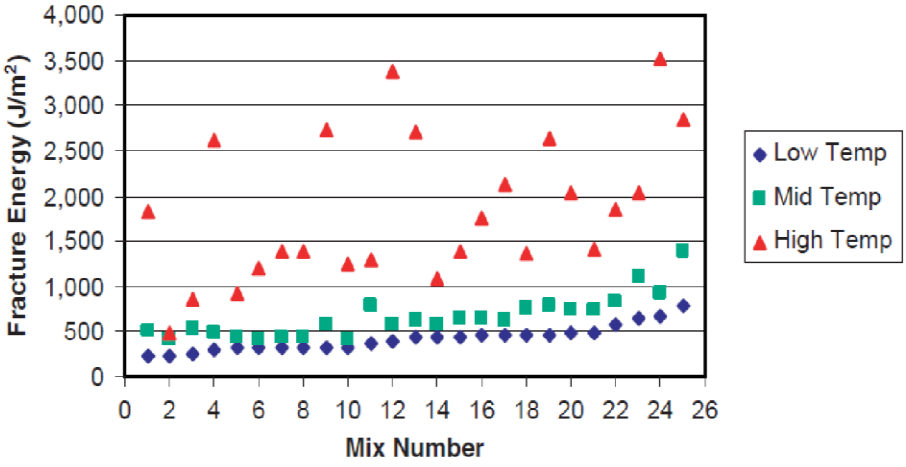

Figure 2-12 Effect of Test Temperature on Fracture Energy (Braham et al., 2007)

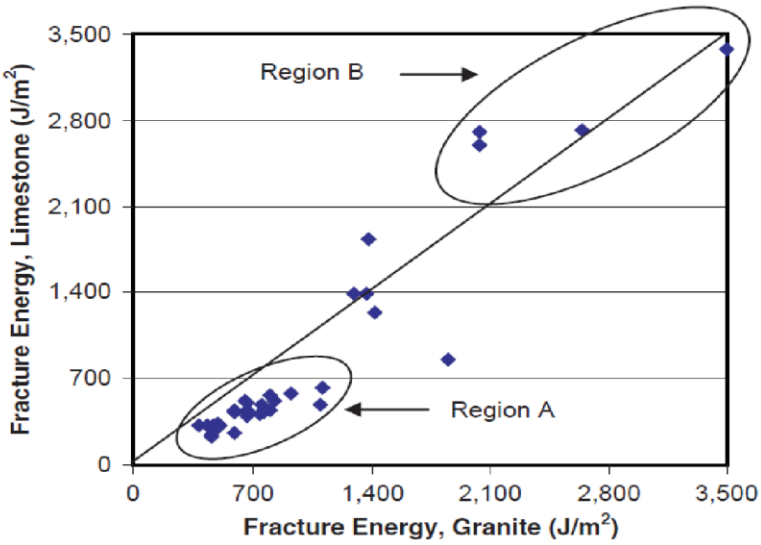

Figure 2-13 Effect of Aggregate Type on the Fracture Energy (Region A = Limestone, Region B = Granite) (Braham et al., 2007)

The effect of binder content on fracture energy is shown in Figure 2-14. For this particular study, it was found that 0.5% additional binder did not make a difference at the low-temperature fracture energy. The results in that study also suggested that the specimens tested at two air void levels did not show any significant difference in fracture energy (Figure 2-15).

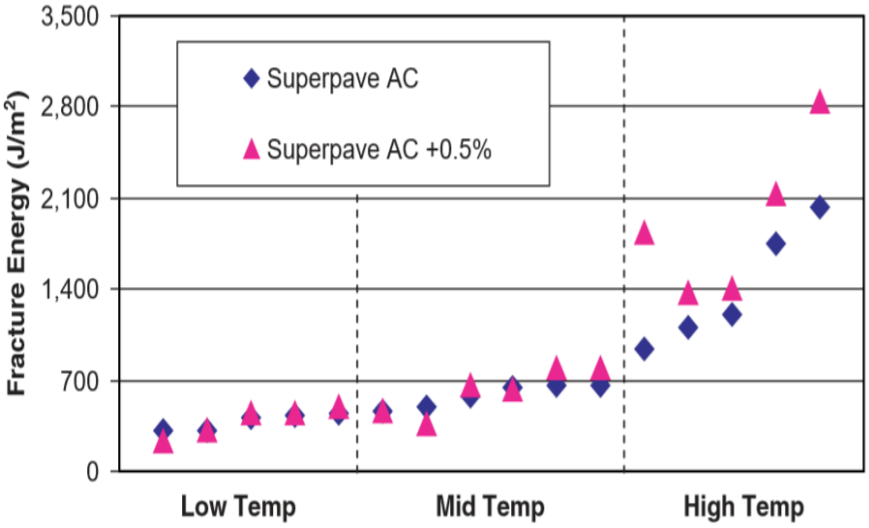

Figure 2-14 Effect of Binder Content on the Fracture Energy (Braham et al., 2007)

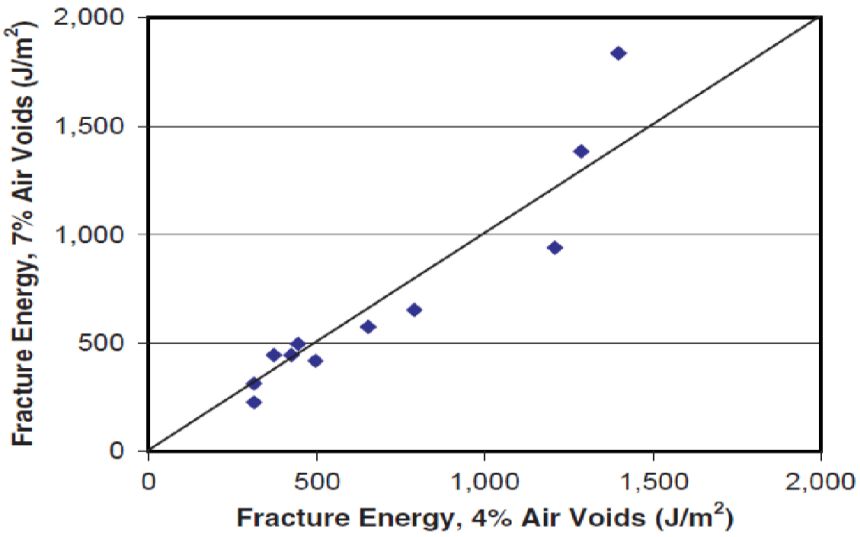

Figure 2-15 Effect of Air Voids Percentage on the Fracture Energy (Braham et al., 2007)

2.3.4.5 Volumetric parameters of the low-volume road asphalt mixtures

Vitillo et al. (2006) conducted a study to compare the volumetric properties of asphalt mixtures designed by the Superpave and Marshall Methods. This study is included in this report to document the volumetric parameters of low-volume road mixtures for a wet freeze climate state, New Jersey, in this case. The study considered four different asphalt mixes collected from four suppliers. For each of the four mixes, asphalt concrete specimens were reproduced by the Marshall method and Superpave method matching the original Job Mix Formula (JMF). The design air voids for the Marshall and Superpave methods were 4.5% and 4%, respectively. PG 64-22 binder and the nominal maximum aggregate size was 9.5 mm. Table 2.7 shows the volumetric parameters of the asphalt mixtures including % air voids, VMA, VFA, dust to binder ratio, etc. The VMA for the mix ranges between 15.3 to 18.5%.

Table 2.8 shows the asphalt film thickness of the mixes used in that study, which ranges between 7 and 10 microns.

Table 2.7 Volumetric Properties of Low-volume Road Asphalt Mixtures for a Study Conducted in New Jersey (Vitillo et al., 2006)

	Optimum Asphalt	% Air Voids	VMA	VFA	Stability	Flow	G_{mm}	Dust to Binder
Supplier A								
JMF	5.6	4.5	18.2	76.6	2510	8	2.653	
Marshall	*5 6*	4.5	18.1	75.1	2610	9.1	2.654	1.07
Superpave	5.1 (5.05)	4	15.3	*75.1*			2.710	1.17
Supplier B								
JMF	*5.7*	4.1	169	75.9	2115	11.8	2.449	
Marshall	*5.8*	4.5	17	7J.5	2000	8.8	2.4J6	1.0
Superpave	6 0(5.95)	4	16.5	75.8			2.435	0.96
Supplier C								
JMF	*5.5*	4.3	17.4	75.3	2461	11.7	2.605	
Marshall	*5.5*	4.5	17.2	74.4	3731	9.7	2.560	1.12
Superpave	5.3 (5.25)	4	15.9	74.8			2.568	1.16
Supplier D								
JMF	5.6	4.2	17.2	75.6	3140	11	2.450	
Marshall	5.2 (5.15)	4.5	16.3	72.4	3300	11.9	*2.552*	1.49
Superpave	5.3	4	17.7	77.4			2.505	1.48

Table 2.8 Asphalt Film Thickness Values of Low-volume Road Asphalt Mixtures for a Study Conducted in New Jersey (Vitillo et al., 2006)

	Marshall				Superpave			
Supplier	Thickness	VMA	%Binder	D to B ratio	Thickness	VMA	%Binder	D to B
A	9.8	18.1	5.6	1.07	7.9	15.3	5.1	1.17
B	9.5	17	5.8	1.0	10.0	16.5	6.0	0.96
C	7.2	17.2	*5.5*	1.12	7.2	15.9	5.3	1.16
D	7.0	16.3	5.2	1.49	7.1	17.7	5.3	1.48

2.3.4.6 MnROAD findings

MnRoad is a pavement test track owned by MnDOT. It consists of many test sections used for research. Worel et al. (2007) summarized the lessons learned from the MnRoad's low-volume asphalt roads, emphasizing the effects of design variables on the transverse and fatigue cracking and rutting. Table 2.9 summarizes the key distresses that were responsible for the failure of the pavements in different test cells.

Table 2.9 Failure Mechanisms of Low-volume Asphalt Road Cells (Worel et al., 2007)

Test Cell		Major Contribution to Failure		
(Construction Number)	Description of Cells	LTC	Fatigue	Rutting
24, a 25a	HMA on sand subgrade	X		
26(1),26(2)	HMA full depth		X	
27, a27(2),28a	3-inch HMA over granular base		X	X
27(3). 28(2)	Oil gravel over large Slone base		X	
29.a 30. a 31a	HMA over granular base	X		X
31(2)	Mesabi HMA over granular base (new)			
33(2)	Superpave HMA over granular base	X		X
34(2)	Superpave HMA over granular base			X
35(2)	Superpave HMA over granular base	X	X	X
Note: LTC = low-temperature cracking a = Original 1994 test cell				

Based on the performance and distress data, it was found that Cells 26 through 28 did not fail by transverse cracking. Authors hypothesized that the warm-mix or cold-mix technology used during the construction probably reduced the aging of the asphalt binder, allowing the binder to remain soft for an extended period. The performance of the Cells 33 (PG58-28), 34 (PG58-34) and 35 (PG58-40) revealed that the cell with PG 58-34 binder experienced far fewer transverse cracks compared to the other two cells. Figure 2-16 shows that most cells experienced transverse cracks during a cold snap that occurred in 1996 and the transverse crack did not increase afterward. Authors noted that the added friction at the interface between the asphalt layer and Class 6 base in Cell 25 probably resulted in a large amount of thermal cracking compared to the cell that had full-depth asphalt (Cell 25). The study also noted that the softer and wet subgrade under Cell 26 helped allow sliding of the asphalt layer, reducing the tensile stress build-up and transverse cracks. Figure 2-17 and Figure 2-18 show the rutting history of different cells. Based on the rutting trends observed, the authors noted that the number of load repetitions was more influential than the load magnitude. More load repetitions with a lighter load configuration (80K) resulted in more rutting than smaller number of repetitions with a heavier load configuration (102K) for given ESALs. A similar trend was also noticed for fatigue cracks.

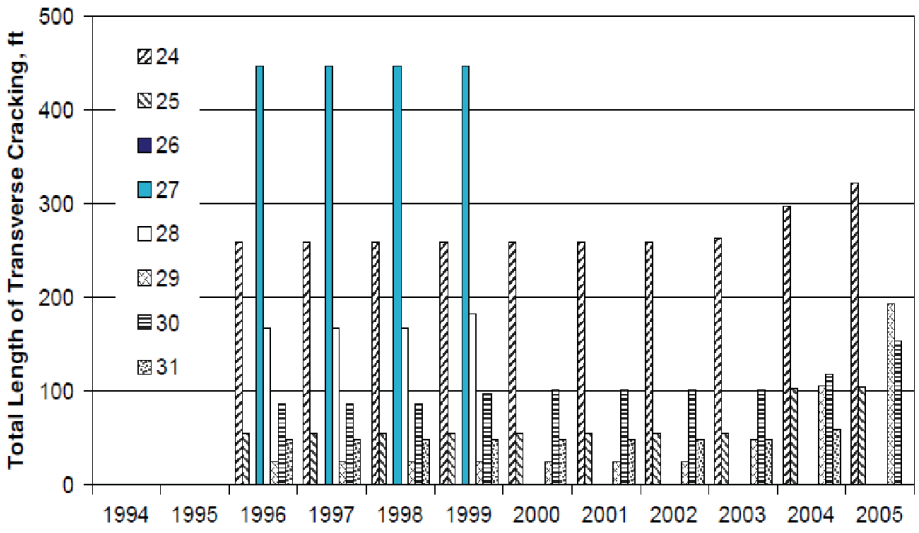

Figure 2-16 Transverse Crack History for Different Cells in Worrel et al. (2007) Study

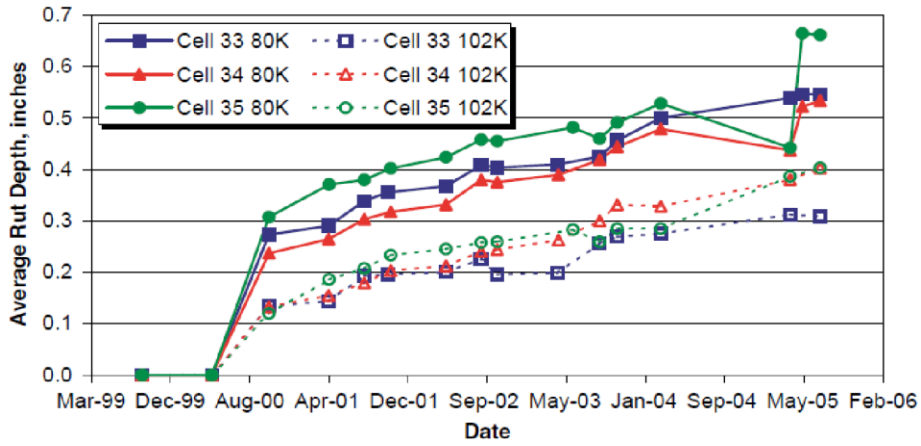

Figure 2-17 Asphalt Rutting History for Various Cells in Worrel et al. (2007) Study

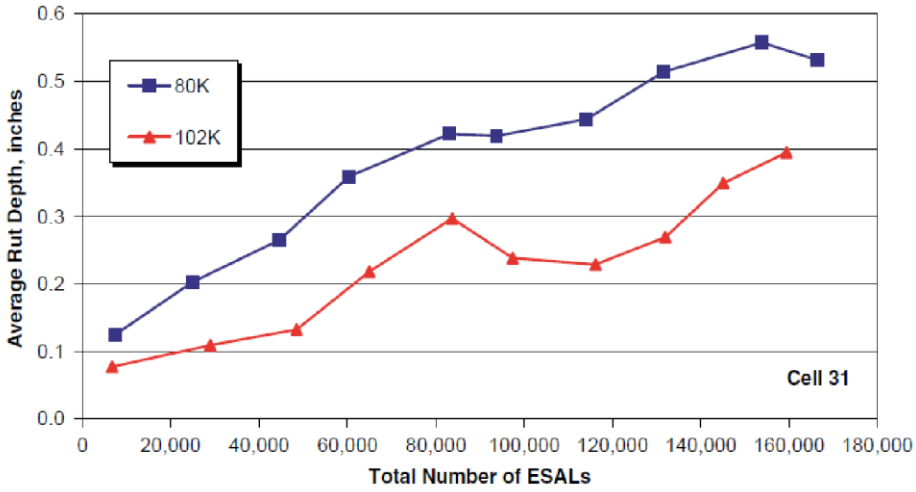

Figure 2-18 Asphalt Rutting versus ESALs in Worrel et al. (2007) Study

2.3.4.7 Correlation between the number of gyrations and field densities

The state of Colorado started implementing the Superpave mix design method in 1995. A study conducted by Harmelink and Aschenbrener (2002) investigated the correlation between the number of gyrations and field densities of 25 different projects. The objective of the study was to validate the number of gyrations that shall be used for Superpave mix design. The major finding of this research was that asphalt mostly densifies in the first three years, and after that, field density does not change significantly. Figure 2-19 shows the relationship between the field air voids (y-axis) and air voids at N_{design}. It was found that after six years, the field air voids percentage was approximately 1.2% higher than the design air voids percentage. The observed trends indicate that field air voids are probably never going to match the design air voids. The study concluded that the N_{design} values were higher than necessary, which resulted in stiffer mixes in the lab. The study recommended lowering the number of gyrations or to adjust the target air voids contents.

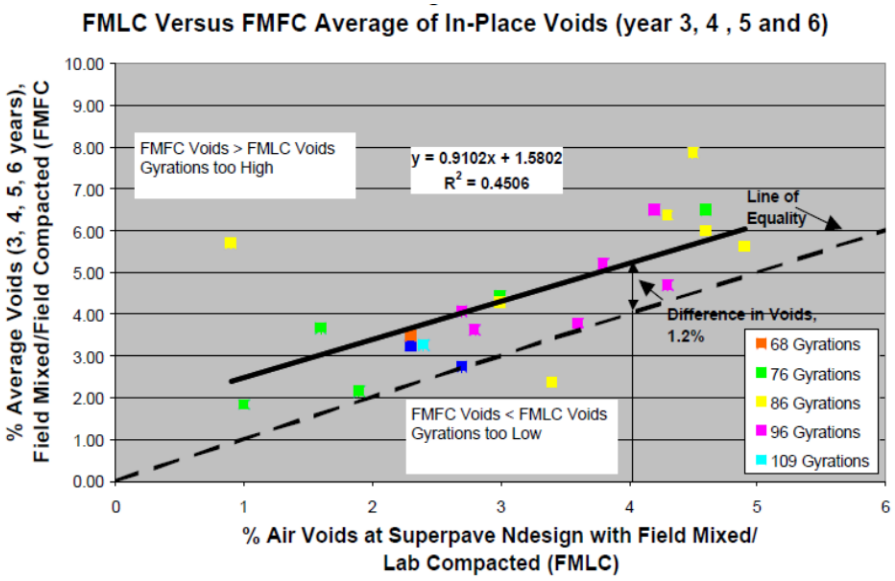

Figure 2-19 Relationship Between the Field Air Voids and Laboratory Air Voids at Ndesign in Harmelink and Aschenbrener (2002) Study

2.3.4.8 Effect of mixture design properties on the field compaction

Engle (2004) conducted a study in Iowa to determine the issues that might affect the implementation of Superpave mix design in low-volume roads. The influence of various mixture design parameters, such as aggregate gradation, laboratory air voids on the field compacted air voids were studied for eight county low-volume roads. In the Scott County project, the main emphasis was on aggregate gradations and three different aggregate gradations were used. A stronger "S" shape gradation was used to increase VMA, as shown in Figure 2-20. According to Figure 2-21 and Figure 2-22, the use of coarser gradation was able to increase the lab and field air voids. However, while the lab air voids varied within the upper and lower allowable limits, the field air voids exceeded the upper allowable limits, when the coarseness of the gradation was increased. The author noted that the reason for the higher voids for the coarser gradation was the less workability of mixes which influenced compaction in the field. The asphalt film thickness for all mixes was determined and found to be meeting the minimum requirement for low-volume roads. The seven other projects dealt with many variables such as the use of fine aggregate gradation, local aggregates, aggregate size, underlying layers, etc. A comprehensive discussion on those projects is available in the Engle (2004) report.

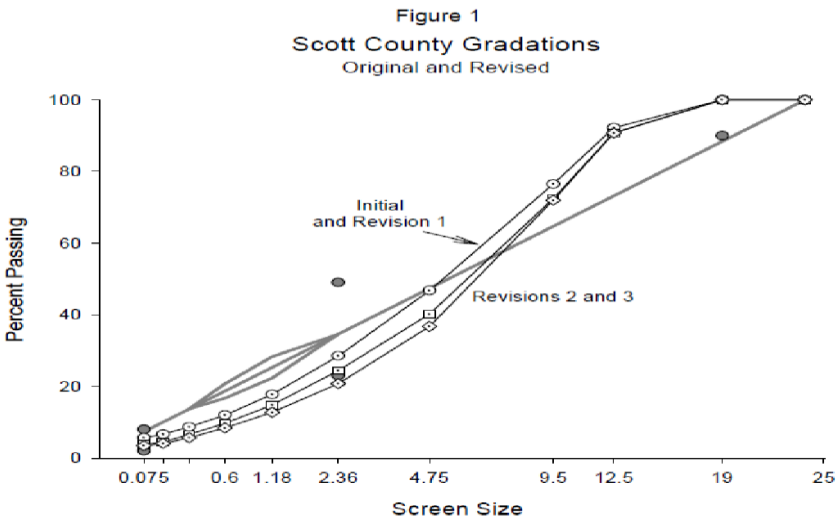

Figure 2-20 Aggregate Gradation used in Scott County Project in Engle (2004) Study

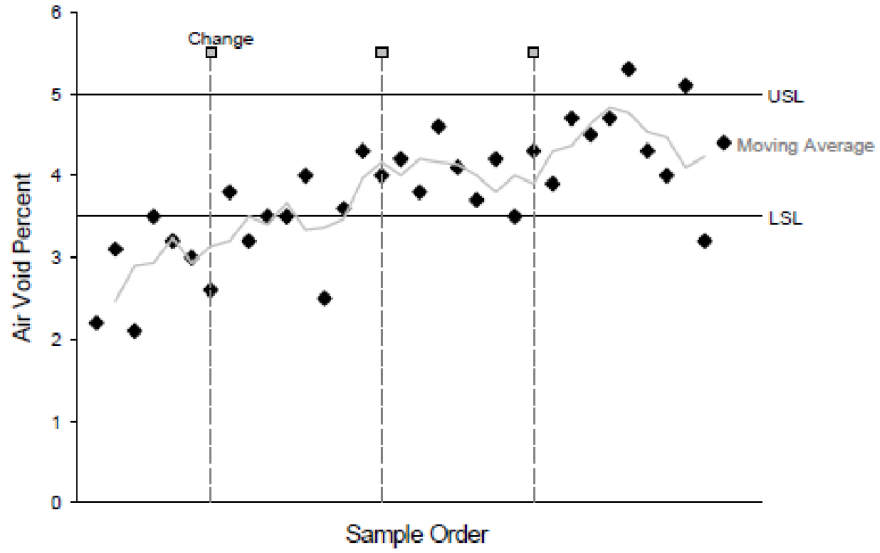

Figure 2-21 Air Voids for the Laboratory Samples for the Scott County Project in Engle (2004) Study

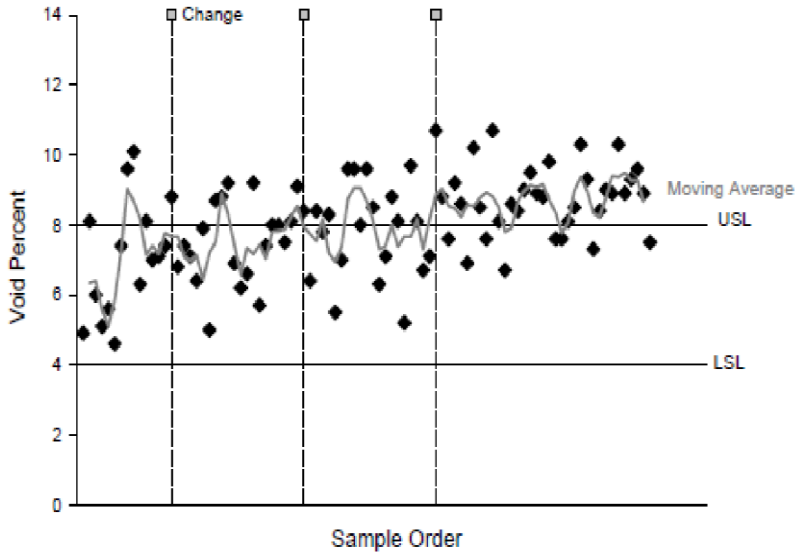

Figure 2-22 Field Air Voids for the Scott County Project in Engle (2004) Study

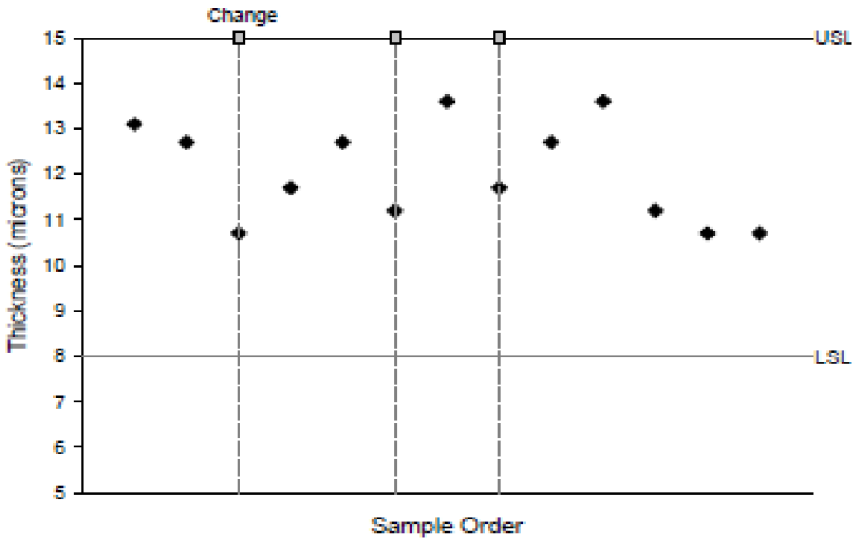

Figure 2-23 Asphalt Film Thickness for the Scott County Project in Engle (2004) Study

2.3.4.9 Effect of regressed air void mix design on the field performance

West et al. (2018) conducted a study for the Wisconsin Department of Transportation (WisDOT) to investigate the impact of regressed air void mix design on cracking, rutting, and moisture damage resistance of asphalt mixes. The use of increased binder contents results in regressed air voids. Once the job mix formula (JMF) and aggregate proportions are finalized, the binder content is then increased by 0.3% to 0.4% to reduce the design air voids percentage from 4% to 3%.

The study included a total of six asphalt mixes for various traffic levels (low, medium, and high) with various contents of RAP and RAS. The performance tests conducted on these mixtures were (i) Illinois

Flexibility Index Test (I-FIT) per AASHTO TP 124 to evaluate intermediate temperature cracking resistance, (ii) Disc-Shaped Compacted Tension (DCT) Test per ASTM D 7313 to evaluate low temperature cracking resistance, and (iii) Hamburg Wheel Tracking Test (HWTT) per AASHTO T 324 to evaluate rutting and moisture damage resistance. As shown in Figure 2-24, the flexibility index increased with the decrease in air voids percentage. The higher the flexibility index, the better the crack resistance. Figure 2-25 shows the DCT fracture energy results for the low-volume road mixes (test conducted at -18°C). The fracture energy did not increase as much as the flexibility index, nevertheless, when the air voids decreased to 3%, the fracture energy met the minimum required value of 400 J/m^2.

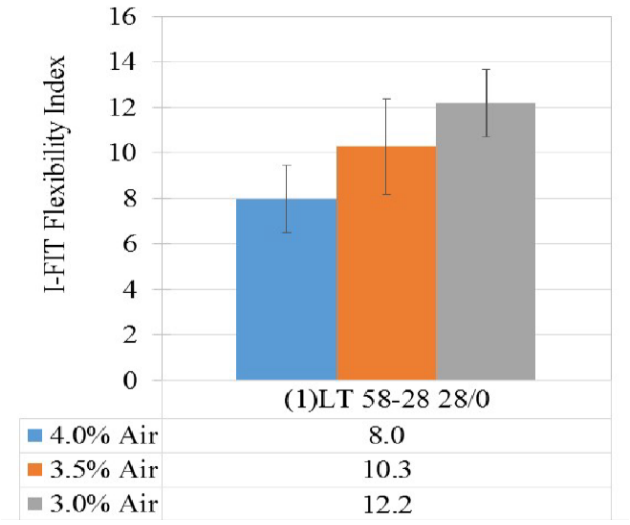

Figure 2-24 Flexibility Index versus Air Voids for Low-volume Road Mixes in West et al. (2018) Study

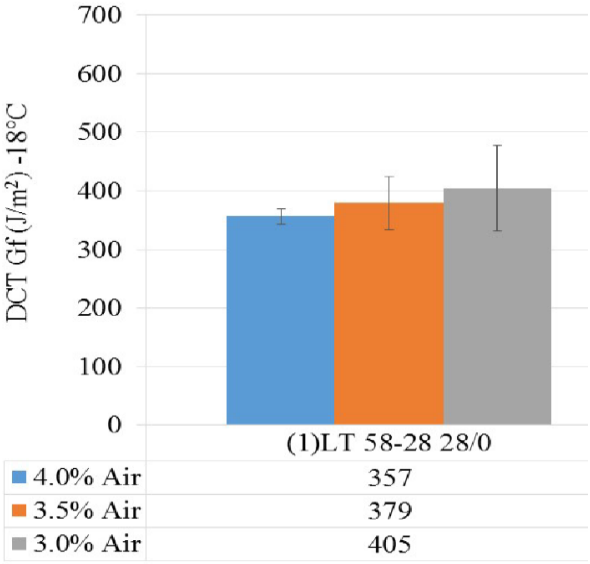

Figure 2-25 DCT Fracture Energy versus Air Voids for Low-volume Road Mixes in West et al. (2018) Study

2.4 Summary

1. It was found that most of the compaction occurs during the first three years and the field air void percentage never matches the design air voids.
2. MnROAD's test section's performance and other key studies suggested using PG58-34 binder is advantageous to minimize the transverse cracking, which is critical to the low-volume roads.
3. It was found that the asphalt mixtures possessing DCT test-measured fracture energy equal to 400 J/m^2 or SCB test-measured fracture energy equal to 350 J/m^2 provide good resistance against thermal cracking.
4. Implementation of the balanced mix design procedure is likely to enhance the performance of the asphalt pavement.
5. The literature review suggests that the regressed air void design concept and Superpave-5 mixture design concept are promising. This study thereby will consider evaluating mixtures designed according to the two above-mentioned methods.

Chapter 3: Survey Results

An online survey was conducted to collect information related to the current practice of materials and mixture designs for low-volume roads and their performance. A questionnaire was prepared after consultation with the Technical Liaison of the project. The survey was conducted through SurveyMonkey.com®. As many as 29 counties have participated in the survey as shown in Table 3.1. The key survey questions and responses are presented in this chapter.

Table 3.1 Participating Agencies in the Survey Conducted in this Study.

Agency	Responder
Dodge County Hwy Dept	Guy Kohlnhofer
Clearwater	Dan Sauve
Brown County	Wayne Stevens
Wright County Highway Department	Pete Forare
Nobles County	Stephen Schnieder
Meeker County	Michele
Rock County Highway Department	Mark Sehr
Carlton County	Greg J.Thompson
Faribault County	Mark Daly
Anoka County	Jerry Auge
Nicollet County	Seth Greenwood
Cottonwood County	Nick Klisch
Pipestone County	Nick Bergman
Carver County	Andrew Engel
St. Louis County	Matt Hemmila
Lincoln County	Joe Wilson
Pennington County	Mike Flaagan
Pope County	Brian Giese
Stevens County Highway Department	Jon Maras
Beltrami County	Bruce Hasbargen
Traverse County Highway	Chad Gillespie
Houston County	Brian Pogodzinski
Aitkin County	John Welle
Roseau County	Daryle Dahl
Blue Earth County	Nick Engel
Wabasha County	Dietric h Flesch
Hubbard County	Jed Nordin
Lac qui Parle County	Sam Muntean
Mcleod County	John Brunkhorst

Question 1: What pavement design method does your agency use in designing low-volume road pavements?

Response: The response summary for the Question 1 is provided in Figure 3-1. It appears that more than 50% of responders use MnDOT Flexible Pavement Design, R-value Method. Around 30% of respondents mentioned of using State Aid Design Charts. MnPAVE is used by a couple of counties.

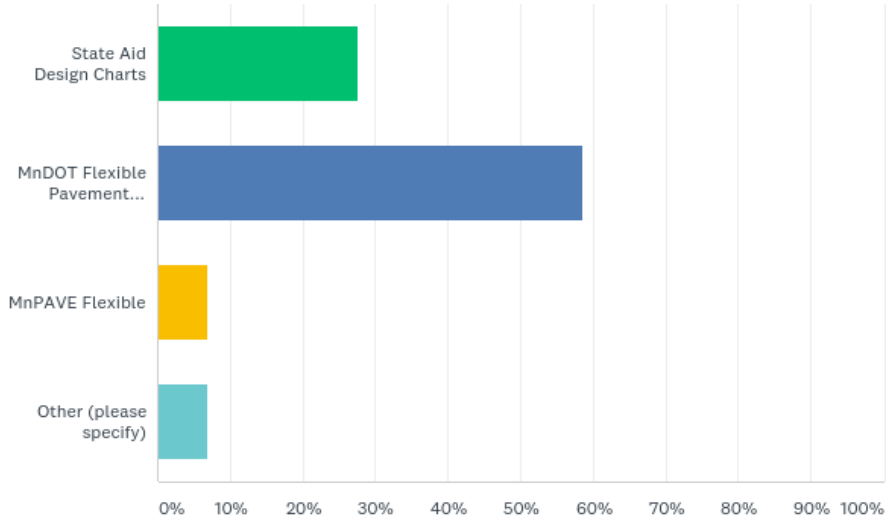

Figure 3-1 Response Summary for the Question 1

Question 2: Do you use the current MnDOT 2360 Asphalt Mix specification for the design of your low-volume Roads (<400 AADT, <1M ESAL's)?

Response: The response summary is provided in Figure 3-2. All the responders mentioned of using the MnDOT 2360 Asphalt Mix specification for designing their asphalt mixtures, either directly or with some modification.

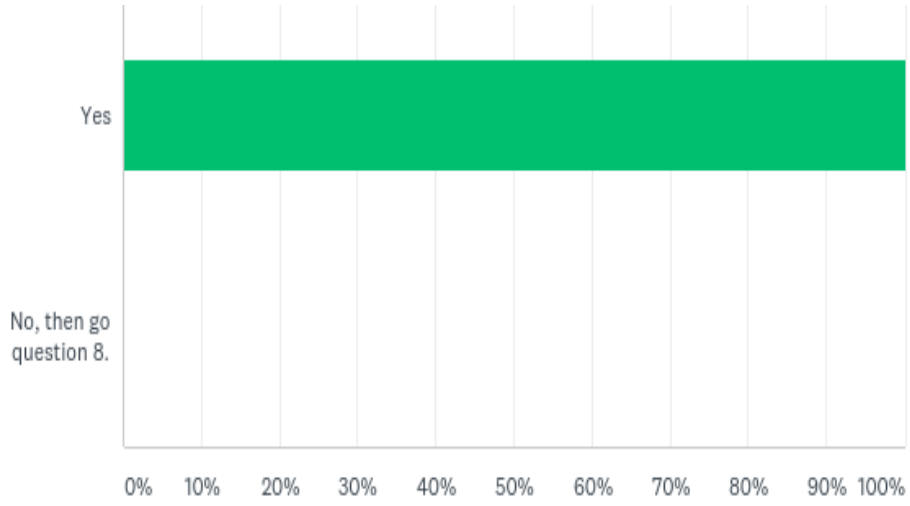

Figure 3-2 Response Summary for the Question 2

Question 3: Do you modify the current MnDOT 2360 Asphalt Mix specification for the design of your low-volume roads (< 400 AADT, <1M ESAL's)?

Response: The response summary is provided in Figure 3-3. Around 70% of respondents mentioned of not modifying the MnDOT 2360 procedure, while 30% used some modifications, as indicated in the responses to the following two questions.

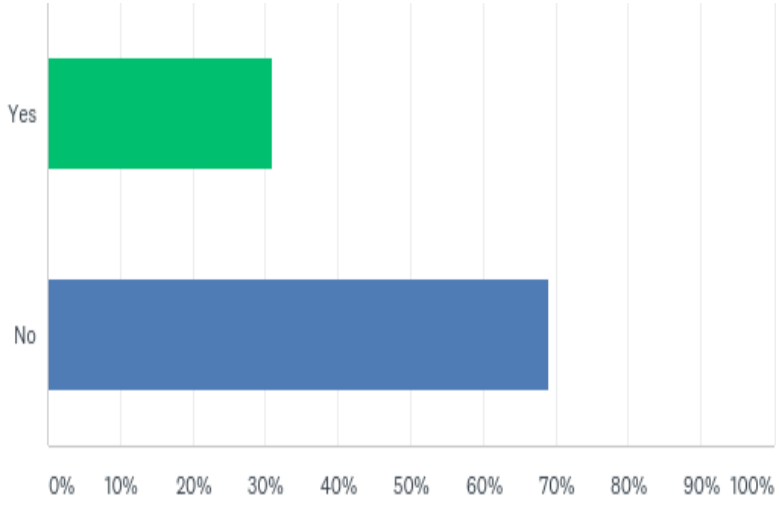

Figure 3-3 Response Summary for the Question 3

Question 4: Are you modifying the adjusted asphalt film thickness (AFT)?

Response: The response summary is provided in Figure 3-4. Most of the responders mentioned using the MnDOT's 2360 recommended AFT, which is 8.5 microns for low-volume roads (traffic level 2). Five counties mentioned using AFT as 9 microns. One county noted that they require a minimum VMA of 14% in addition to the AFT requirement.

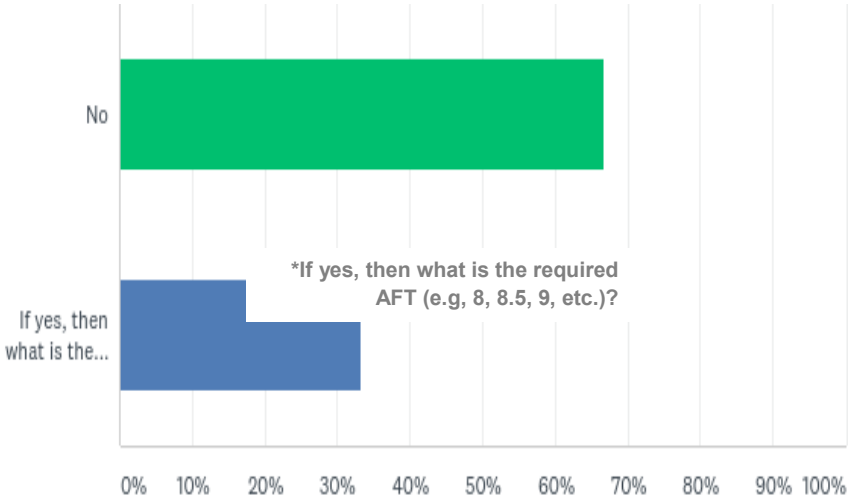

Figure 3-4 Response Summary for the Question 4

Question 5: Are you modifying the design air voids?

Response: The response summary is provided in Figure 3-5. Only about 20% responders mentioned using a different design air voids percentage than what is recommended by MnDOT's 2360. Three counties mentioned using target air voids as 3% instead of 4% for the wearing courses.

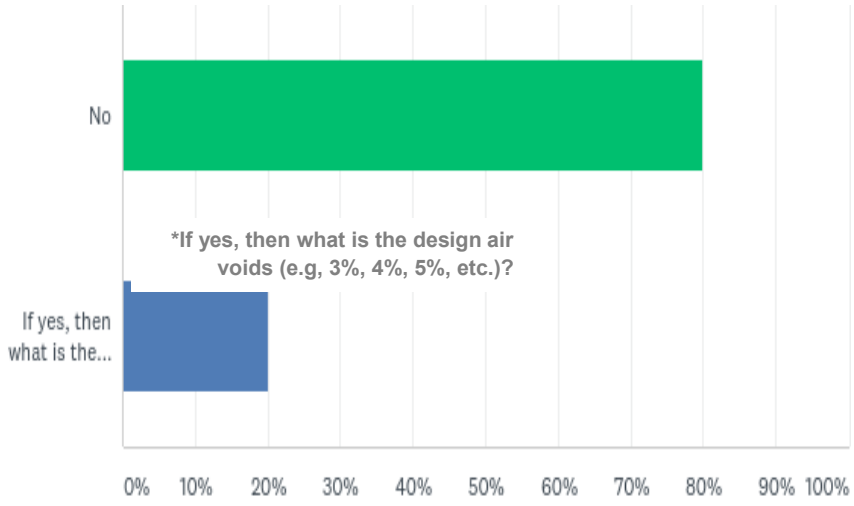

Figure 3-5 Response Summary for the Question 5

Question 6: What aggregate size do you specify in your low-volume road asphalt mixes?

Response: The response summary is provided in Figure 3-6. Around 50% of the responders use SP 9.5 aggregate gradation and 35% use SP 12.5. The comments received for this question are provided in the Figure 3-6 as well.

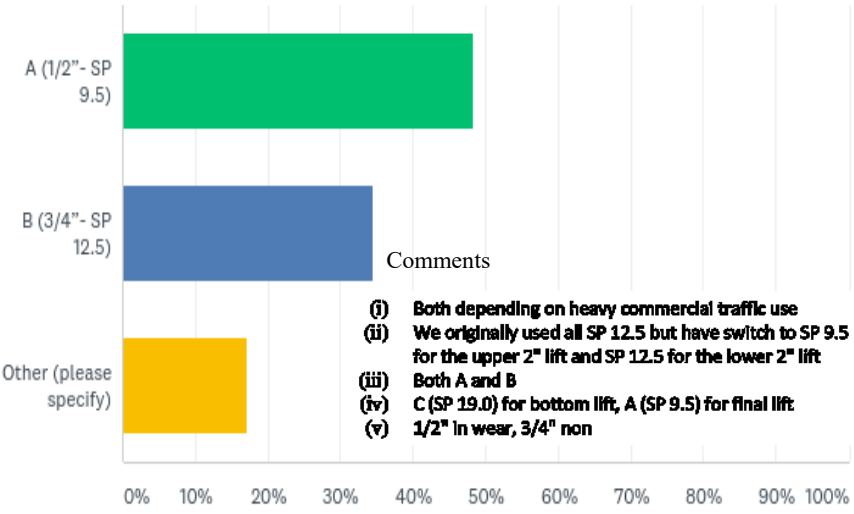

Figure 3-6 Response Summary for the Question 6

Question 7: Do you require QC/QA testing of low-volume road asphalt mixes?

Response: It appears that most of the counties perform some QC/QA tests as shown in Figure 3-7. The comments made by different responders are provided in Figure 3-7.

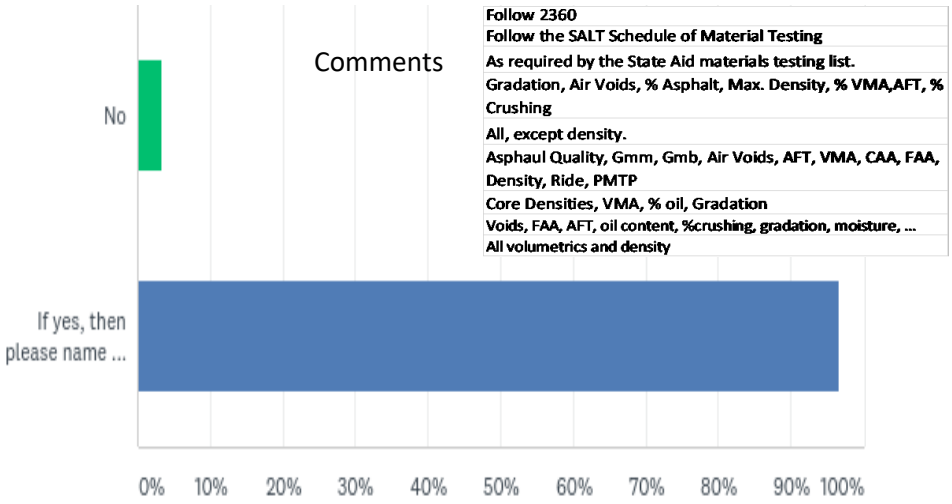

Figure 3-7 Response Summary for the Question 7

Question 8: What is the single most "predominant distress" observed on your low-volume road pavements?

Response: As anticipated, more than 75% of respondents consider transverse cracking as the most predominant distress. See Figure 3-8

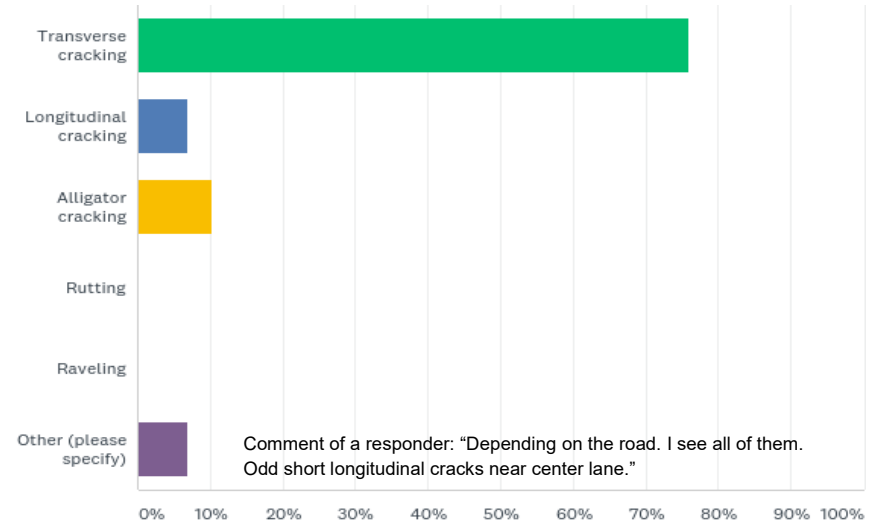

Figure 3-8 Response Summary for the Question 8

Question 9: What is the time in years before your first major rehabilitation (mill & overlay, CIR, FDR, etc.) of your low-volume road pavements experienced by your agency?

Response: As shown in Figure 3-9, low-volume roads are not rehabilitated before 15 years, most of the rehabilitation work occurs between 15 and 25 years.

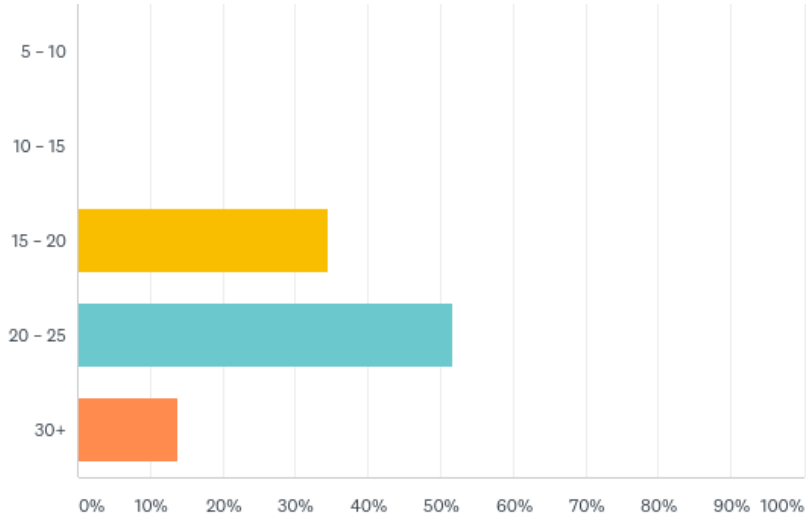

Figure 3-9 Response Summary for the Question 9

3.1 Summary

1. The survey conducted in the study indicated that more than 75% of responders consider transverse cracking as the single most predominant distress.
2. Aggregate gradation 'A' with a maximum aggregate size of 12.5 mm (SP 9.5) is mostly used for low-volume roads in Minnesota. The survey indicated some counties also use other gradations, such as SP 12.5.
3. RAP is used in low-volume asphalt mixtures; the maximum allowable limit varies among the counties.
4. The majority of the counties follow the MnDOT 2360 manual for mixture design, some counties apply some modifications, such as a minimum AFT of 9 microns, design air voids for wear course as 3%, etc.

Chapter 4: Field Study on the Asphalt Layer Densification and Common Distresses

The low-volume asphalt road densification was studied by collecting field cores from various counties of Minnesota. Two sets (Data sets 1 and 2) of core data have been used to study the asphalt layer densification. Data Set 1 was provided by Mr. Ron Bumann, a former State-aid technician. Data Set 2 was generated by the research team by collecting and testing cores from various locations. The first part of this chapter provides details of the project locations from where the cores were collected, the volumetric analysis results, and key findings about the layer densification.

Field study was also extended to document the common distresses in the low-volume roads. The second part of this chapter discusses the distresses observed in the field study.

4.1 Asphalt Layer Densification Study

4.1.1 Core Data Set 1

4.1.1.1 Project Locations

The data was collected from various roads in seven different counties: Polk, Crow Wing, Morrison, Pope, Lake, Cass, and Clearwater Counties. Figure 4-1 shows the locations of the roadways in different counties in the Google Map, and presents detailed information about roadway type, location, mixture type, AADT, etc. Data like AADT, roadway type, etc., was collected from the relevant MnDOT webpages based on the project name associated with the core data provided by Mr. Bumann. Project information and traffic data for the roadways are presented in Table 4.1.

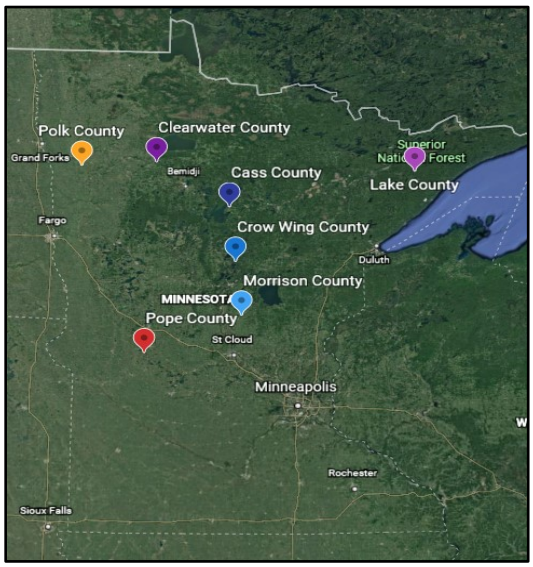

Figure 4-1 Locations for the roadways in different counties

Table 4.1 Project information and traffic data for the roadways where cores were collected

County	Project #	Road Type	Location	Mix Type	Average AADT
Polk County	60-619-015	Major Collector	CSAH 19 from 130 st SW to 150 st SW to 400 Ave SW	WEB240B (Jun 2013)	1077
	60-614-19	Major Collector	CSAH 14 from S. County line to CSAH 41 and CSAH 41 to CSAH 45	WEB240B (Aug 2011)	328
	60-641-022	Minor Collector	CSAH 41 from CSAH 14 to US TH 75	WEB240B (Aug 2009) NWB230B (Aug 2009)	185
Pope County	61-618-032	Major Collector (rural undivided)	CSAH 18 from 4.5 mi. E of CSAH 1 and TH 29	WEB230A (Jun 2010) NWB230A (Jun 2010)	602
	61-601-013	Major Collector	CSAH 1 from Jct. CSAH 2 and Jct. 255 st.	WEB230A (Jun 2012) NWB230A (Jun 2012)	295
Crow Wing County	18-127-004	Local Collector	CR 127 from CR 115 to CR 137	WEB240B (Jun 2012)	835
	18-104-001	Local Collector	CR 104 from CSAH 22 to CSAH 23	WEB240B (Aug 2011)	50
	18-610-005	Major Collector	CSAH 10 Btw. MN Trunk HWY 18 and CSAH 14 in Bay Lake Twnshp	WEB240B (Apr 2010)	790
Lake County	38-614-010	Major collector	CSAH 14 from CSAH 2 to County line	WEB340C (Jul 2012) WEA340C (Jul 2012) NWB330B (Jul 2012)	407
Morrison County	49-647-014	Major Collector	On CSAH 47 from CSAH 23 to TH 27	WEB240B (Jul 2010)	520
	49-637-010	Minor Collector	On CSAH 37 from CSAH 26 to 39	WEB230B (Aug 2011)	308
	49-240-012	Local Collector	TH 25 to CSAH 37	WEB240B (Jul 2012)	260

Cass County	11-608-014	Major Collector	On CSAH 8 (TH 200 to Cass CO CR 157)	WEA230C (Oct 2012) NWB230C (Oct 2012)	730
Clear Water County	15-614-009	Minor Collector	On CSAH 14 from N of Leonard NCL (E of TH 223) to CSAH 4, from Bagley Lake Rd. (N of CSAH 4) to CSAH 11	WEB340B (Sep 2013)	315

4.1.1.2 Volumetric Properties

The different volumetric parameters considered are the Bulk Specific Gravity of mixture (G_{mb}), air voids percentage (V_a), MA, density, and relative density (%). The variations of these parameters with the age and ESALs (Equivalent Single Axle Load) applied to them between the construction year and the core collection year were studied. The ESAL was calculated from AADT (Average Annual Daily Traffic) data referring to the State-Aid Excel Spreadsheet. The percentage of trucks in each vehicle category and their directional distribution were considered; the growth rate of the truck factor was considered as 0.

4.1.1.3 Bulk Specific Gravity (G_{mb})

Table 4.2 shows the bulk specific gravity of the cores collected right after the construction and at various years after the construction. While the exact locations of the cores are not available to the research team; however, as the objective of the core collection was to study the field density over time, it is assumed that cores were collected from the same vicinity from each project location, along the wheel path. In Table 4.2, 'Year 0' indicates the time right after the construction. 'Year 1' through 'Year 5' indicates the number of the year(s) aged before the core was collected. There was no core data available to the research team between the 'year 0' and 'year 1'. It is seen from Table 4.2 that in all the projects, G_{mb} values increased with pavement age, in general. Interestingly, G_{mb} values also show some correlations with the ESALs for the projects within a county. The difference in the G_{mb} values is more for higher ESALs. For example, project 60-619-015 in Polk County, which had 28,000 ESALs in a year, experienced a 1.6% change in the G_{mb} values compared to 0.7% change of the same for the project 60-641-22 (Polk County), which had 14,000 ESALs in three years. Similar observations can also be found in other counties.

Table 4.2 G_{mb} values of the cores

County	Project	*Total ESALs	G_{mb} (in different years of pavement aging)						% Difference
			Year 0	Year 1	Year 2	Year 3	Year 4	Year 5	
Polk	60-619-015	28000	2.348	2.386					1.6
	60-614-19	19000	2.386			2.407			0.9
	60-641-22	14000	2.329					2.345	0.7
Pope	61-618-32	43000	2.289				2.363		3.2
	61-601-13	13000	2.280		2.316				1.6
Crow Wing	18-127-04	41000	2.325		2.354				1.3
	18-104-01	3000	2.334			2.342			0.3
	18-610-05	62000	2.359				2.384		1.1
Lake	38-614-10	20000	2.347		2.368				0.9
	38-614-10	20000	2.349		2.368				0.8
Morrison	49-647-14	39000	2.317				2.349		1.4
	49-637-10	17000	2.336			2.376			1.7
	49-240-12	11000	2.349		2.364				0.6
Cass	11-608-14	40000	2.323		2.367				1.9
Clearwater	15-614-09	12000	2.314	2.333					0.8

**Total ESALs = ESALs applied between the construction year and core collection year. Example: for the Polk County project no. 60-614-19, the ESAL for the period between 'year 0' and 'year 3' (three years) is 19,000.*

4.1.1.4 Air Voids

Table 4.3 shows the air voids measured at different ages. The in-situ air voids at Year 0 range between 5.3% and 7.2% (average = 6.32%). It may be noted that the design air voids for some of the projects were 3%, but the in-situ air voids (Year 0) for those projects, compared to the projects constructed with 4% design air voids, were not distinctly low. The air voids of the aged (Year 1 through 5) pavements were found to be lower than the 'Year 0' air voids, which indicates that some degrees of compaction occur in the low-volume roads. Regarding the air voids percentage vs. ESALs relationship, air voids percentage change was generally more prominent for the projects with higher ESALs than the projects with lower ESALs in the same county, irrespective of the age.

Table 4.3 Air void percentages of the cores

County	Project	Total ESALs	Air voids (in different years of pavement aging)						% Difference
			Year	Year	Year	Year	Year	Year	
Polk	60-619-015	28000	5.7	4.1					28.1
	60-614-19	19000	5.3			4.5			15.1
	60-641-22	14000	6.4					5.8	9.4
Pope	61-618-32	43000	5.8*				2.7		53.5
	61-601-13	13000	6.3*		4.8				23.8
Crow Wing	18-127-04	41000	6.4		5.3				17.2
	18-104-01	3000	7.2*			6.9			4.2
	18-610-05	62000	6.2				5.2		16.1
Lake	38-614-10	20000	7.1		6.3				11.3
	38-614-10	20000	7.0		6.3				10.0
Morrison	49-647-14	39000	6.8				5.5		19.1
	49-637-10	17000	6.3*			4.7			25.4
	49-240-12	11000	5.9		5.3				10.2
Cass	11-608-14	40000	5.9*		4.1				30.5
Clearwater	15-614-09	12000	6.5	5.8					10.8
* Indicates the design air voids percentage was 3%									

4.1.1.5 Void in Mineral Aggregates (VMA)

VMA represents the void spaces between mineral aggregate particles in compacted asphalt mixtures. Table 4.4 presents the VMA values of different projects at each of the seven counties. It is observed from Table 4.4 that the VMA values decreased with age in general, irrespective of the mix type. However, a notable trend could not be observed because of limited yearly data and variations in the AADT. This general decrease in the VMA is probably due to the layer densification, oxidation of the binder, and decreased air voids. Regarding the VMA vs. ESALs relationship, like the air void percentage trend, the VMA change was more prominent for the projects with higher ESALs than the projects with lower ESALs in the same county, irrespective of age.

Table 4.4 VMA values of the cores

County	Project	Total ESALs	VMA (in different years of pavement aging)						% Difference
			Year 0	Year 1	Year 2	Year 3	Year 4	Year5	
Polk	60-619-015	28000	13.8	12.4					10.1
	60-614-19	19000	13.4			12.6			5.7
	60-641-22	14000	11.8					11.2	5.1
Pope	61-618-32	43000	14.6				11.8		18.9
	61-601-13	13000	14.5		13.2				9.3
Crow Wing	18-127-04	41000	15.9		14.9				6.6
	18-104-01	3000	14.5			14.2			2.0
	18-610-05	62000	14.6				13.7		6.2
Lake	38-614-10	20000	15.1		14.3				5.0
	38-614-10	20000	15.3		14.6				4.5
Morrison	49-647-14	39000	14.6				13.4		8.1
	49-637-10	17000	13.5			12.0			11.0
	49-240-12	11000	13.9		13.4				4.0
Cass	11-608-14	40000	14.7		13.1				11.0
Clearwater	15-614-09	12000	13.5	12.8					5.3

4.1.1.6 Density of Cores

Table 4.5 shows core density with age. Both wearing and non-wearing courses were considered in this analysis. In general, the density was found to increase in both courses. As anticipated, the wearing course had densified more than the non-wearing course (marked with '#'), as the non-wearing courses are lower in the pavement structure and experience less stress.

Table 4.6 shows the relative density values, which are expressed as the ratio of average bulk specific gravity (G_{mb}) of cores and the theoretical maximum specific gravity of loose mixes (G_{mm}) multiplied by 100%. Numerically, the relative density is also equal to '100 - air void percent (Va)'. Based on density and relative density values provided in Table 4.5 and Table 4.6, it can be seen that the differences in the densities between the cores from aged pavement (various years) and new pavement lie between 0.3% to 3.2%, with an average value of 1.27% (standard deviation = 0.71%).

Table 4.5 Core densities

County	Project	Total ESALs	Core Density (pcf) (in different years of pavement aging)						% Difference
			Year 0	Year 1	Year 2	Year 3	Year 4	Year 5	
Polk	60-619-015	28000	146.3	148.6					1.6
	60-614-19	19000	148.6			150.0			0.9
	60-641-22	14000	145.1					146.1	0.7
	60-641-22#	14000	146.9					148.1	0.8
Pope	61-618-32	43000	142.6				147.2		3.2
	61-618-32#	43000	142.8				145.7		2.0
	61-601-13	13000	142.0		144.3				1.6
	61-601-13#	13000	142.2		144.0				1.3
Crow Wing	18-127-04	41000	144.8		146.7				1.3
	18-104-01	3000	145.4			145.9			0.3
	18-610-05	62000	147.0				148.5		1.0
Lake	38-614-10	20000	146.2		147.5				0.9
	38-614-10	20000	146.3		147.5				0.8
	38-614-10#	20000	145.5		146.3				0.5
Morrison	49-647-14	39000	144.3				146.3		1.4
	49-637-10	17000	145.5			148.0			1.7
	49-240-12	11000	146.3		147.3				0.7
Cass	11-608-14	40000	144.7		147.5				1.9
	11-608-14#	40000	144.0		147.2				2.2
Clearwater	15-614-09	12000	144.2	145.3					0.8
	15-614-09#	12000	-	141.6					
# non-wearing courses									

Table 4.6 Relative densities

County	Project	ESALs	Relative density (in different years of pavement aging)						% Difference
			Year 0	Year 1	Year 2	Year 3	Year 4	Year 5	
Polk	60-619-015	28000	94.3	95.9					1.7
	60-614-19	19000	94.7			95.5			0.8
	60-641-22	14000	93.6					94.2	0.6
	60-641-22#	14000	94.7					95.5	0.8
Pope	61-618-32	43000	94.2				97.3		3.3
	61-618-32#	43000	94.3				96.2		2.0
	61-601-13	13000	93.8		95.2				1.5
	61-601-13#	13000	93.8		95.1				1.4
Crow Wing	18-127-04	41000	93.6		94.7				1.2
	18-104-01	3000	92.8			93.1			0.3
	18-610-05	62000	93.8				94.8		1.1
Lake	38-614-10	20000	92.9		93.7				0.9
	38-614-10	20000	93.0		93.7				0.8
	38-614-10#	20000	92.6		93.1				0.5
Morrison	49-647-14	39000	93.2				94.5		1.4
	49-637-10	17000	93.7			95.3			1.7
	49-240-12	11000	94.1		94.7				0.6
Cass	11-608-14	40000	94.1		95.9				1.9
	11-608-14#	40000	94.0		96.1				2.2
Clearwater	15-614-09	12000	93.5	94.2					0.7
	15-614-09#	12000	-						
# non-wearing courses									

4.1.1.7 Impact of Pavement Age and Traffic on Air voids Percentage and Pavement Densification

Figure 4-2 presents the air voids percentage measured from the cores extracted in different years for all seven counties together. The average of in-situ air voids for all the projects at Year 0 was 6.30%, with a standard deviation of 0.62%, as shown in Table 4.7. This table shows the average air voids percentage at different years of aging. It should be noted that the number of data points for the aged cores is very limited, so a strong conclusion is not possible. Figure 4-2 also shows that although the air voids decrease with age in LVRs, it rarely goes below 4%. One data point in Figure 4-2, which shows the 2.7% air voids after four years of aging, was recorded in Pope County. The total ESALs for that road was 14,000, and the mix type was WEB230A. All other measured air voids were around 4% or higher. A reasonable correlation is not achieved between the age and air voids percentage, based on the trendline of the air voids and year of aging in Figure 4-2. Figure 4-3 presents the variation of air voids percentage with respect to the ESALs; this correlation is slightly better than the previous one. Figure 4-4 shows the

correlation of the relative density change with respect to ESALs plotted separately for each of the four counties with at least three data points. The correlations are significantly better than what was seen in the two other correlations discussed above. The reason for this could be the use of similar materials and mixture designs within the counties, which creates a similar densification of the pavement layer with respect to the traffic.

Lastly, based on the above volumetric analysis of the cores (Core Data Set 1), it can be stated that pavement age and ESALs influence the air voids in general, but intuitively ESALs have a higher influence on pavement densification. However, the air voids percentage in the low-volume roads does not seem to go below 4%, at least for the type of the road sections considered in this analysis. Therefore, it may be beneficial to adopt mixture designs with a higher initial density like Superpave-5 mixture design, where the initial air voids percentage is close to 5%, lower than the in-situ densities achieved in conventional Superpave mixes.

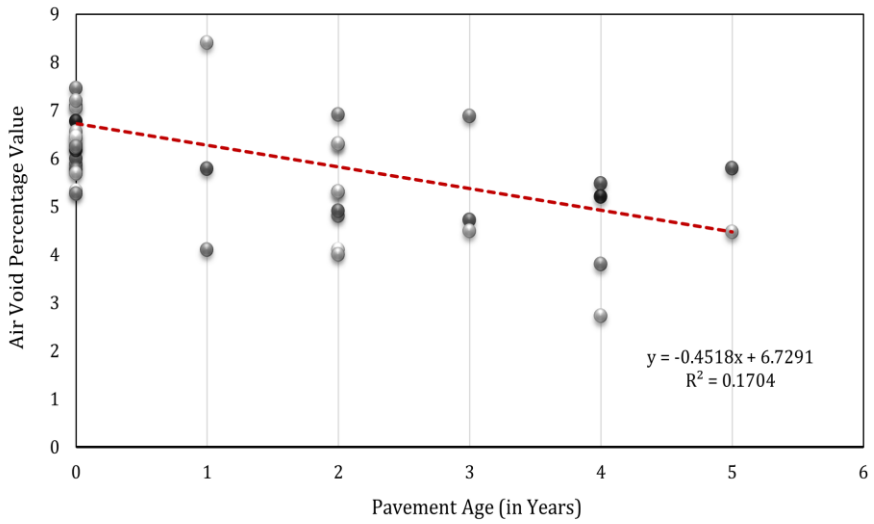

Figure 4-2 Air void percentage measured in different years

Table 4.7 Air Voids

	Number of data points	Average	Standard deviation
Year 0	19	6.30	0.62
Year 1	3	6.09	2.17
Year 2	9	5.32	1.01
Year 3	3	5.36	1.32
Year 4	4	4.30	1.28
Year 5	2	5.12	0.94

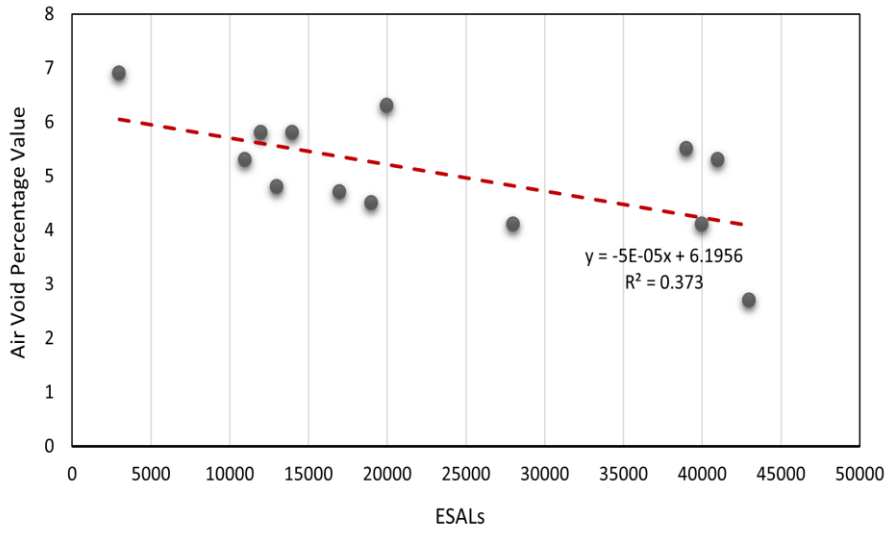

Figure 4-3 Air void percentage vs. Total ESALs value

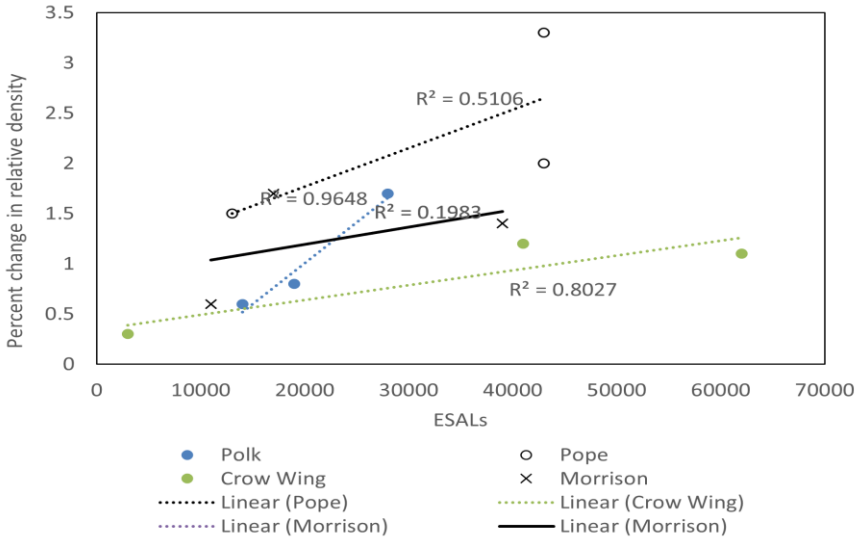

Figure 4-4 Air void percentage vs. Total ESALs value

4.1.2 Core Data Set 2

Field visits were conducted in four different counties across Minnesota under the scope of the current study. As shown in Figure 4-6, field core samples were collected on LVRs from the wheel path in Koochiching County, Pope County, Beltrami County, and Saint-Louis County. Figure 4-7 shows a photograph of the core collection on CR-18 in Pope County. Figure 4-8 and Figure 4-9 show photographs of the typical cores, showing the top and bottom surfaces of the cores, respectively. All the cores were collected using a 6-inch core drill bit.

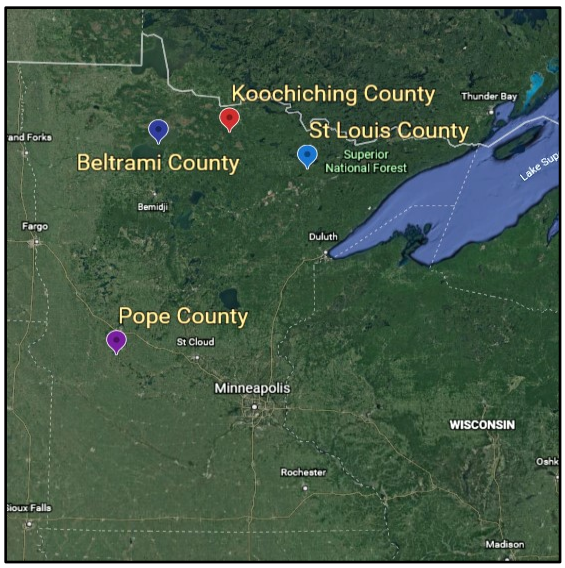

Figure 4-5 Core collection sites in Minnesota

Figure 4-6 A photograph of core collection in Pope County

Figure 4-7 Top surface of field cores

Figure 4-8 Bottom surface of field cores

4.1.2.1 Project Locations

In Beltrami County, cores were collected from the Bemidji area, where the county office is located. Four different CSAH sections were considered in this county: CSAH 8, CSAH 4, CSAH 46, and CR 404. In Koochiching County, cores were collected from Big Falls, International Falls, and Little Fork areas on four different CSAH routes: CSAH30, CSAH 1, CSAH 9, and CSAH 2. In Pope County, cores were collected from four different CSAH sections: CSAH-18 (at two locations), CSAH-16, and CSAH-1. Figure 4-9 through Figure 4-12 show the locations of roads from which cores were collected in Beltrami, Koochiching, and Pope counties. Three to four cores were cut out from each location. In addition to the above, six cores were collected from a newly paved road in St. Louis County. These cores were not extracted by the research team but provided by the St. Louis County lab.

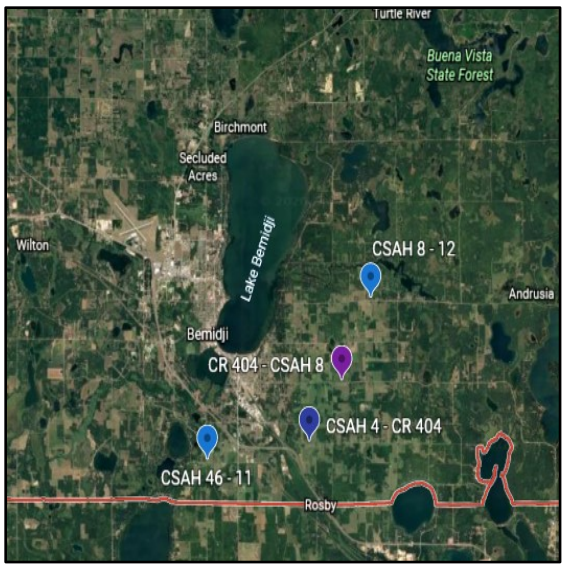

Figure 4-9 Location of core collection sites in Beltrami County

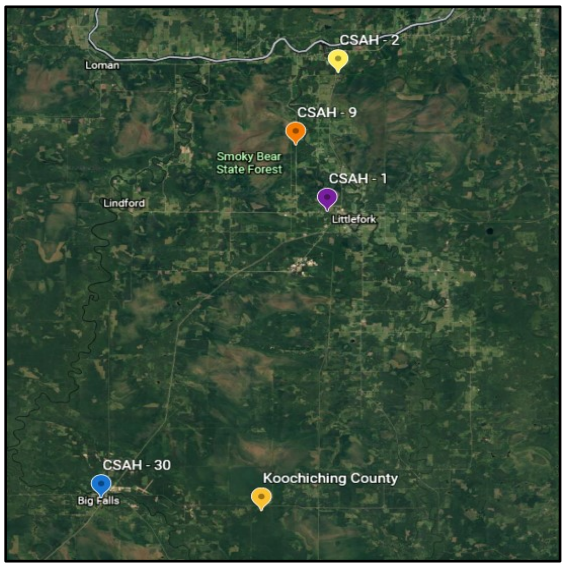

Figure 4-10 Location of core collection sites in Koochiching County

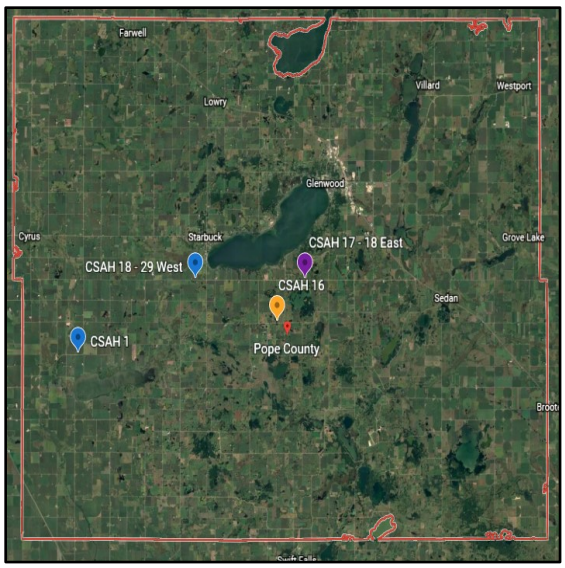

Figure 4-11 Location of core collection sites in Pope County

4.1.2.2 Volumetric Properties and Density of cores

The volumetric parameters such as G_{mb}, G_{mm}, and density have been calculated for all the cores. Asphalt Institute's method was followed to determine the G_{mm}. For this purpose, the specific binder type used in different locations was determined (PG 58-28 and PG 58-34). Two cores were selected at random from each location and heated to the normal mixing temperature. One percent binder by the total weight of the mix was added to thoroughly coat all the aggregate particles. Crushed cores visibly found to have sufficient binder coating on all the aggregates were not subjected to this procedure. G_{mm} testing was conducted as usual, and equation (1) was used to determine the final G_{mm} value.

Theoretical Maximum Specific Gravity = A–J / (A+D) – (E+K) (1)

Where, A = mass of the oven-dry sample in air, gm;

B = mass of the container filled with water at 25°C, gm;

E = mass of the container filled with sample and water at 25°C, gm;

J = mass of the added asphalt binder in air, gm;

K = volume of the added asphalt binder (cc or ml) = J/G_b, where G_b is the specific gravity of the binder.

Table 4.8 through

Table 4.11 present G_{mb} and density values of cores collected from different sections in all four counties. The core densities measured for the projects in this section are plotted together with all the projects discussed in the previous section, as shown in Figure 4-12. Among all the aged core density results, a

few projects in Beltrami, Koochiching, and Pope counties have shown lower densities than others. The average densities of the cores collected from all the aged pavement is 146.81 pcf (standard deviation = 2.66 pcf); whereas the same for the unaged asphalt layers is 145.44 pcf (standard deviation = 1.1 pcf). The difference in the densities between aged and unaged cores is 1.37 pcf. It shall also be noted that this average difference may be misleading as the standard deviations of the densities measured for the cores are quite high. Nevertheless, the moderate difference in the densities between aged and unaged cores indicates that the asphalt layers in the low-volume roads considered do not achieve significant densification.

Table 4.8 G_{mb} and density of cores collected from Beltrami County

Sample #	G_{mb}				Density (pcf)			
	CR 404-CSAH 8	CSAH 8-12	CSAH 4-404	CSAH 46-11	CR 404-CSAH 8	CSAH 8-12	CSAH 4-404	CSAH 46-11
1	2.385	2.295	2.430	2.309	148.82	143.21	151.63	143.71
2	2.374	2.279	2.397	2.308	148.14	142.21	149.57	143.65
3	2.37	2.288	2.435	2.326	147.89	142.77	151.94	144.77
4	2.346	2.284			146.39	142.52		
Ave.	2.369	2.287	2.421	2.314	148.82	143.21	151.63	144.04
Std. Deviation	0.016	0.007	0.021	0.010	1.03	0.42	1.29	0.63

Table 4.9 G_{mb} and density of cores collected from Koochiching County

Sample #	G_{mb}				Density (pcf)			
	CSAH30	CSAH - 2	CSAH - 1	CSAH - 9	CSAH -30	CSAH - 2	CSAH - 1	CSAH - 9
1	2.296	2.383	2.287	2.215	143.2704	148.699	142.709	138.216
2	2.302	2.349	2.299	2.197	143.6448	146.578	143.458	137.0928
3	2.309	2.367	2.302	2.186	144.0816	147.701	143.645	136.406
4		2.36		2.223		147.264		138.715
5	2.315				144.456			
Ave.	2.306	2.365	2.296	2.205	143.863	147.560	143.270	137.608
Std. Deviation	0.008	0.014	0.008	0.017	0.52	0.89	0.50	1.05

Table 4.10 G_{mb} and density of cores collected from Pope County

Sample #	G_{mb}				Density (pcf)			
	CSAH-18	CSAH 18	CSAH 16	CSAH 1	CSAH-18	CSAH 18	CSAH 16	CSAH 1
1	2.39	2.37	2.374	2.337	149.14	147.89	148.14	145.83
2	2.374	2.365	2.382	2.345	148.14	147.58	148.64	146.33
3	2.382	2.363		2.361	148.64	147.45		147.33
4		2.371				147.95		
5		2.387				148.95		
Ave.	2.382	2.371	2.378	2.348	148.64	147.96	148.39	146.49
Std. Deviation	0.008	0.009	0.006	0.012	0.50	0.59	0.35	0.76

Table 4.11 G_{mb} and density of cores collected from St. Louis County

Sample #	G_{mb}	Density (pcf)
1	2.366	147.6384
2	2.381	148.5744
3	2.412	150.5088
4	2.363	147.4512
5	2.348	146.5152
6	2.383	148.6992
Ave.	2.376	148.231
Std. Deviation	0.022	1.373

Table 4.12 shows the air void percentage values calculated for cores using the Asphalt Institute method explained earlier. Figure 4-13 provides a comparison of air void percentage values from 10 counties in Minnesota (both Core Data Set 1 and Core Data Set 2). The average air voids and standard deviation for unaged and aged cores are 6.3% (standard deviation = 0.44%) and 5.6% (standard deviation = 1.92%), respectively. It is observed from the plot that although there is a decrease in the average air void percentage from unaged to aged cores, the difference is not significant. Some air void percentage values for the road sections in Koochiching and Beltrami counties were found to be very high. The exact reason for this is unknown; it is suspected that the asphalt layer might have lost some materials because of very high traffic or distresses. For example, in Beltrami County, it was noticed that the daily traffic on CSAH 8-12 (around 4000) was almost 67 times higher than CSAH 4 – 404 (around 60) (Traffic Mapping Application, MnDOT). CSAH 8-12 has 9.35% air voids in comparison to an average of 3.2% air voids on CSAH 4 – 404. This observation may seem surprising and contrary to the air voids percentage vs. ESALs relationship discussed previously, but excessive traffic and distresses can lead to material loss as well.

Table 4.12 Air void percentage value for different counties

Beltrami County			
CR 404 - CSAH 8	CSAH - 8 - 12	CSAH - 4 - 404	CSAH 46-11
4.3	9.4	2.5	6.7
3.4	9.3	4.0	5.4
Koochiching County			
CSAH -30	CSAH - 2	CSAH - 9	
6.0	6.9	9.4	
7.6	8.0	10.0	
6.9			
Pope County			
CSAH 18 (Good road)	CSAH 18	CSAH 16	CSAH 1
5.6	4.4	4.2	4.2
2.7	5.0	4.1	--

-- outlier

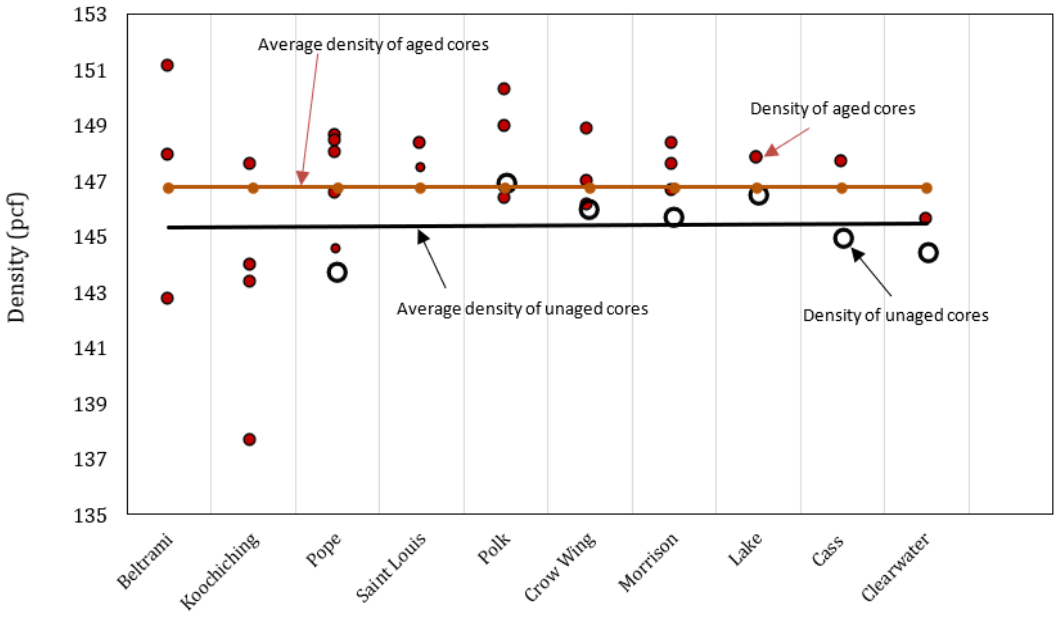

Figure 4-12 Comparison of density of cores from unaged and aged pavement

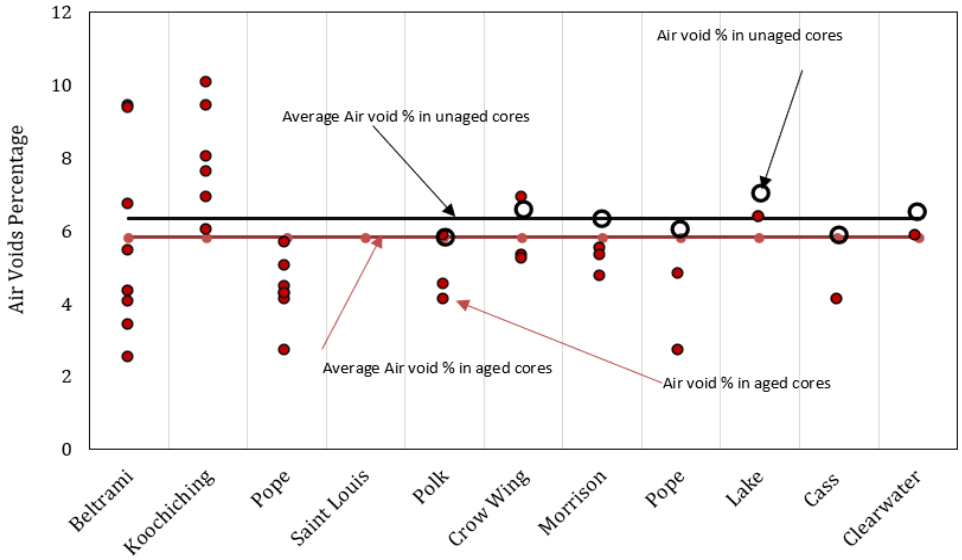

Figure 4-13 Comparison of air void percentage of cores from unaged and aged pavements Low-Temperature Fracture Characterization of Field Cores

4.2 Observed Pavement Distresses

During the core collections in Beltrami, Koochiching, and Pope County, pavement distress surveys were also performed to document key distresses. The most common distresses observed were the transverse cracks, longitudinal cracks, and cracks along the lane joints.

Figure 4-14 shows a photograph of a longitudinal crack found on a low-volume road at Koochiching County. The severity of this type of distress ranges from at least 3-feet long to a crack with significant adjacent random cracks (12 inches or more apart). Figure 4-15 shows a low severity longitudinal joint crack. Figure 4-16 shows transverse cracks in Koochiching County.

Figure 4-14 Medium severity longitudinal cracking in Koochiching County

Figure 4-15 Low severity longitudinal joint cracking

Figure 4-16 Closely spaced transverse cracks on a road in Koochiching County

In addition to the abovementioned three distresses, low severity rutting was noticed on a couple of roads. In one site at CSAH 18 at Pope County, moderate washboarding was observed. Figure 4-17 shows a photograph of rutting observed in CSAH 18 in Pope County.

Figure 4-17 Rutting on CSAH 18 West

Table 4.13, Table 4.14, and Table 4.15 provide the statistics of the distresses observed in the Beltrami, Koochiching, and Pope counties. Transverse cracking is the most dominant distress for all three counties, at least for all the project sites considered in this study. This observation also matches with the findings from the online survey conducted for this project; more than 75% of responders in the online survey stated that the transverse cracking is dominant distress in the low-volume asphalt roads.

Table 4.13 Pavement distresses observed in the low-volume roads of Beltrami County

Pavement Distress	Severity Level	# of Cracks
Transverse Cracking	Low	42
	Medium	6
Longitudinal Cracking	Low	8
	Medium	6
Longitudinal Joint Cracking	Low	19
	Medium	2

Table 4.14 Pavement distresses observed in the low-volume roads of Koochiching County

Pavement Distress	Severity Level	# of Cracks
Transverse Cracking	Low	25
	Medium	22
	High	3
Longitudinal Cracking	Low	15
	Medium	5
	High	1
Longitudinal Joint Cracking	Low	12
	Medium	6

Table 4.15 Pavement distresses observed in the low-volume roads Pope County

Pavement Distress	Severity Level	# of Cracks
Transverse Cracking	Low	9
Longitudinal Cracking	Low	3
Longitudinal Joint Cracking	Low	6

4.3 Summary

This chapter included the volumetric analysis of the cores collected from the low-volume roads of various counties of Minnesota. Two sets of core data were collected. Core data set 1 was collected from the former State-Aid Technician, Mr. Ron Bumann. The research team has gathered the Core data set 2 by collecting cores from four different counties. The volumetric analysis of the cores reveals that the initial air voids of the asphalt layer right after the construction ranges between 5.3 and 7.2%, with an

average value of 6.32%. The air voids slightly decrease with age, but traffic or the ESALs play a considerable role in densifying the asphalt layer. But as the traffic or ESALs is less in the low-volume road, the air voids percentage was not found to decrease close to the design air voids (3 or 4%) or lower.

The field distress survey showed three major distress types in Beltrami, Koochiching, and Pope counties, namely longitudinal cracking, longitudinal joint cracking, and transverse cracking. These cracks are generated due to environmental factors. Transverse cracking was the dominant distress, which is also supported by the online survey conducted in this study as discussed in Chapter 3.

Lastly, it seems that the improvement in mix design for the low-volume roads can be achieved by creating high-density asphalt mixtures, which will result in better fracture energy G_f and eventually decrease the low-temperature thermal cracking or other environmental force driven distresses. The research team thereby focused on investigating the use of Superpave 5 design for the low-volume roads and comparing the fracture toughness of the same with the mixtures produced by the conventional Superpave mix design.

Chapter 5: Experimental Methodology and Test Materials

This chapter discusses the test materials and experimental methodology. In the laboratory study, mechanical properties of asphalt mixes prepared with conventional Superpave design procedure, Superpave-5 design procedure and regressed air voids methods were compared. Different materials were used to create seven mix designs, and performance tests were conducted to determine the fracture resistance, strength, modulus, and moisture sensitivity of the asphalt mixes. State-of-the-art testing techniques were adopted to characterize the performance of laboratory-produced and laboratory-compacted specimens. Figure 5-1 illustrates the experimental approach adopted in this chapter, including the different tests conducted to determine the mechanical performance of the asphalt mixes.

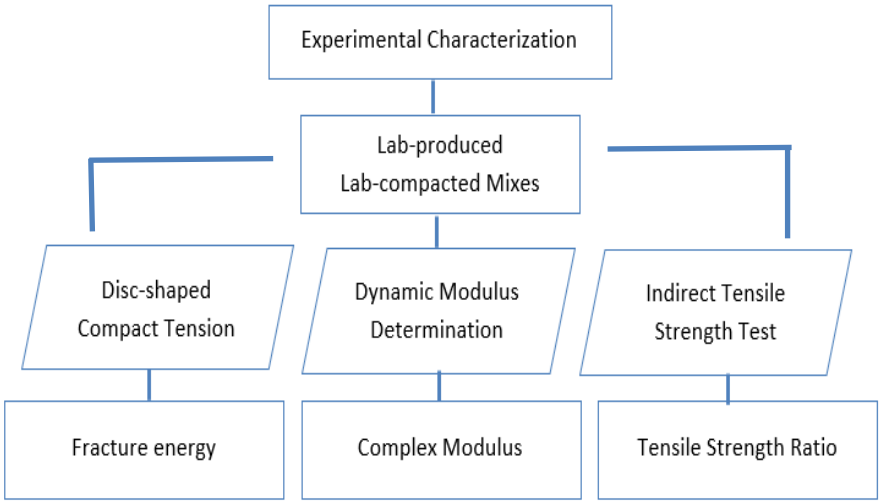

Figure 5-1 Illustration of the experimental methodology adopted in this study

5.1 Materials

5.1.1 Asphalt Binder

PG 58S-28 asphalt binder, which is generally used in the state of Minnesota, was used in this task.

5.1.2 Aggregate

Four different aggregates, i.e., crusher fines, sand, ½" coarse aggregate, and fine RAP, were used in all the mixes except one (4N/40 (A)), in which a fifth aggregate, Taconite Tailing, was also used. Figure 5-2(a) shows photographs of the four different aggregates used in the laboratory investigation. The individual gradation for each of the four aggregate types is shown in Figure 5-2 (b).

(a)

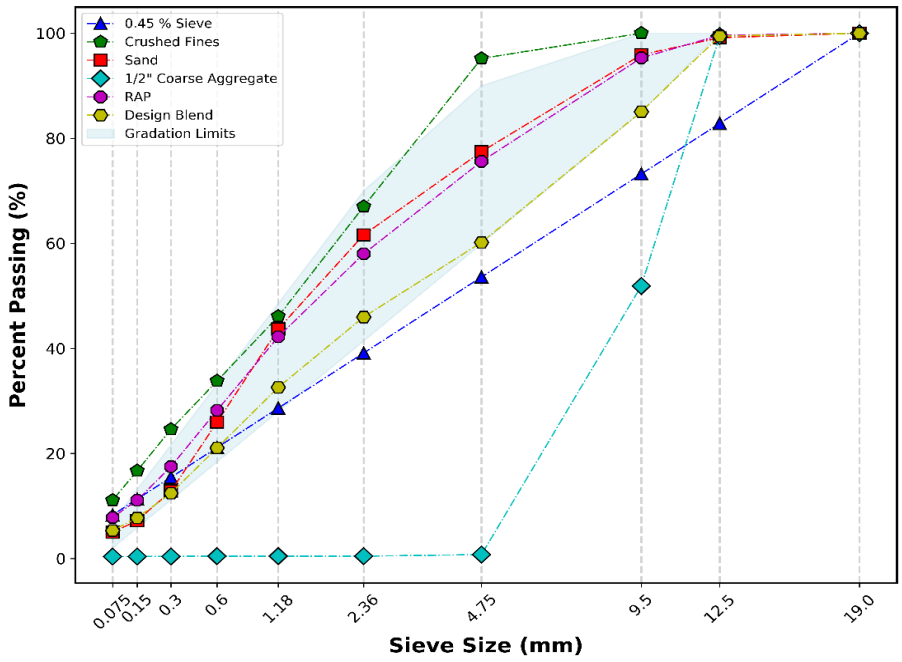

(b)

Figure 5-2 (a)Aggregates used for the mixture, from the left-crushed fines, sand ½" rocks, RAP, and (b) Individual aggregate gradation and Design blend used for preparing the laboratory asphalt mixture

In Minnesota, a minimum of 80% of virgin or added asphalt binder to total binder is recommended for PG58H-34 binder and a minimum of 70% of virgin or new added asphalt binder to total binder is recommended for PG 58S-28 binder type. In this project, 18% ½" RAP collected from Northland Constructors was used for every mix design.

5.1.3 Asphalt Mix Designs

A total of seven mix designs were considered for this laboratory study. The focus was obtaining the target air voids and number of gyrations that will provide an asphalt mix with considerable resistance against environmentally induced distresses. As shown in Figure 5-3, the target air voids, and the number of gyrations were varied among the mixes. The flow chart below shows different mix designations. For example, 4N/40 (A) indicates a mix that is designed with 4% air voids, 40 number of gyrations, and '(A)' represents one of the three trials (A, B, and C) for this specific combination of air void and the number of gyrations. The mix designs presented in Figure 5-3 were correlated in different ways, as shown in Figure 5-4. Aggregate gradations for the different mix designs are provided in Figure 5-5. More detailed aggregate gradation information is provided in Table 5.1.

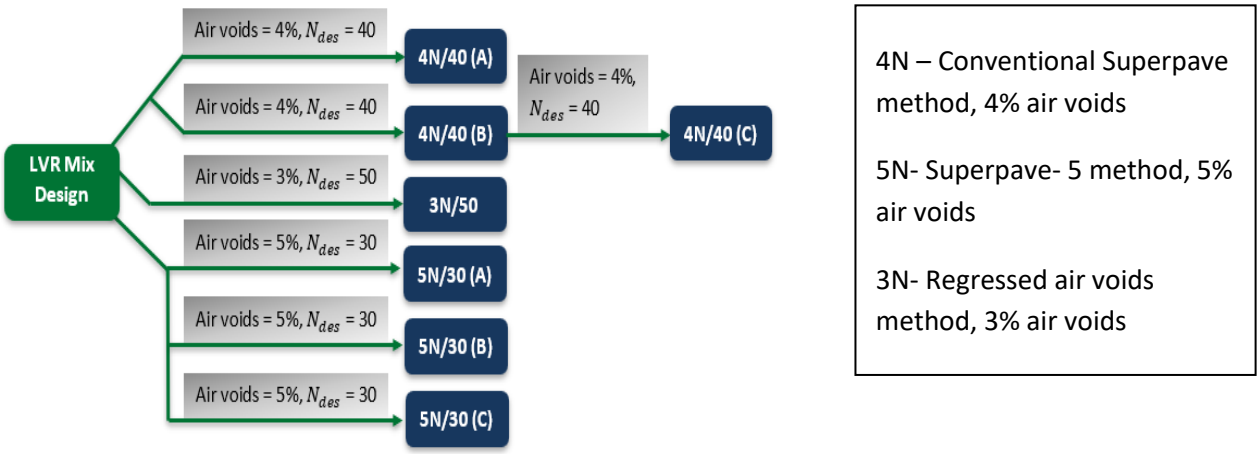

Figure 5-3 Mix designs prepared for the study.

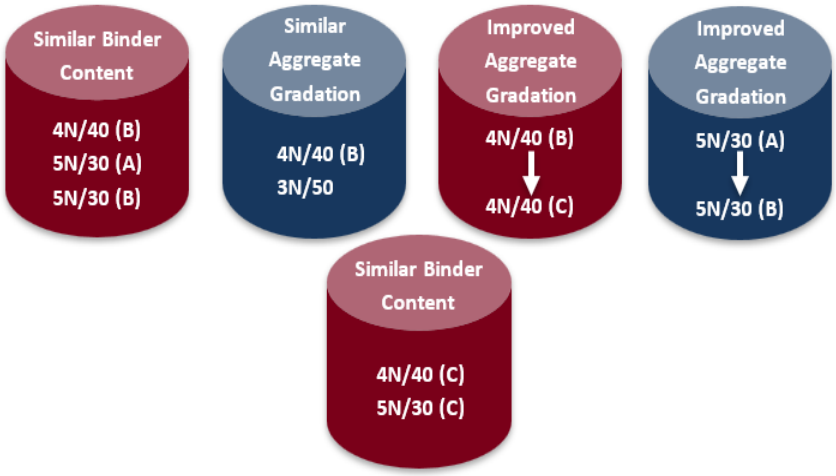

Figure 5-4 Correlation between different mix designs

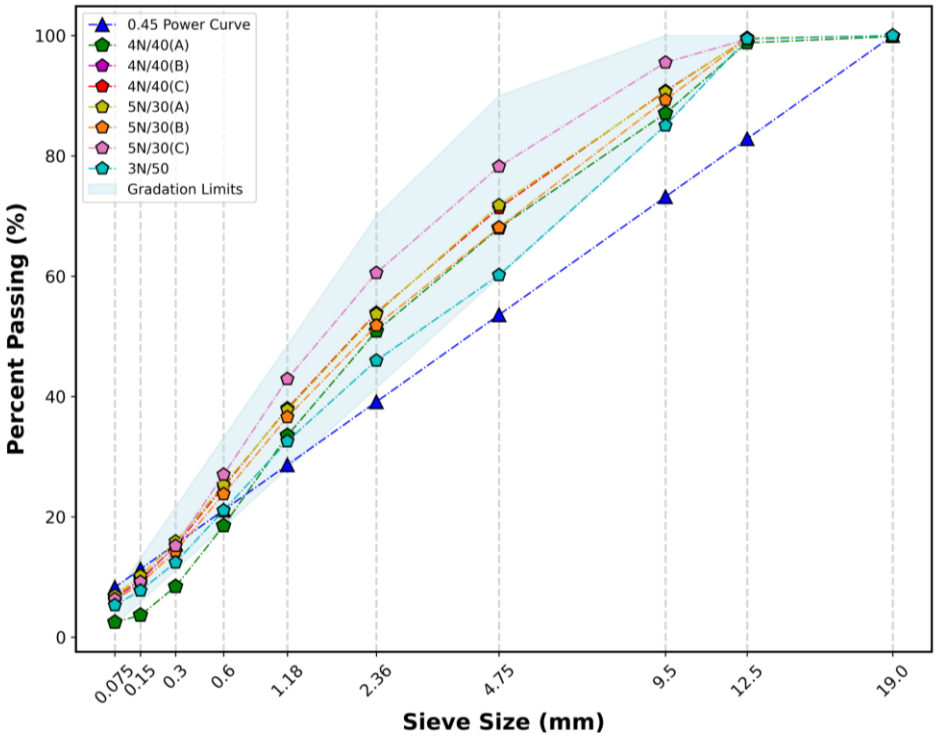

Figure 5-5 Gradations of different mix designs

Table 5.1 Aggregate gradation for different mix designs

Opening (mm)	Percentage Passing (%)						
	4N/40 (A)	4N/40 (B)	4N/40 (C)	5N/30 (A)	5N/30 (B)	5N/30 (C)	3N/50
19	99.8	100	100	100	100	100	100
12.5	98.8	99.5	99.5	99.6	99.5	99.4	99.5
9.5	87.1	85.1	90.8	90.6	89.3	95.5	85.1
4.75	68.0	60.2	71.3	71.8	68.1	78.2	60.2
2.36	50.9	46.0	53.9	53.7	51.8	60.5	46.0
1.18	33.5	32.6	38.0	37.8	36.6	42.9	32.6
0.6	18.5	21.1	25.0	25.3	23.8	27.0	21.1
0.3	8.4	12.4	15.2	15.9	14.3	15.2	12.4
0.15	3.7	7.8	9.6	10.2	8.9	9.2	7.8
0.075	2.5	5.3	6.6	6.9	6.1	6.3	5.3

A comparison of aggregate gradations of 5N/30 Superpave-5 mix designs (5N/30 (A) and 5N/30 (B)) prepared in this study and a 5N/30 mix prepared in Indiana (Marasteanu et al., 2019) is provided in Figure 5-6. The NMAS, design gyrations, and traffic levels considered were similar for all the mixes compared; however, the aggregate types used in Indiana were different from the ones used for this research.

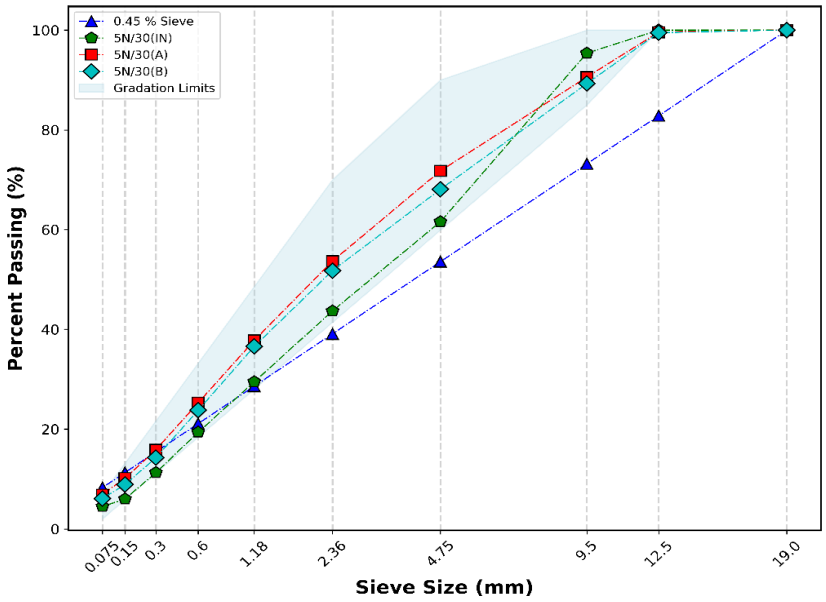

Figure 5-6 Comparison of aggregate gradation for different Superpave-5 mixes

Table 5.2 provides the aggregate percentage and asphalt percentage used for the various mix designs. It should be noted that the mix 4N/40 (A) used Minorca tailings in the mix along with other aggregates used in the rest of the mix designs.

Table 5.2 Composition for different mix designs

Mix Component	4N/40 (A)	4N/40 (B)	4N/40 (C)	5N/30 (A)	5N/30 (B)	5N/30(C)	3N/50
Crusher Fines (%)	15	17	28	35	23	15	17
Sand (%)	36	39	40	32	42	65	39
½”Coarse Aggregate (%)	18	26	14	15	17	2	26
RAP (%)	15	18	18	18	18	18	18
Minorca Tailings (%)	16	0	0	0	0	0	0
Virgin asphalt binder (%)	5.5	5.5	5.0	5.5	5.5	5.0	4.9

Table 5.3 Comparison of volumetric property values for the different mix designs

Parameter	4N/40(A)	4N/40 (B)	4N/40 (C)	5N/30(A)	5N/30 (B)	5N/30(C)	3N/50
Gyration	40	40	40	30	30	30	50
Total Asphalt Content (%)	6.3	6.3	5.8	6.3	6.7	6.3	5.7
Virgin asphalt binder (%)	5.5	5.5	5.0	5.5	5.5	5.0	4.9
Air Voids (%)	3.9	4.2	4.3	5.2	5.1	5.5	3.1
VMA (%)	16.4	15.9	16.0	16.9	16.8	15.9	15.2
VFA (%)	76.3	73.7	73.1	69.2	69.7	65.4	79.5
P_{be} (%)	5.3	5.0	5.0	5.1	5.0	5.0	5.1
AFT	13.8	9.4	9.1	9.4	8.6	9.0	9.6

5.2 Performance Testing Methods

5.2.1 Disc Shaped Compact Tension (DCT) Test

Disc Shaped Compact Tension (DCT) test was conducted to determine the low-temperature fracture energy of asphalt mixes and field cores. The specimen geometry shown in Figure 5-7 allows the compacted asphalt samples or field cores to be tested to determine the mix fracture characteristics. The testing is conducted in accordance with the ASTM standard D7313. A single edge notched sample is loaded in tension at a temperature of -18°C, 10°C warmer than the low-temperature PG grade (-28°C, in this case). The test is run in Crack Mouth Opening Displacement (CMOD) controlled mode, i.e., applied force on a specimen is varied according to the rate of opening of the crack mouth, at a rate of 1mm/min. A Universal Testing Machine, UTM-30 manufactured by IPC Global®, equipped with a 30kN servo-hydraulic labyrinth bearing actuator assembly and a dual-axis control and data acquisition system, was used to run the test. The typical load-CMOD displacement curves for different asphalt mixtures are shown in Figure 5-8.

The thermal cracking resistance of asphalt mixtures can be determined by calculating the fracture energy parameter. The fracture energy of a material is generally defined as the energy required to create a new unit fracture surface in the material. The DCT fracture energy, denoted as G_f, is determined by calculating the work of fracture, W_f, which is the area under the load-CMOD curve. Fracture work is normalized by the fracture surface area to determine the fracture energy as shown in equation (2).

$G_f = W_f / (t \times a)$ (2)

Where, G_f = Fracture Energy (J/m^2).

t = thickness of the specimen (mm); and

a = ligament length (mm).

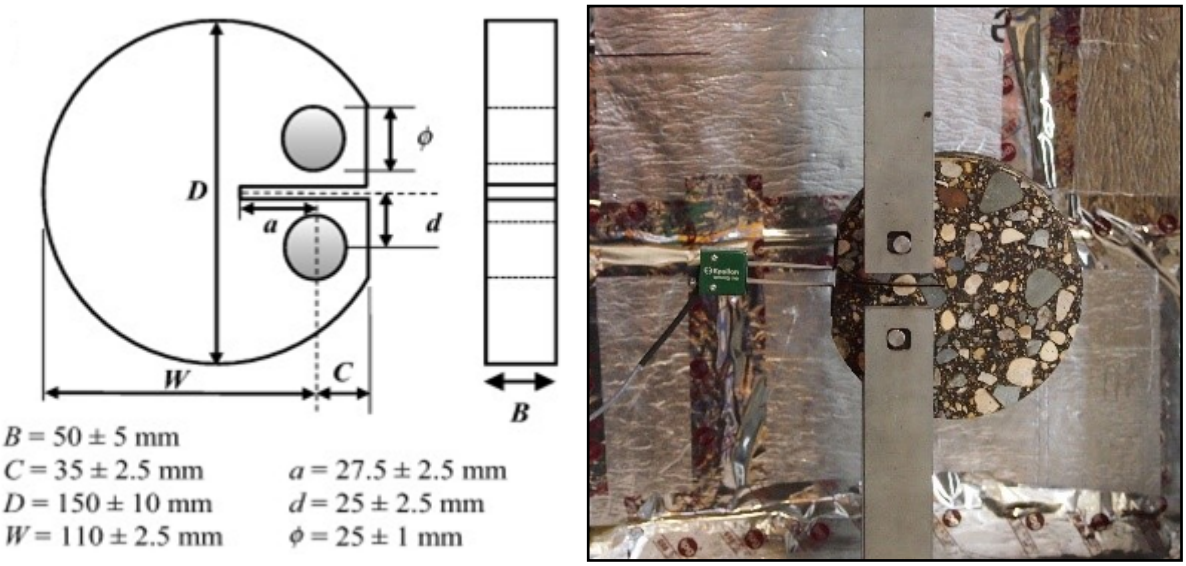

Figure 5-7 DCT specimen geometry and sample installation in UTM-30

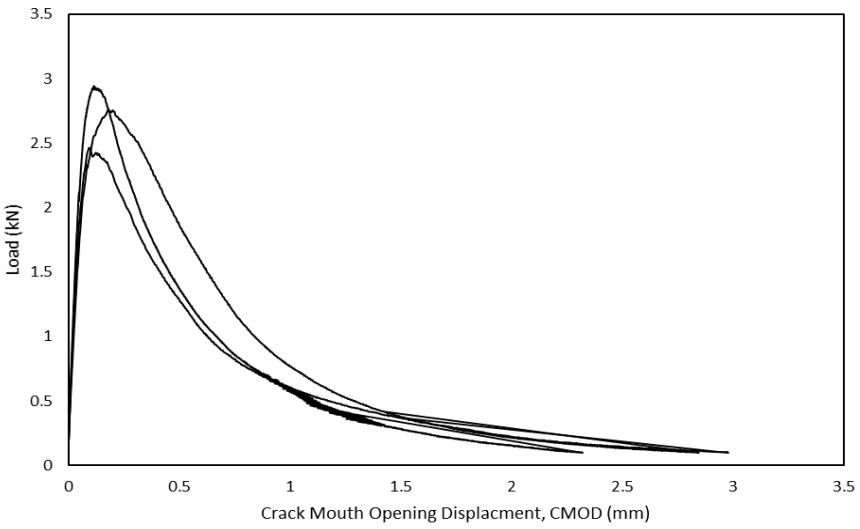

Figure 5-8 Load-CMOD curves for different asphalt mixtures

5.2.1.1 Fracture Energy Indices

Besides fracture energy (G_f), researchers developed other parameters over the years to characterize the fracture performance of asphalt mixes, e.g., Flexibility Index (FI), Toughness Index (TI), Stress intensity factor (SIF), etc. Fracture energy can be normalized with different post-peak slopes to determine the impact of softening behavior of the material in addition to the energy required to develop a crack. Three different post-peak slopes, as shown in Figure 5-9, can be used to calculate normalized fracture energy indices.

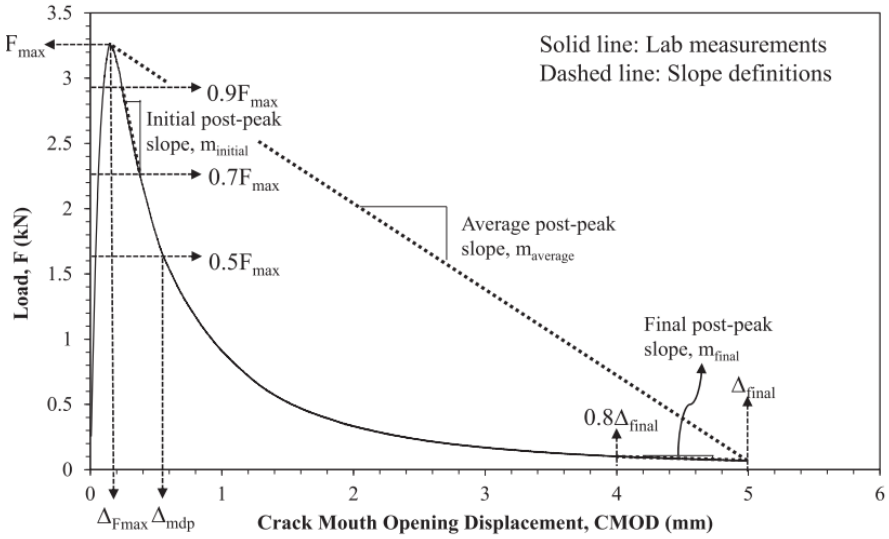

Figure 5-9 Different variables used in the calculation of fracture testing energy indices (Zhu et al.)

If the post-peak slope is denoted by the symbol 'm', the initial post-peak softening slope, the final post-peak slope, and the average post-peak slope can be identified as $m_{initial}$, m_{final}, and $m_{average}$ respectively. The different relationships are explained in Equation 3.

$$\begin{matrix} M_{initial} \\ m_{average} \\ m_{final} \end{matrix} = \left\{ \begin{matrix} \text{average slope between } 0.9F_{max} \text{ and } 0.7F_{max} \\ \text{average post} - \text{peak slope} \\ \text{average slope between } 0.8\Delta_{final} \text{ and } \Delta_{final} \end{matrix} \right\} \quad (3)$$

In Figure 5-9, 70% peak load represents initial crack propagation, and 90% peak load represents the complete formation of a fracture process zone near the tip of the notch. Based on the three slope values given in Equation 3, three normalized fracture energy parameters can be calculated, which are $Gf/m_{initial}$, $Gf/(m_{initial} - m_{final})$ and $Gf/m_{average}$. To characterize the post-peak behavior, Toughness index (TI) can also be calculated using Equation 4.

$$TI = G_f^{Post-peak}(\Delta_{mdp} - \Delta_{Fmax}) \cdot 10^{-3} \quad (4)$$

Where, Δ_{mdp} = displacement corresponding to 50% peak load, Δ_{Fmax} = displacement corresponding to peak load displacement, as shown in Figure 5-9.

Apeagyei et al. (2006) proposed another parameter called Fracture Strength (S_f) based on the Stress Intensity Factor (SIF) defined in the ASTM E399 standard. S_f can be calculated using the DCT fracture test peak load value and the specimen geometry, as given in Equation 5.

$$S_f = \frac{2F_{max}(3L-a)}{t \times a^2} \quad (5)$$

Where, F_{max} = peak load, L = ligament length, t = thickness, and a = defined in Equation 2.

It may be noted that before performing any calculation on the load vs. CMOD curve, a polynomial pre-smoothing of the curve was done. A summary of the different parameters used for a detailed analysis of DCT results is given in Table 5.4.

Table 5.4 Different parameters used for DCT analysis

Fracture Parameter		Symbol	Physical Interpretation
Energy Indices	Fracture Energy	G_f	Energy needed to create a new unit fractured surface
	Pre-peak Facture Energy	$G_f^{Pre-peak}$	Energy needed in the pre-peak region to initiate crack
	Post-peak Fracture Energy	$G_f^{Post-peak}$	Energy needed in the post-peak region to propagate crack
Fracture Strength		S_f	Indicator of peak load required to induce fracture
Normalized Fracture Energy Indices	Initial Post-peak Slope Flexibility Index	$G_f/m_{initial}$	Represents initial material softening. $m_{initial}$ corresponds to the upper asymptote of the load-CMOD softening curve
Normalized Fracture Energy Indices	Average Post-peak Slope Flexibility Index	$G_f/m_{average}$	$m_{average}$ is the average of the tangent post-peak slopes at every point

	Flexibility index using the initial and final slope values	$G_f / m_{initial} - m_{final}$	m_{final} is the average post-peak slope in the 20% CMOD at the tail-end
	Toughness Index	TI	Normalized post-peak fracture energy

5.2.1.2 Freeze-Thaw Testing

A set of three samples for each mix were subjected to a freeze-thaw cycle to determine the Fracture Energy Ratio (FER). Apeagyei et al. (2006) followed a similar approach to study the resistance of asphalt mixes against thermal cracking. This practice was followed to better replicate the impact of low-temperature freezing and subsequent thawing of asphalt mixes in the Minnesota-like weather. The FER was calculated as the ratio of fracture strengths of wet to dry test samples.

ASTM D4867 standard was adopted to induce a freeze-thaw phenomenon in compacted specimens. Three samples were saturated within 60-80% by applying a partial vacuum pressure at 25±1°C of about 254 mm (10 in) of mercury. The specimens were then removed from the vacuum chamber, and submerged mass and surface saturated dry mass values were determined to calculate percent saturation. This process was repeated until the desired percent saturation value was reached. After saturation, the sample was wrapped thoroughly with plastic film and placed inside a ziplock bag with 3 ml of distilled water. The bag was then placed in a freezer at -18°C for a minimum of 15 hours. Thereafter, the samples were removed from the freezer and placed in a water bath at 60°C for 24 hours without any covering. After a day, the samples were taken out from the water bath and conditioned at 25±1°C for a period of 1 hour. At the end of the freeze-thaw cycle, the samples were tested as usual in the DCT test set up to determine the fracture resistance of moisture-conditioned specimens.

5.2.2 Indirect Tensile Strength Determination

The Indirect Tensile Strength test (ITS) estimates the potential for cracking in accordance with the ASTM D4867 standard. For this purpose, ten samples were prepared for most mix designs; seven of them were tested dry, and the rest after subjected to one freeze-thaw cycle.

The compacted specimens of 95 mm (3.74 in) height and 150 mm (6 in) diameter were prepared with a target air void content of 7+0.5% air voids for 4N/40 mixes and 5+0.5% for 5N/30 mix design specimens. The samples were then placed in an air bath at 25±1 °C (77 °F) for a minimum of 4 hours. After the conditioning period, the sample was placed between the loading strips such that the strips were centered on the vertical diametrical plane. A displacement-controlled test was performed with a vertical compressive load that was applied with a rate of deformation of 50+5 mm/min (about 2 in/min). Photographs of an ITS sample before and after the test are shown in Figure 5-10.

The ITS strength was determined using Equation 6:

$$S_t = 2000 \times P/(\pi \times t \times D) \quad (6)$$

Where, S_t = ITS Strength (kPa), P = maximum load (N), t = specimen height immediately before the test (mm), and D = specimen diameter (mm).

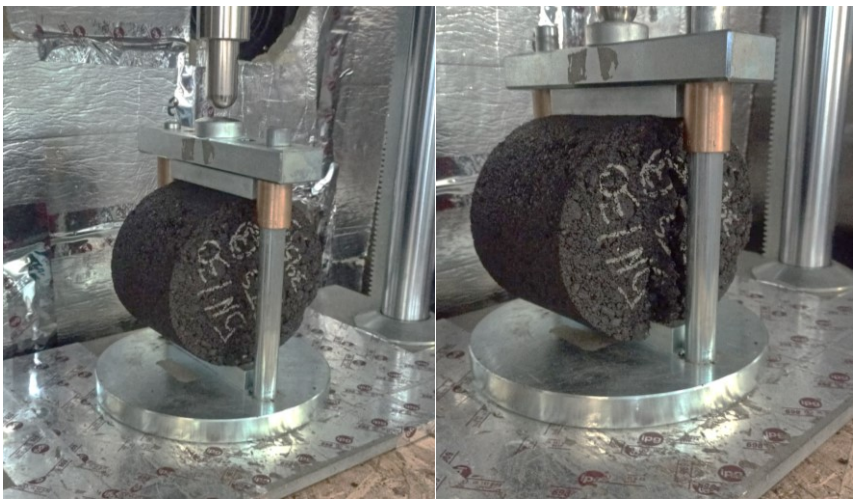

Figure 5-10 Indirect Tensile Strength testing setup

5.2.2.1 Freeze-Thaw Testing

In the case of ITS testing, the Tensile Strength Ratio (TSR) of dry and wet specimens were determined. Three specimens were subjected to moisture conditioning by following the steps mentioned in ASTM D4867.

5.2.3 Dynamic Modulus and Master Curve

The dynamic modulus test was conducted on the UTM-30 equipment in accordance with the standard AASHTO T 378-17; sinusoidal (haversine) compressive loading was applied at different frequencies on the sample at a fixed temperature. During the test, applied stresses and strains were measured with respect to time to calculate the dynamic modulus and phase angle values. To ensure a non-destructive test procedure, the tests were run with an increasing temperature and decreasing frequency.

The Superpave gyratory compactor was used to produce asphalt mix specimens that were 165.1 mm (6.5 in) long with a diameter of 150 mm (6 in). After compaction, the samples were cored to a diameter of 101.6 mm (4 in) and cut on both ends to obtain a smooth surface. The air void percent was maintained at 7+0.5% air voids (5+0.5% for 5N/30 mix design specimens). Three to four replicates were tested for each mix design. To measure axial displacement during testing, three axial LVDTs were mounted 120° apart on hexagonal studs with a gauge length of 75 mm that were glued to the sides of the test sample with the help of vacuum pressure in a gauge point fixing jig. Greased double-latex end-friction reducers sheets were also used before starting the test.

The samples were tested at four different temperatures and frequencies as shown in Table 5.5. An extra frequency of 0.01 was used at a higher temperature to ensure broader coverage of the master curve. During testing, the average micro strain was dynamically controlled to be within a value of 75 to 125 μm/m, as mentioned in the standard.

Table 5.5 Test parameters for determining the Dynamic Modulus

Test Temperature °C (°F)	Test Frequency (Hz)
-10 (14)	0.1, 1, 10
4 (39.2)	0.1, 1, 10
20 (68)	0.1, 1, 10
35 (95)	0.01, 0.1, 1, 10

It has been noticed that as the loading frequency increases, the loading becomes more instantaneous, and the material becomes stiffer and vice versa for low-frequency values. As a result, higher frequency corresponds to a low-temperature asphalt behavior, and low-frequency displays the performance at high temperature. Based on the results obtained from the dynamic modulus testing, master curves were developed in accordance with the Time-Temperature Superposition Principle (TTSP), wherein the modulus vs. frequency curves at every temperature was shifted to a reference temperature (20 °C). The shifting of individual curves to a single curve was performed by changing the test frequencies to reduced frequency values using a shift factor, α_T. A common relationship between shift factors and temperature is given by the William-Landel-Ferry Equation 7.

$$\alpha_T = -C_1 (T - T_0)/(C_2 + (T - T_0)) \quad (7)$$

Where, T_0 = reference temperature, T = input temperature, and C_1 and C_2 = equation constants.

On a log-log scale, the single master curve resembles a sigmoid curve which is fitted using the MEPDG sigmoidal model as given in Equation 8.

$$\log(|E^*|) = \delta + \frac{\alpha}{1 + e^{\beta + \gamma (\log f_r)}} \quad (8)$$

Where, $|E^*|$ = Dynamic modulus, $\alpha, \beta, \delta, \gamma$ = fitting constants, and f_r = reduced loading frequency.

Further, to assist in the predictive analysis of the viscoelastic behavior of asphalt, an explicit analytical form of a Generalized Maxwell Model with a Prony or Dirichlet series of decaying exponentials can be used. The Prony series representation, as given in Equation 9, was fitted to the average modulus data of different replicates in the time domain instead of frequency domain.

$$E(t) = E_\infty + \sum_{i=1}^{n} E_i \, e^{-t/\tau_i} \quad (9)$$

Where, E_∞ = Equilibrium modulus, E_i = relaxation modulus, and τ_i = relaxation times.

5.3 Summary

Chapter 5 gave a detailed description of the different mix types considered in this study. Information about the aggregate gradation, binder type, and other volumetric properties was provided. Three different test methods conducted to evaluate the mix performance were also explained, and an account of different parameters calculated for data post-processing was given.

Chapter 6: Performance Test Results

Seven different mixes with three target air void contents of 3%, 4%, and 5% with design gyrations of 50, 40, and 30 gyrations, respectively, were designed and test samples were prepared. The 3N/50 mix represented a reduced/regressed air voids mix design, 4N/40 represented conventional Superpave mix with 4% air voids, and 5N/30 mix represented a high-density asphalt, Superpave-5 mix design. In this chapter, results from the performance tests are first presented. Then a comparison of all the test results (DCT, ITS and DM tests) between the different lab produced mixes are presented. This chapter also included the DCT test results of the field cores collected from four counties as discussed in Chapter 4.

6.1 Case I: Coventional Superpave mixes, Target Air Voids = 4%, Design Gyrations = 40 OR 4N/40 Asphalt Mix

Three different asphalt mix designs were prepared with 4% design air voids. Using the same asphalt binder type (PG 58S-28) and 40 number of gyrations, three mix designs were produced varying the aggregate gradation and asphalt binder content. The performance test results of the three mix designs are presented in the following sections.

6.1.1 4N/40 (A)

A comparison of fracture energy from the DCT tests for the dry and wet tested samples is provided in Figure 6-1. The x-axis denotes the different samples tested in the dry and wet phases.

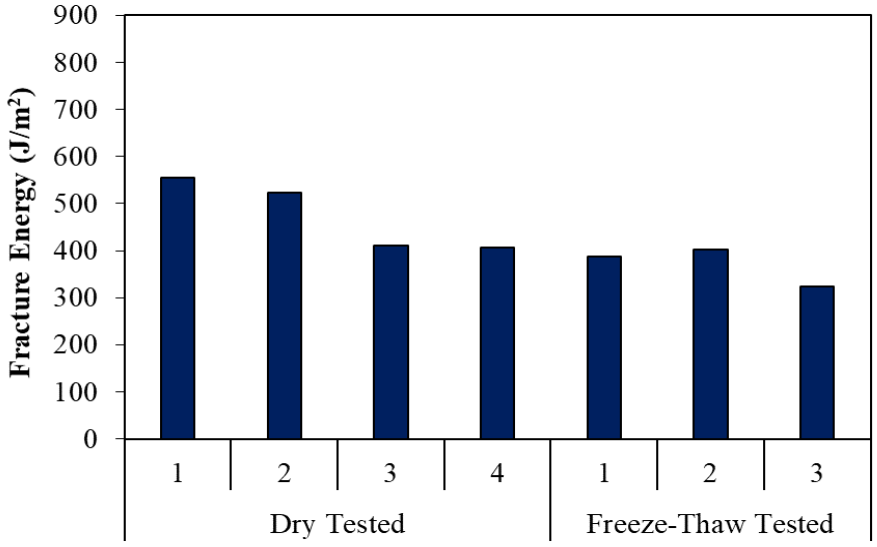

Figure 6-1 DCT test results for 4N/40 (A) asphalt mix

Details of the different fracture energy indices are provided in the individual plot of Figure 6-2 for different replicates of the same mix. The individual plot comparison provides an idea about data

variability and the pre- and post-softening behaviors of a specific mix design. It should be noted that in the $G_f^{Post\text{-}peak}$ vs. Gf plot, red-highlighted data points represent the values for moisture-conditioned specimens. Rest of the plots in Figure 6-2 only present values for the dry test samples. This format is followed for all the similar plots presented for the different mix designs hereafter.

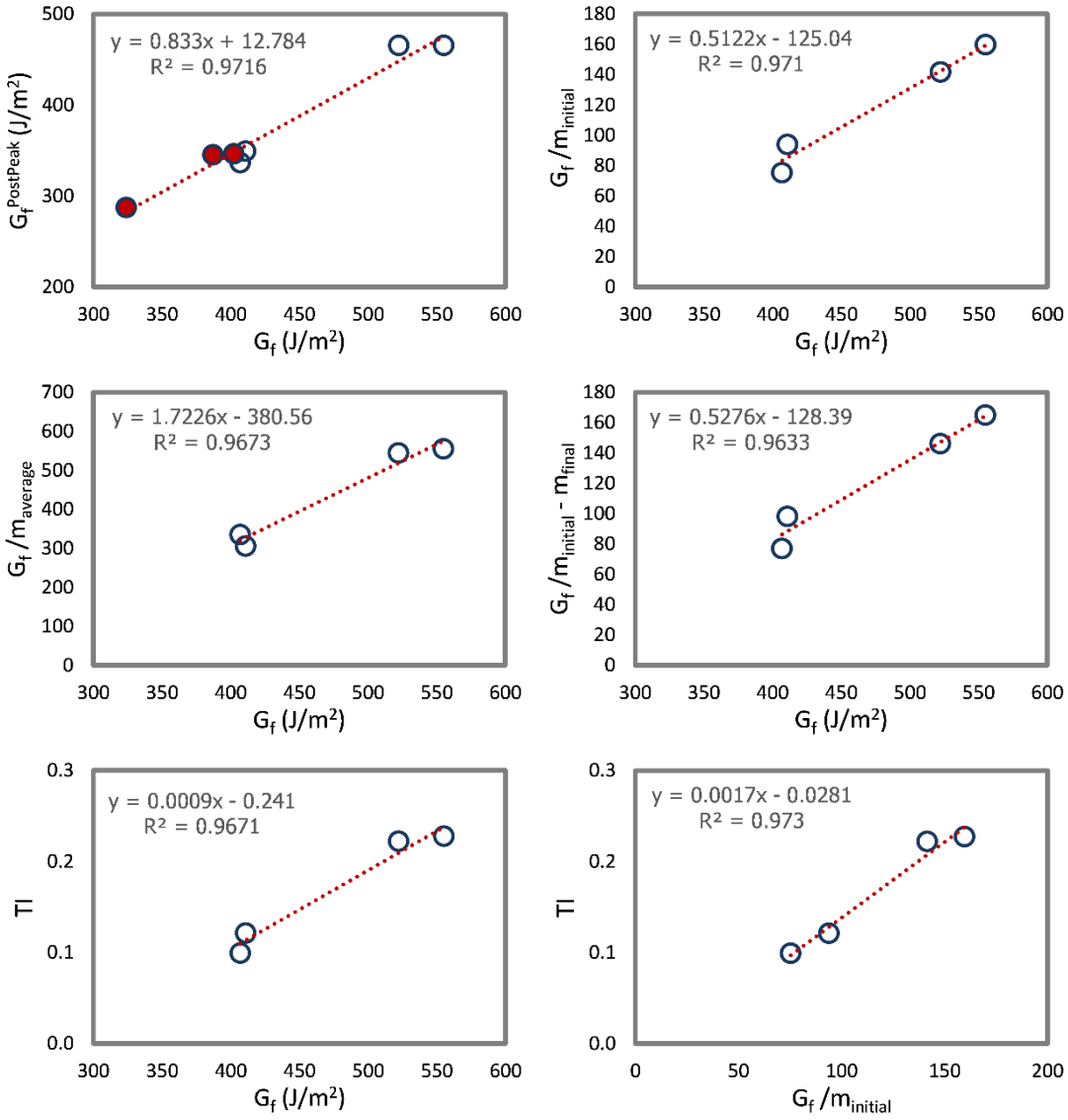

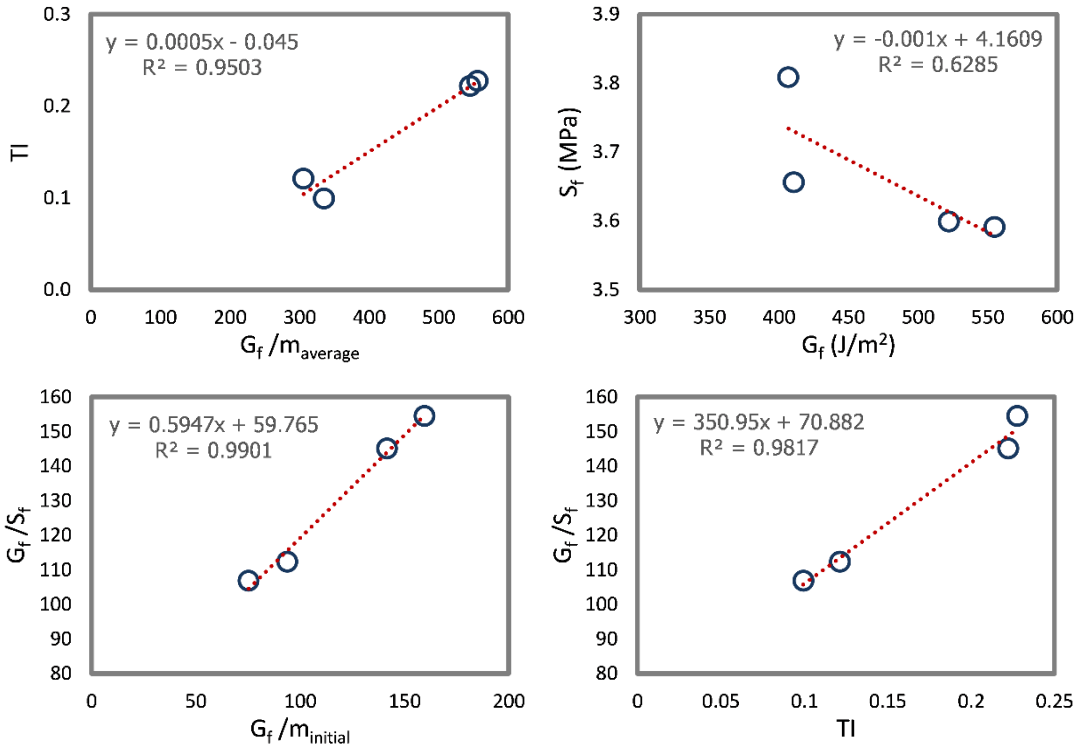

Figure 6-2 DCT fracture energy indices for 4N/40 (A) asphalt mix

It is observed from the figure that various fracture energy parameters show a good fit with the fracture indices and peak-load-related parameters.

Figure 6-3 presents the peak load values from the ITS testing. A comparison of peak load at failure for the dry vs. wet specimens is given.

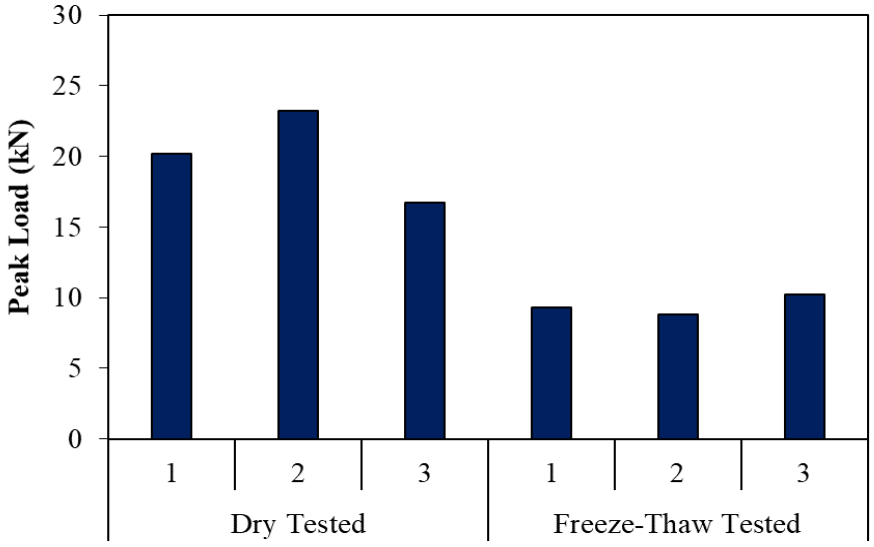

Figure 6-3 ITS test results for 4N/40 (A) asphalt mix

6.1.2 4N/40 (B)

A comparison of fracture energy from the DCT tests for the dry and wet tested samples is provided in Figure 6-4.

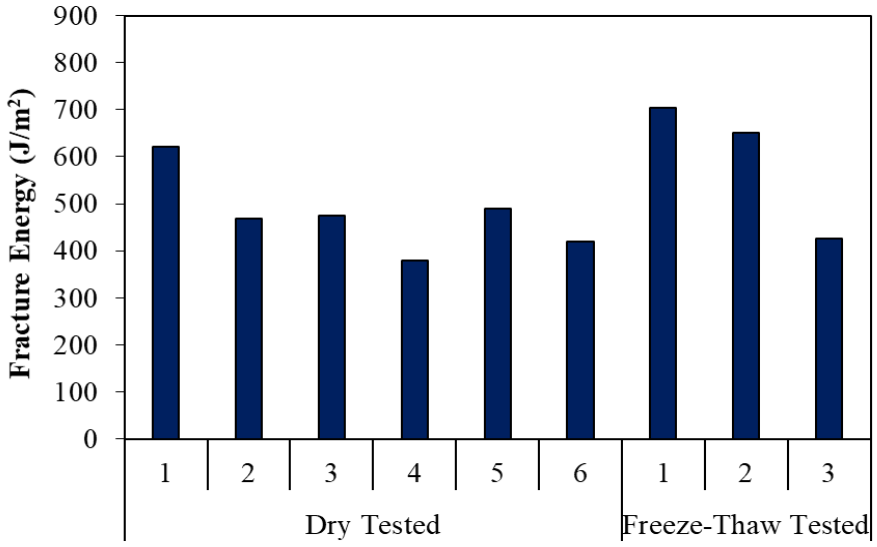

Figure 6-4 DCT test results for 4N/40 (B) asphalt mix

Values for the different fracture energy indices are given in Figure 6-5. Like 4N/40 (A), a good fit among different parameters is observed for the mix 4N/40 (B). However, an unexpected outcome is noticed for the conditioned (or wet) DCT specimens. Two (out of three) conditioned samples show a higher G_f value than the unconditioned (or dry) samples. Regardless, the wet samples had a low peak load at failure value (2.6 kN and 2.9 kN average peak load at failure values for wet and dry samples, respectively). This contrasts with the G_f values for the 4N/40 (A) wet DCT samples, where a comparatively low average G_f than the dry samples is observed. These results imply that 4N/40 (B), which is a denser mix than 4N/40 (A), experienced an increase in strain tolerance but a decrease in peak load carrying capacity after a single cycle of freeze-thaw conditioning. It is stipulated that this outcome was noted because the mix was exposed to a thawed state at 60°C for 24 hours after freezing. While the freezing has an impact on the peak load strength of the sample, the overall crack resistance in the form of sample toughness improved due to the thawing of samples made with a softer binder.

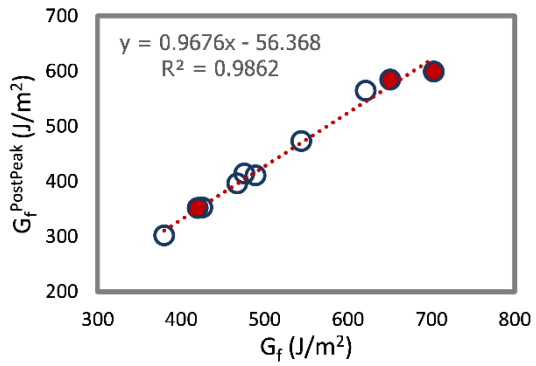
y = 0.9676x - 56.368
R² = 0.9862
$G_f^{PostPeak}$ (J/m²)
G_f (J/m²)

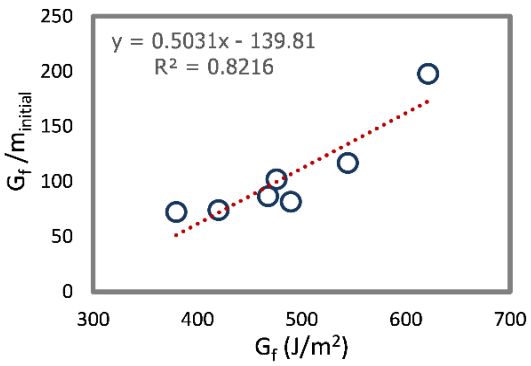
y = 0.5031x - 139.81
R² = 0.8216
$G_f/m_{initial}$
G_f (J/m²)

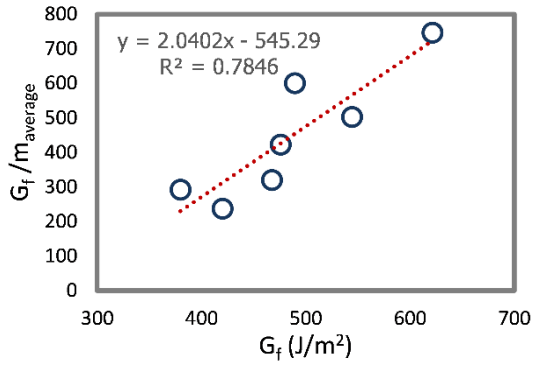
y = 2.0402x - 545.29
R² = 0.7846
$G_f/m_{average}$
G_f (J/m²)

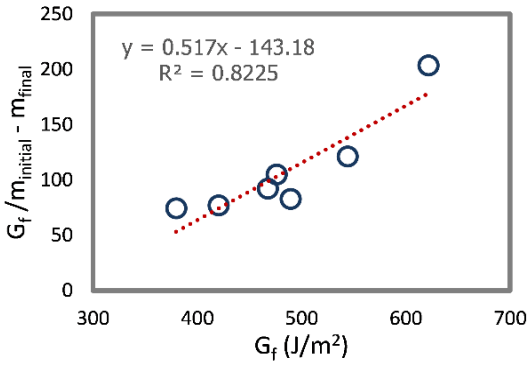
y = 0.517x - 143.18
R² = 0.8225
$G_f/m_{initial} - m_{final}$
G_f (J/m²)

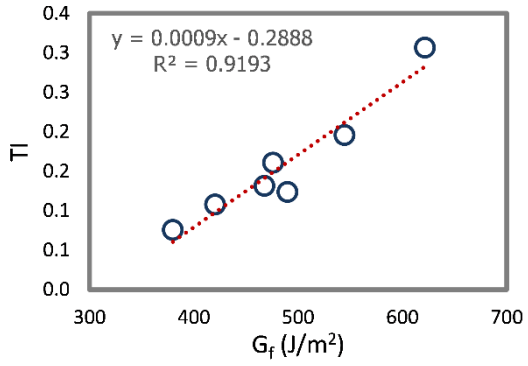
y = 0.0009x - 0.2888
R² = 0.9193
TI
G_f (J/m²)

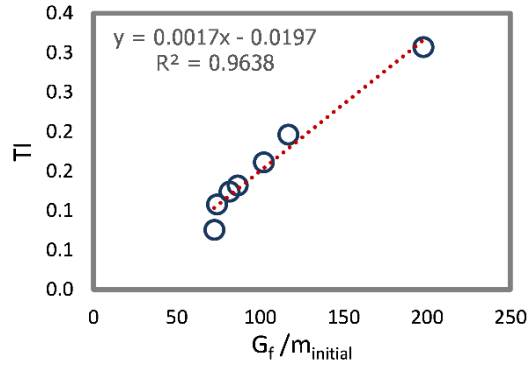
y = 0.0017x - 0.0197
R² = 0.9638
TI
$G_f/m_{initial}$

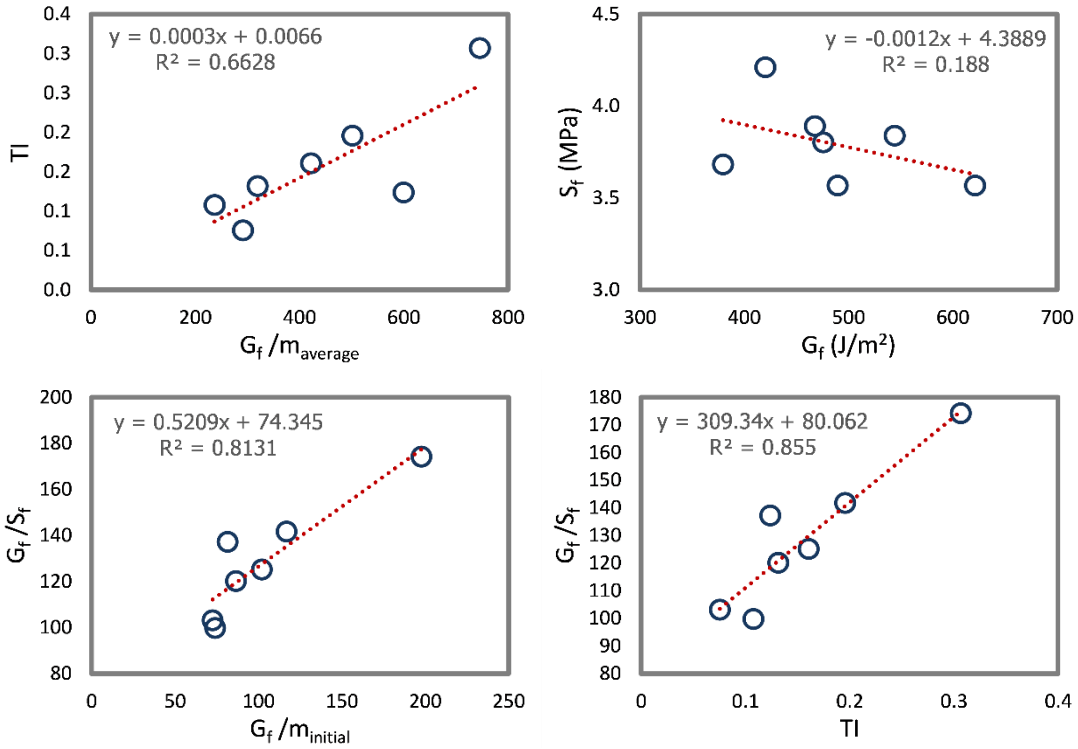

Figure 6-5 DCT fracture energy indices for 4N/40 (B) asphalt mix

Figure 6-6 provides the peak load at failure values for the 4N/40 (B) mix design from the ITS testing.

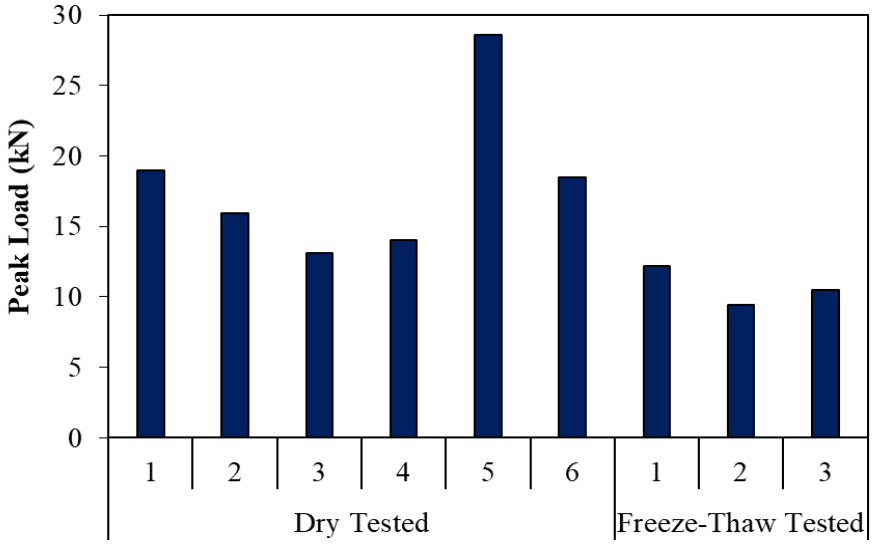

Figure 6-6 ITS test results for 4N/40 (B) asphalt mix

6.1.3 4N/40 (C)

The comparison of fracture energy of the DCT test samples is provided in Figure 6-7. Only four samples were selected for the evaluation of the 4N/40 (C) mix, as few samples were rejected because of erroneous results. Values for the different fracture energy indices are given in Figure 6-8. Figure 6-9 provides the peak load at failure values for the 4N/40 (C) mix design from the ITS testing.

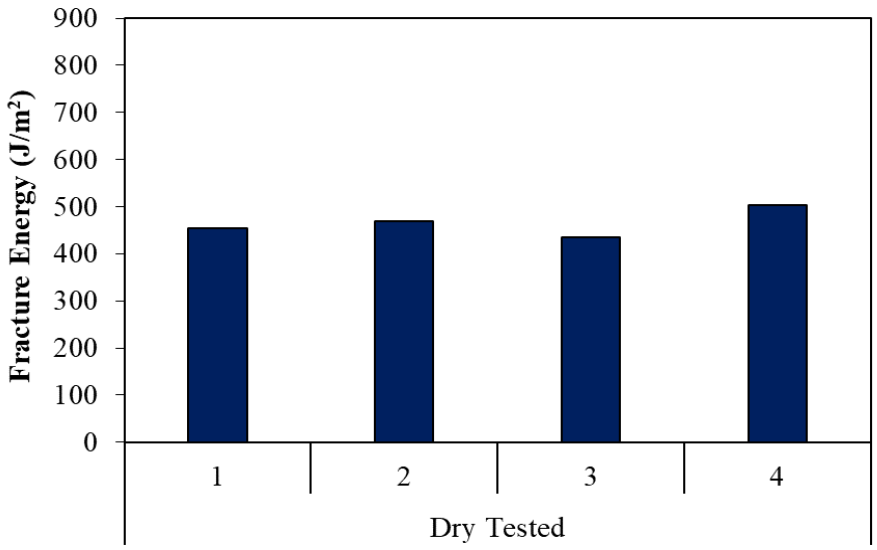

Figure 6-7 DCT test results for 4N/40 (C) asphalt mix

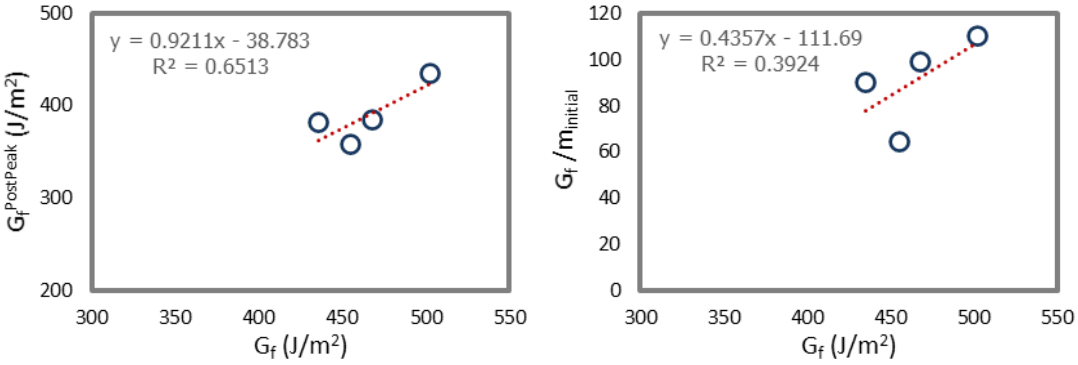

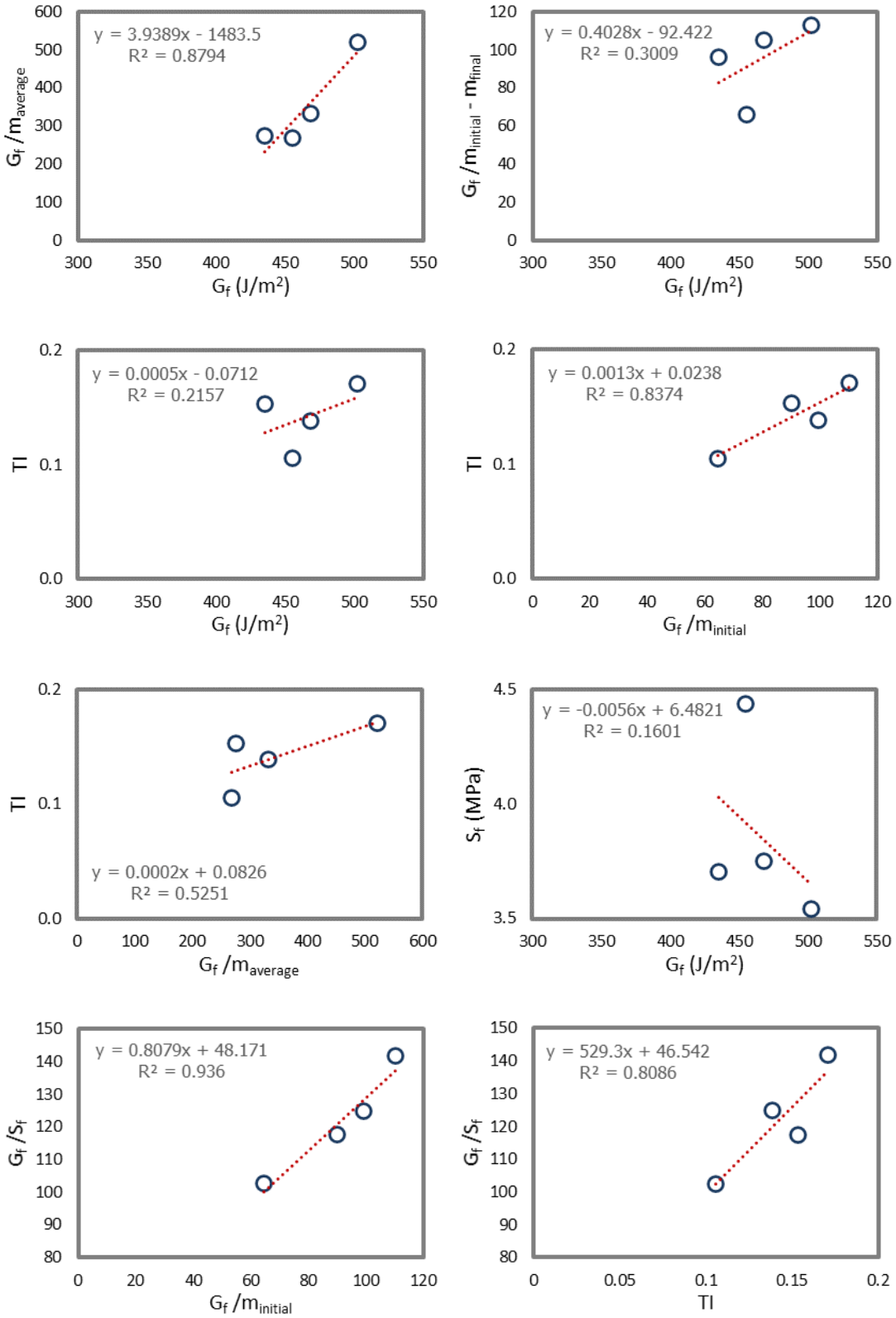

Figure 6-8 DCT fracture energy indices for 4N/40 (C) asphalt mix

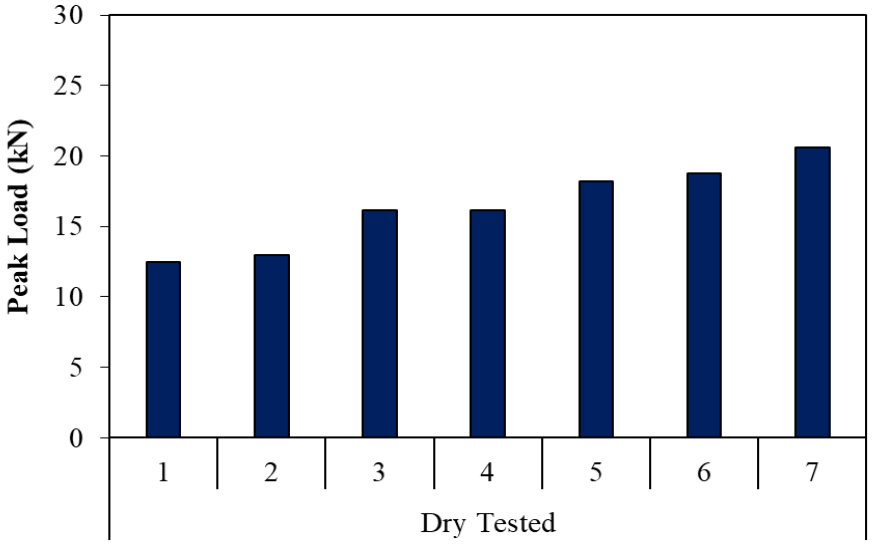

Figure 6-9 ITS test results for 4N/40 (C) asphalt mix

6.2 Case II: Regressed Air Voids Mix, Target Air Voids = 3%, Design Gyrations = 50 OR 3n/50 Asphalt Mix

6.2.1 3N/50

The comparison of fracture energy of the DCT test samples is provided in Figure 6-10. Values for the different fracture energy indices are given in Figure 6-11. In comparison to the 4N/40 mixes, the regressed air void mix showed an opposite pattern for the variation of S_f with respect to G_f. For different replicates of the same mix, a higher fracture energy indicated a higher S_f value. It may be noted that this mix had the same aggregate gradation as 4N/40 mixes, but higher binder content and lower design air voids. This mix showed a brittle performance, resulting in higher peak loads, but lower fracture energy values in comparison to the 4N/40 mix. Figure 6-12 provides the peak load at failure values for the 3N/50 mix design from the ITS testing.

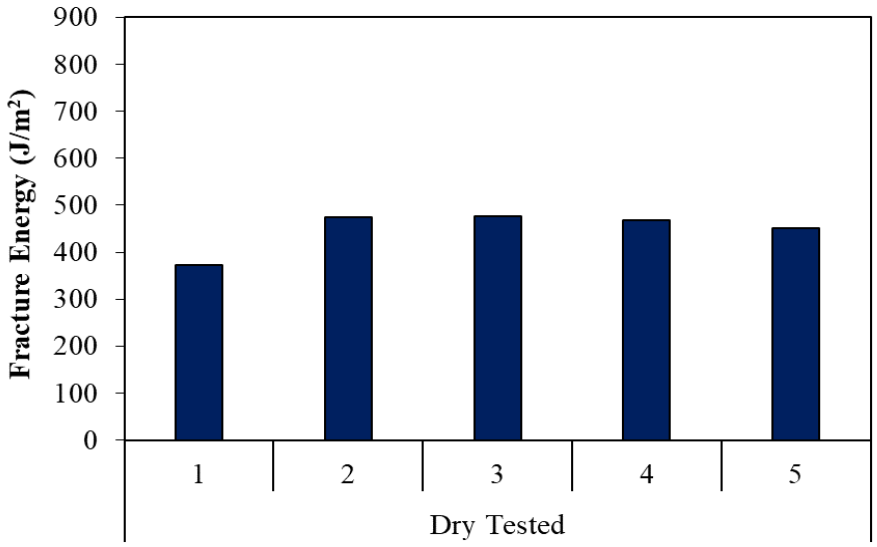

Figure 6-10 DCT test results for 3N/50 asphalt mix

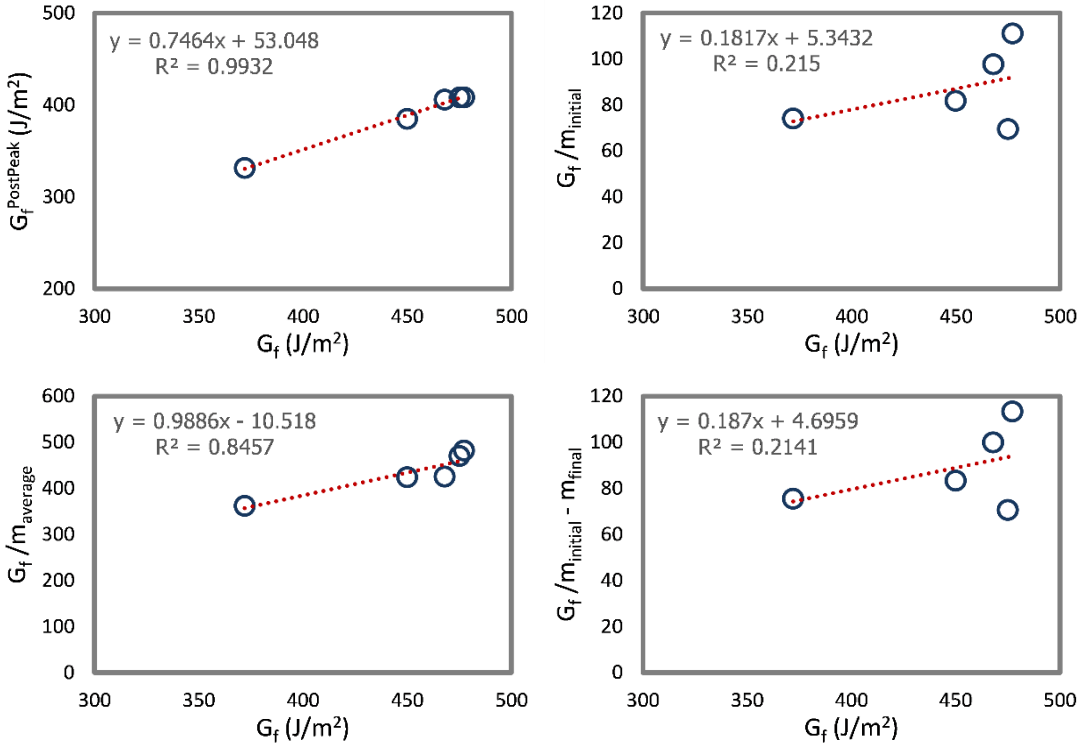

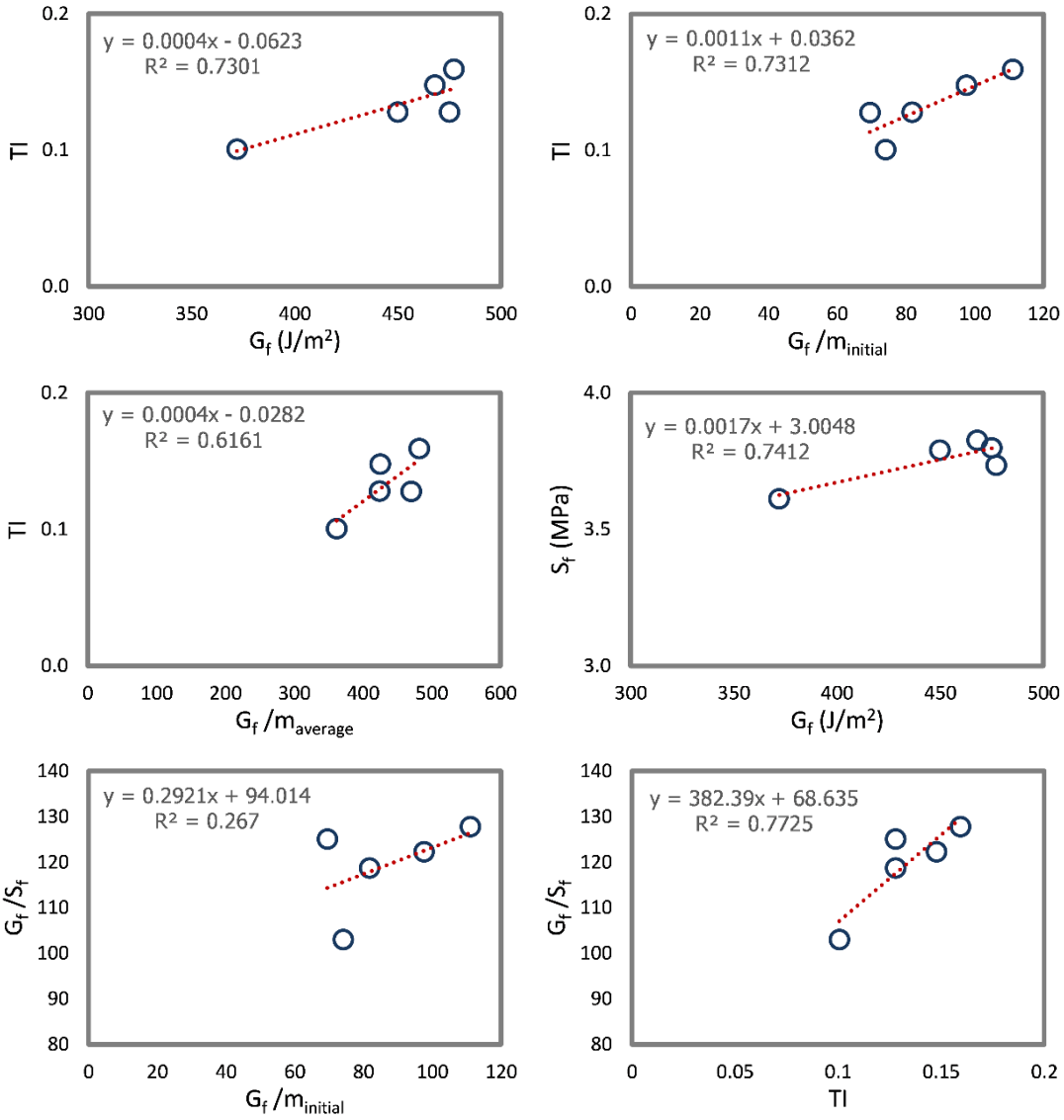

Figure 6-11 DCT fracture energy indices for 3N/50 asphalt mix

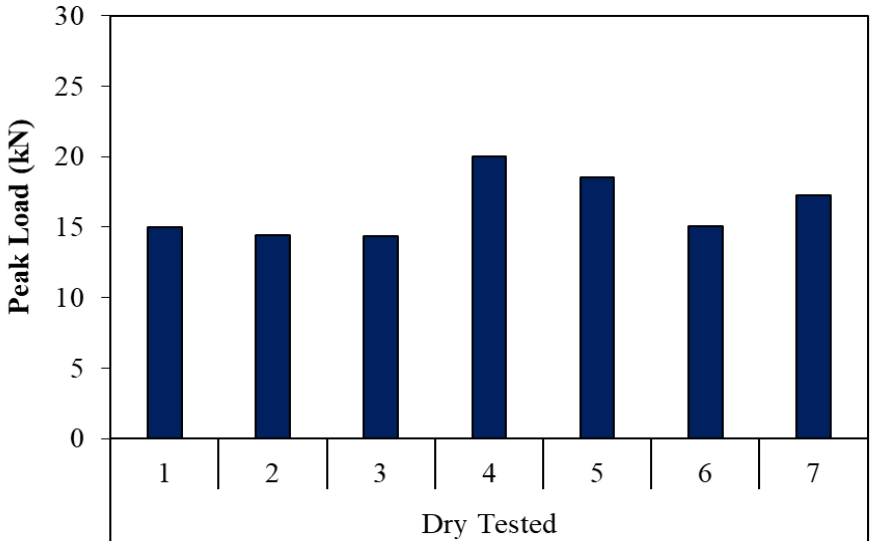

Figure 6-12 ITS test results for 3N/50 asphalt mix

6.3 Case III: Superpave-5 mixes, Target Air Voids = 5%, Design Gyrations = 30 OR 5n/30 Asphalt Mix

6.3.1 5N/30 (A)

A comparison of fracture energy from the DCT tests for the dry and wet tested samples is provided in Figure 6-13. Values for the different fracture energy indices are given in Figure 6-14. It should be noted that one of the data points in the DCT analysis presented in Figure 6-14 had a very high fracture energy value (approx. 1080 J/m^2). However, it is shown in the plots to indicate the measure of variability in test results. Figure 6-15 provides the peak load at failure values for the 5N/30 (A) mix design from the ITS testing.

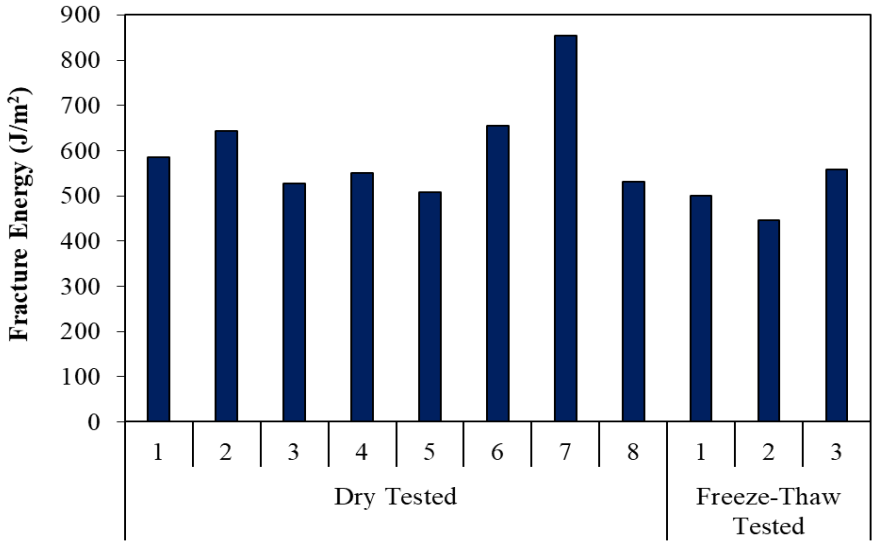

Figure 6-13 DCT test results for 5N/30 (A) asphalt mix

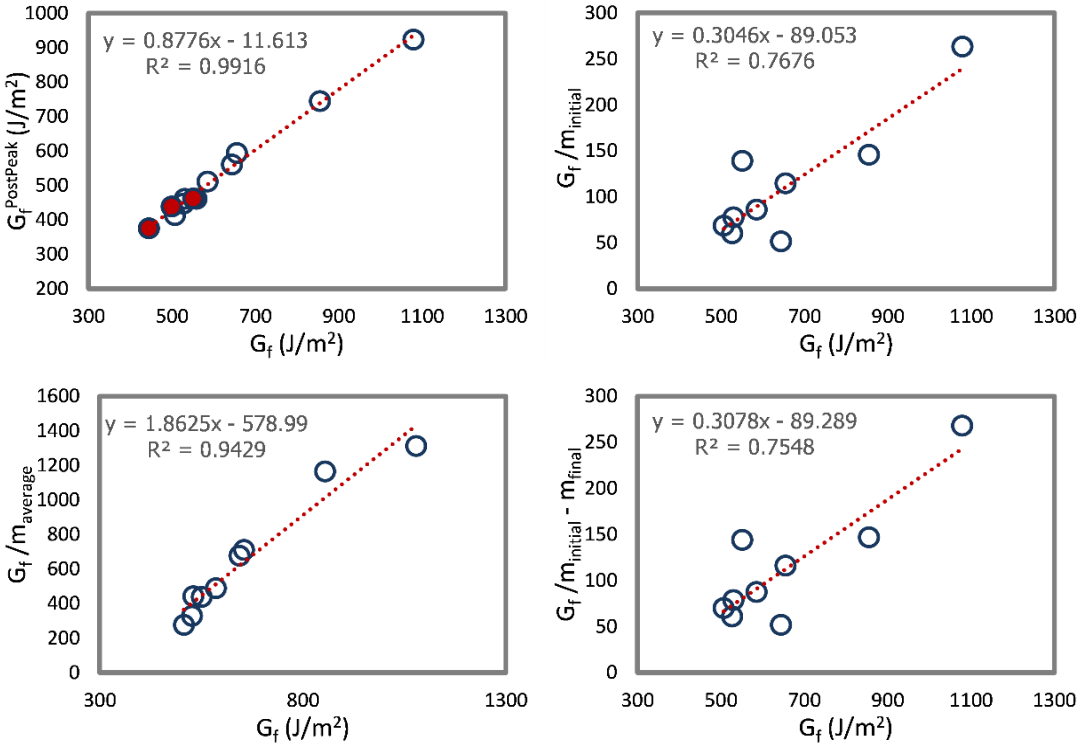

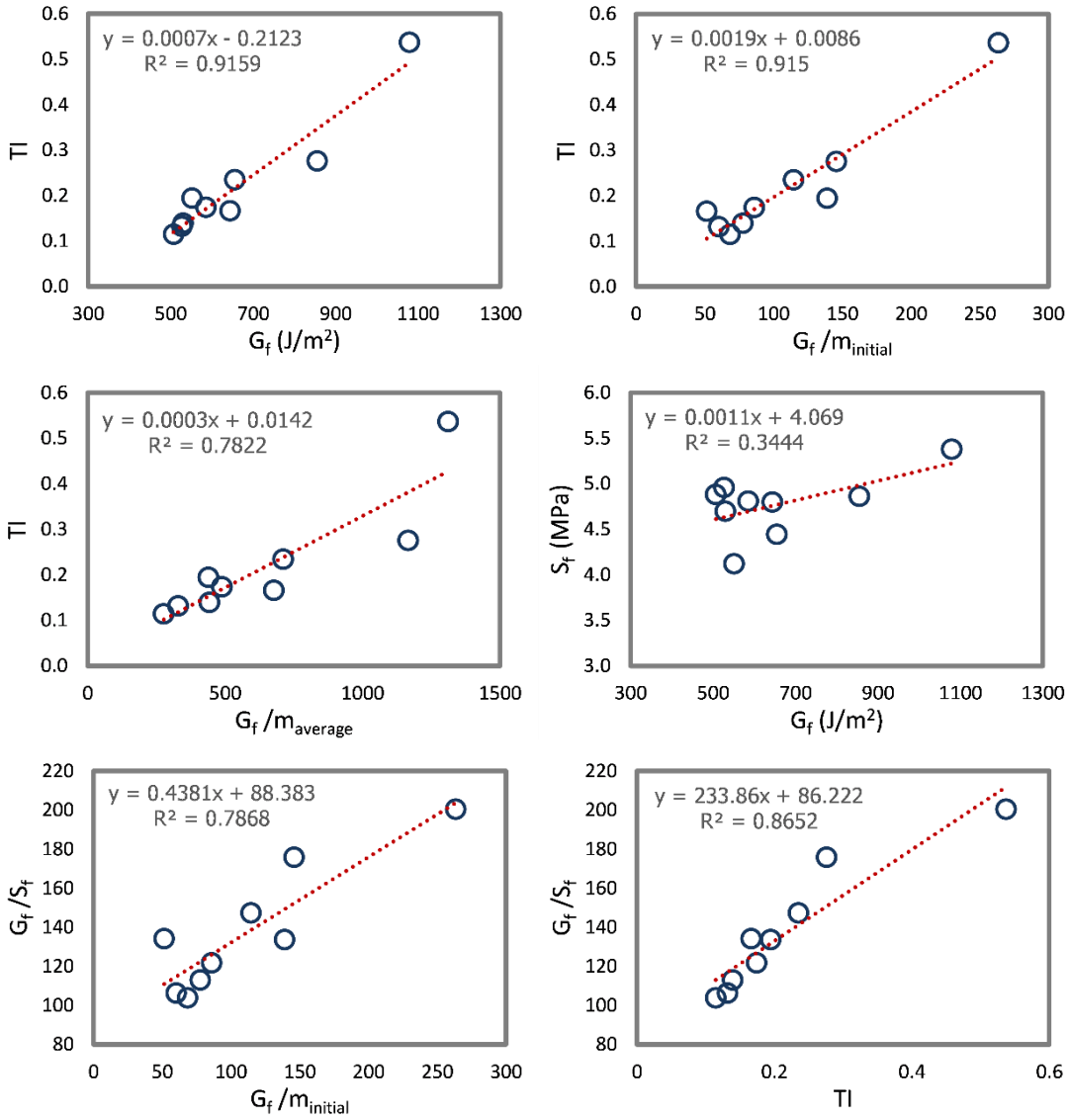

Figure 6-14 DCT fracture energy indices for 5N/30 (A) asphalt mix

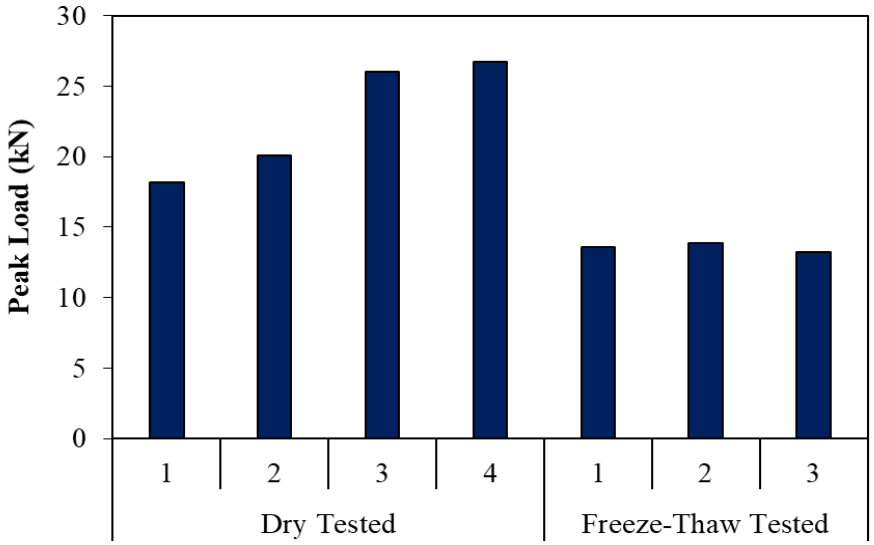

Figure 6-15 ITS test results for 5N/30 (A) asphalt mix

6.3.2 5N/30 (B)

A comparison of fracture energy from the DCT tests samples is provided in Figure 6-16. No wet samples could be tested for this mix. Values for the different fracture energy indices are given in Figure 6-17. Figure 6-18 provides the peak load at failure values for the 5N/30 (A) mix design from the ITS testing.

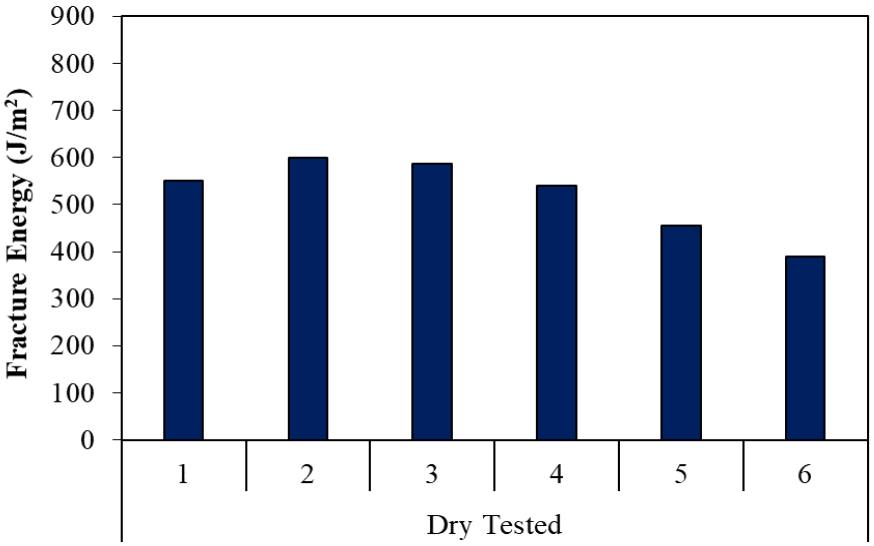

Figure 6-16 DCT test results for 5N/30 (B) asphalt mix

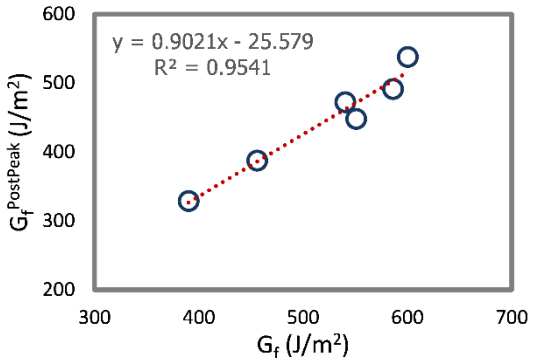
y = 0.9021x - 25.579
R² = 0.9541
$G_f^{PostPeak}$ (J/m²)
G_f (J/m²)

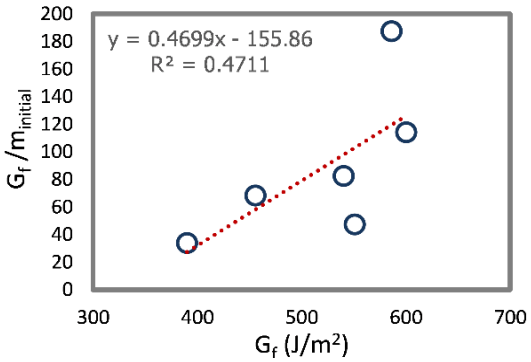
y = 0.4699x - 155.86
R² = 0.4711
$G_f/m_{initial}$
G_f (J/m²)

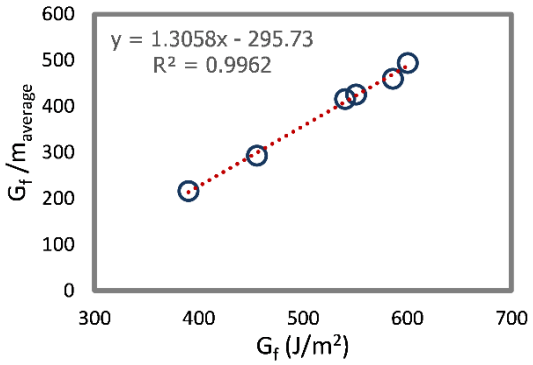
y = 1.3058x - 295.73
R² = 0.9962
$G_f/m_{average}$
G_f (J/m²)

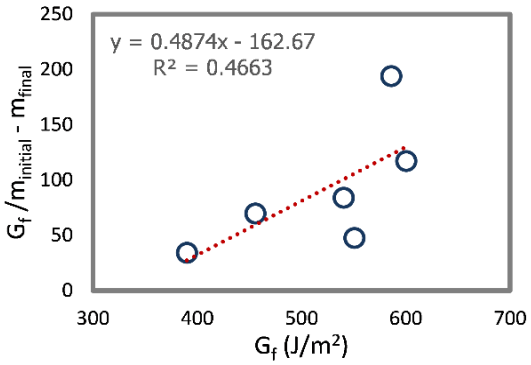
y = 0.4874x - 162.67
R² = 0.4663
$G_f/m_{initial} - m_{final}$
G_f (J/m²)

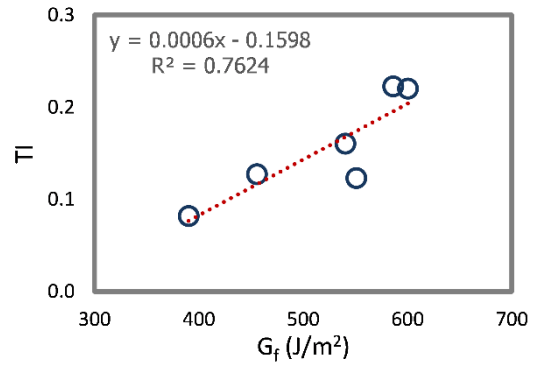
y = 0.0006x - 0.1598
R² = 0.7624
TI
G_f (J/m²)

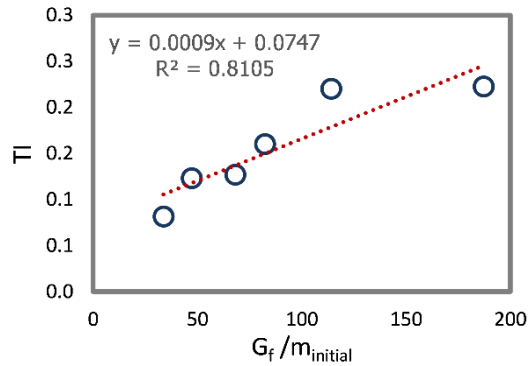
y = 0.0009x + 0.0747
R² = 0.8105
TI
$G_f/m_{initial}$

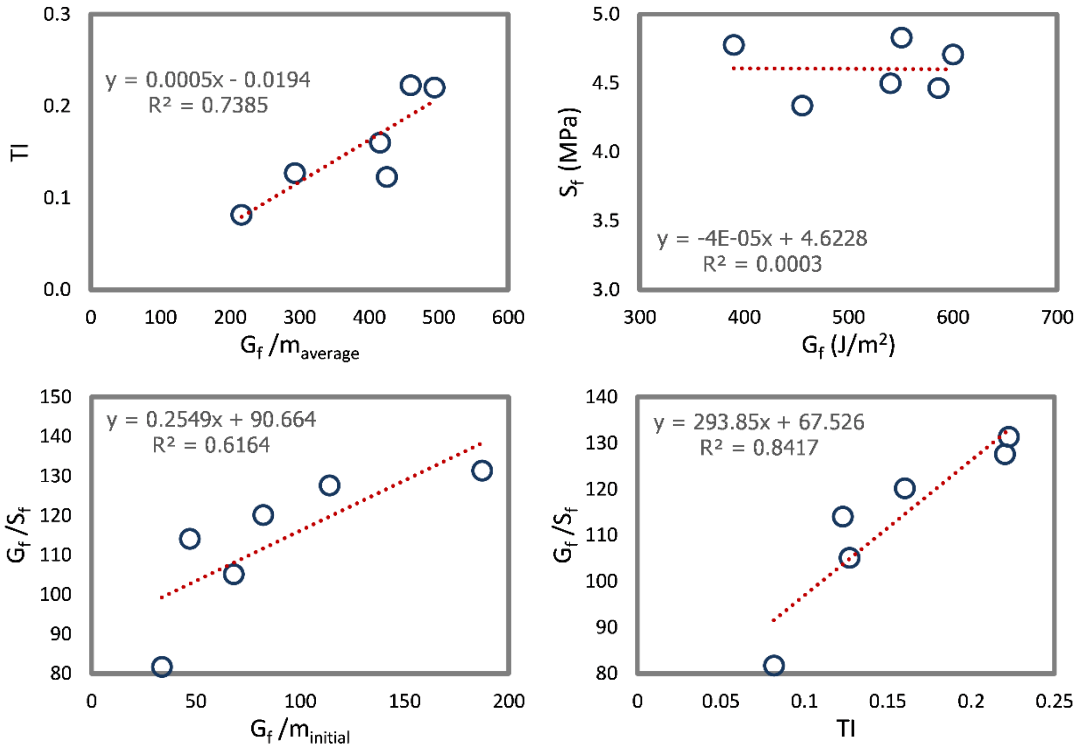

Figure 6-17 DCT fracture energy indices for 5N/30 (B) asphalt mix

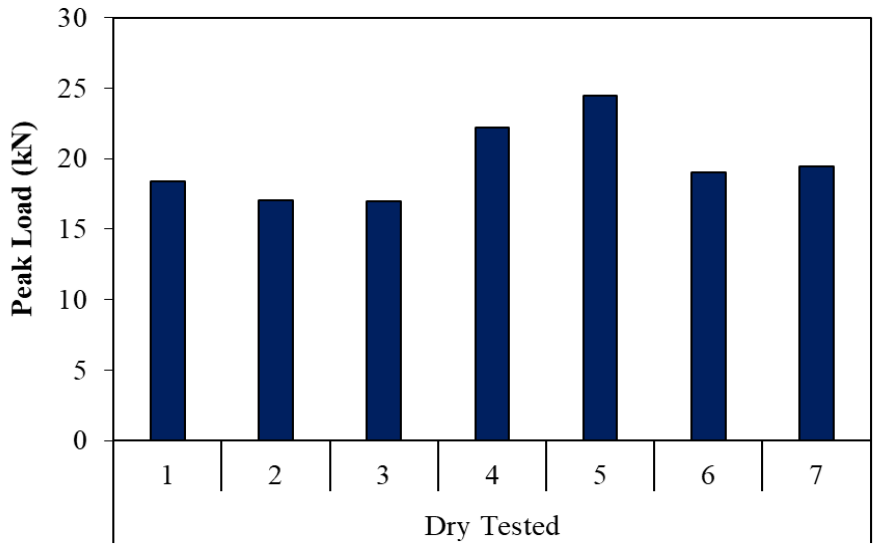

Figure 6-18 ITS test results for 5N/30 (B) asphalt mix

6.3.3 5N/30 (C)

A comparison of fracture energy from the DCT tests for the dry and wet tested samples is provided in Figure 6-19. Values for the different fracture energy indices are given in Figure 6-20. The mix 5N/30 © follows the same trend as that of the other two Superpave-5 mixes. However, a more similarity in trend

can be observed between 5N/30 (B) and 5N/30 (C). It should be noted that one of the data points in the DCT analysis presented in Figure 6-19 had a comparatively higher fracture energy value (approx. 641 J/m^2), which is included in the plots to indicate the measure of variability in test results. Figure 6-21 provides the peak load at failure values for the 5N/30 (C) mix design from the ITS testing.

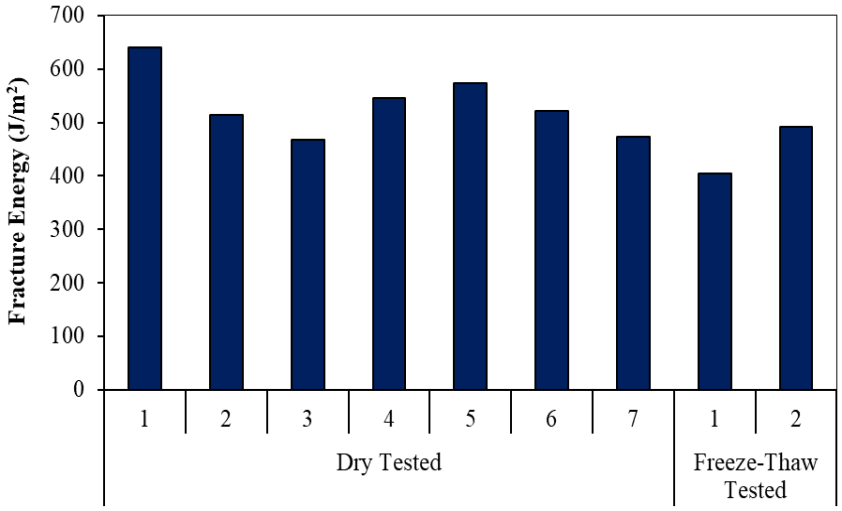

Figure 6-19 DCT test results for 5N/30 (C) asphalt mix

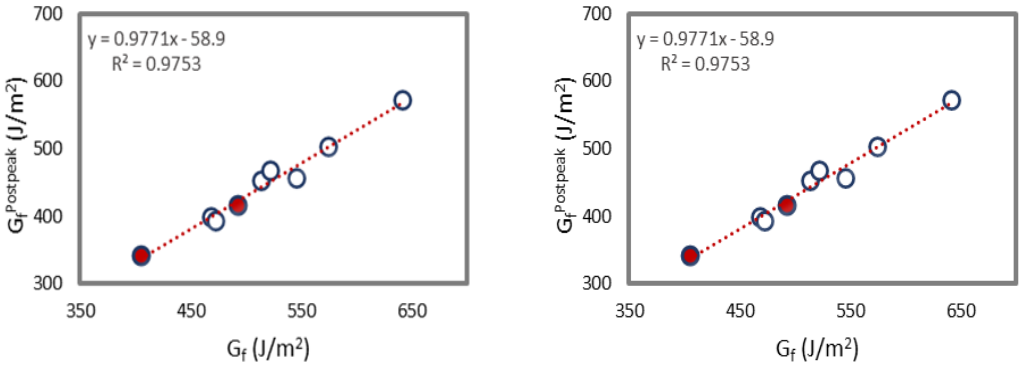

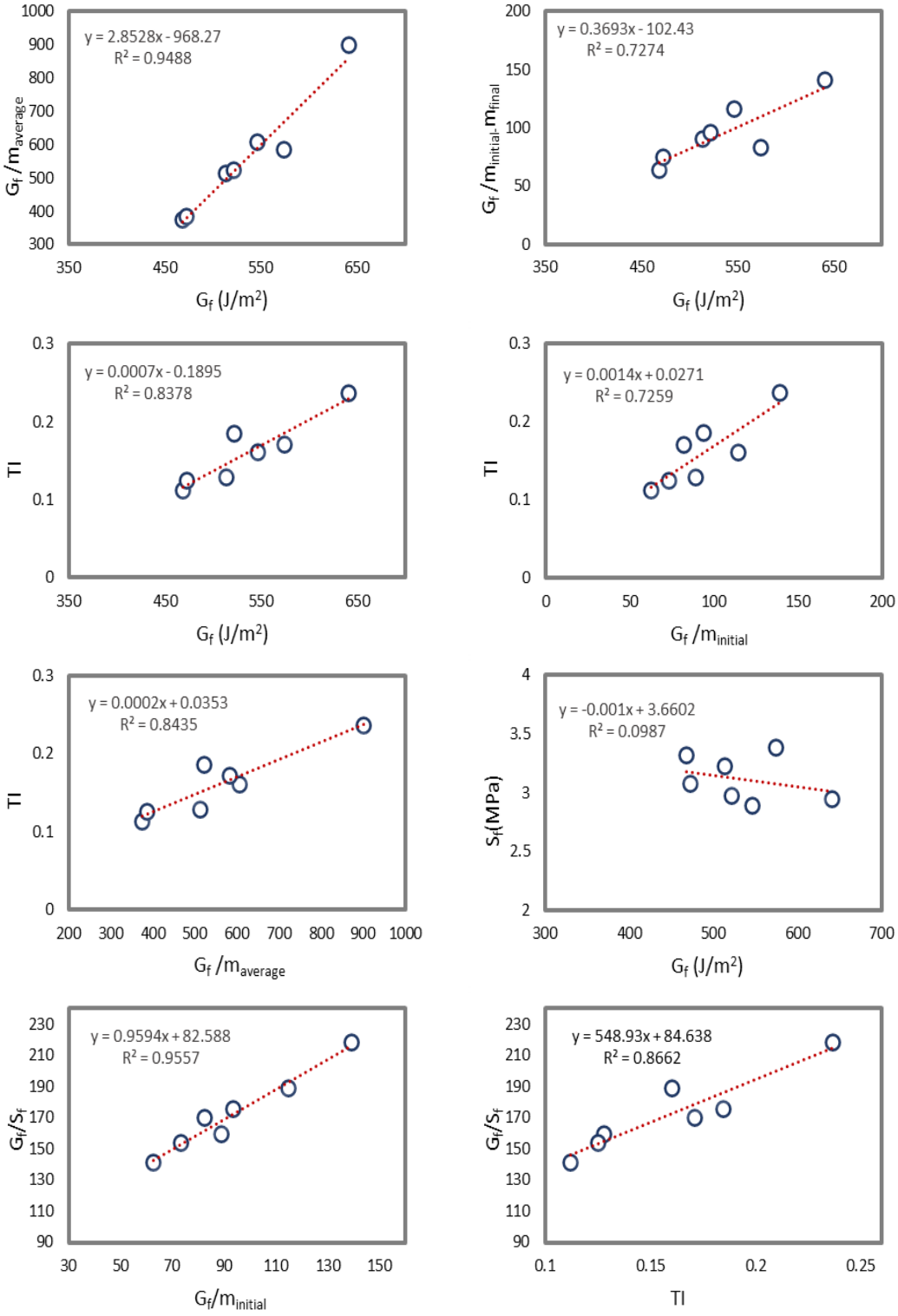

Figure 6-20 DCT fracture energy indices for 5N/30 (C) asphalt mix

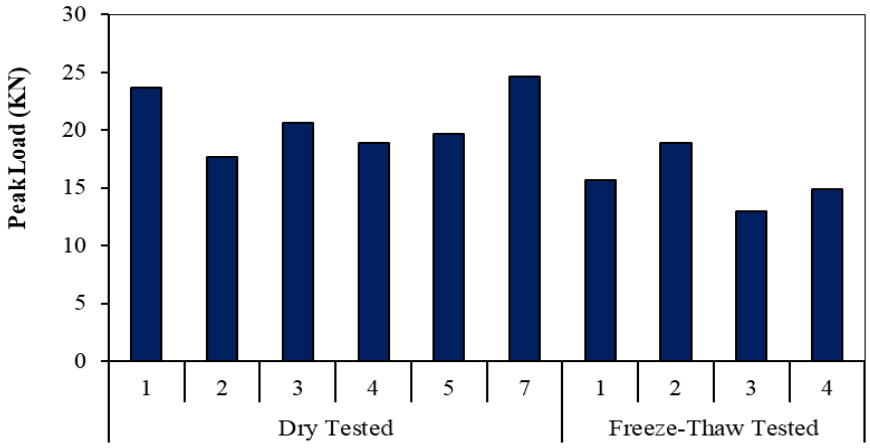

Figure 6-21 ITS test results for 5N/30 (C) asphalt mix

6.4 DCT Test Result Comparison and Discussion

A comparison of the average values of different fracture parameters such as fracture energy and post-peak fracture energy and various other fracture energy indices are provided in Figure 6-22. It is observed from the G_f values shown in the Figure 6-22 that each mix type surpasses the minimum threshold G value (400 J/m^2) recommended for the low-volume roads in Minnesota. The three 4N/40 mixes tested had similar fracture energy values, and the high density (5N/30 Superpave-5) mixes displayed a better fracture performance than the 4N/40 mixes. As far as the post-peak fracture energy (G_f^(post-peak)) is concerned, quite similar rankings of the different mixes are observed. The post-peak fracture energy is about 85% of the total fracture energy.

A different pattern is noticed in the flexibility index values. The initial and final FI values are very close to each other and indicate that mixes in the two individual groups of [4N/40 (A) and 5N/30 (A)], and [4N/40 (C) and 5N/30 (B)] have comparable FI values. Although 4N/40 (A) has lower overall fracture energy, a higher FI (initial) denotes a bigger fracture process zone and a more flexible mix. From the Bailey method analysis, it was found that the 4N/40 (A) mix has significantly less amount of fines, lower than the Bailey recommended value. It also has a coarse aggregate portion higher than 4N/40 (B), but less than the 5N/30 mixes. Although the 5N/30 (C) mix had FI (initial) value higher than 4N/40 (C) and 4N/40 (B), it had the lowest FI (final) value when compared to the other conventional Superpave and Superpave-5 mixes. This observation can be attributed to the presence of more fines in 5N/30 (C) mix. In summary, it can be noticed that the 5N/30 mixes show better flexibility by having a more balanced proportion of coarse and fine aggregates in the mix. This is evident by comparing the FI average values for the different mixes.

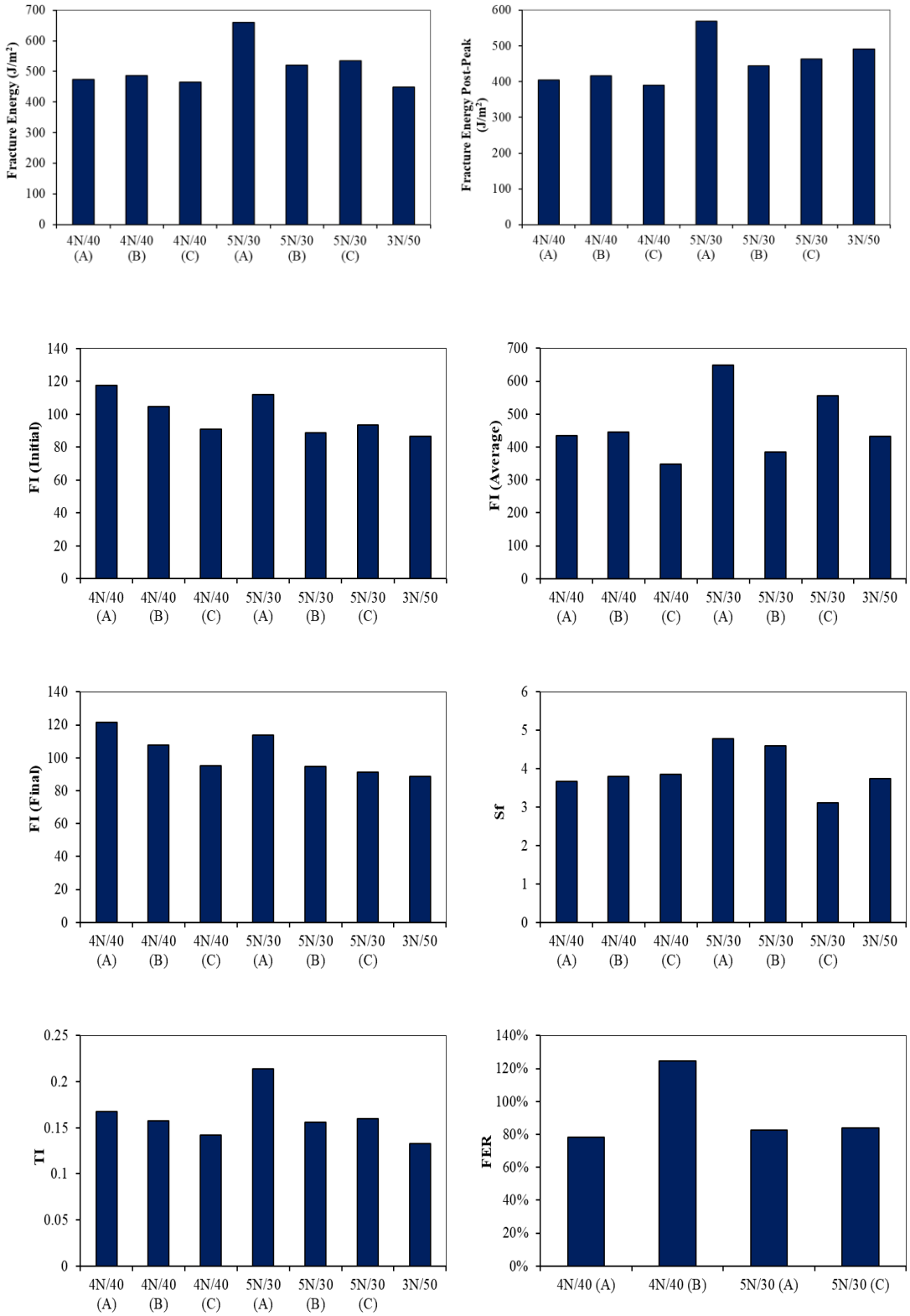

Figure 6-22 DCT test result comparison

In comparison to the strain tolerance evaluation using the fracture energy and FI parameters, the fracture strength is determined using S_f. It is clear from the data presented in Figure 6-22 that 4N/40 (A) and 4N/40 (B) mixes can be classified as soft and flexible in performance. On the other hand, 5N/30 (A) is a stiffer (higher peak load at failure than 4N/40 (A, B or C)) and flexible mix. 5N/30 (B) is also a stiffer mix but has lesser flexibility than the 4N/40 mixes. It can be noted that 5N/30 (C) had the least Sf value which contrasts with the Sf values of other Superpave-5 mixes, and it may be due to the higher quantity of fines in the 5N/30 (C) mix. The impact of a bigger fracture process zone for the 4N/40 (A) mix can be observed in its Toughness Index (TI) value, which is higher than most mixes tested. 5N/30 (A) has the highest TI value among all mixes. A comparison of fracture energy of wet and dry mixes using the FER parameter shows that there is an average of 20% decrease in fracture energy after moisture conditioning of dry specimens. This observation remained comparable for the 4N/40 and 5N/30 mix.

6.4.1 Statistical Analysis of DCT Fracture Energy Results

A one-way ANOVA test was considered for the statistical analysis of the results, especially to determine the significance of the differences in various fracture parameters. Descriptive statistics were calculated, including the impact of data size, homogeneity tests (Levene's test for equality of variance), and tests for normality were performed. Bonferroni's correction was applied in the post-hoc test as it is applicable for equal as well as unequal data sizes.

6.4.1.1 Descriptive Statistics

Mean and standard deviation of fracture energy (Gf) values were determined for the seven different mixes, as shown in Table 6.1. For statistically analyzing the DCT results, one of the data points with an extremely high fracture energy value (approx. 1080 J/m^2) was not included. However, even if it were included in the analysis, the overall conclusion of the statistical analysis remains unchanged.

It can be observed that the 5N/30 mixes have the highest average fracture energy values. A comparison of mean values is shown in Figure 6-23. Error bars represent one standard deviation of the corresponding value. It is noticed that the 4N/40 mixes seem to have almost equal average fracture energy values. In contrast, while the high-density mixes display a better fracture performance, 5N/30 (B) has a lower average G_f than 5N/30(A).

Table 6.1 Descriptive statistics for G_f (J/m^2) values of different mix designs

Mix Type	Mean	SD	COV (%)	N
4N40 (A)	474	76	16.1	4
4N40 (B)	486	79	16.4	7
4N40 (C)	465	28	6.0	4
5N30 (A)	607	114	18.8	8
5N30 (B)	521	82	15.6	6
5N30 (C)	534	59	11	7
3N/50	448	44	9.8	5

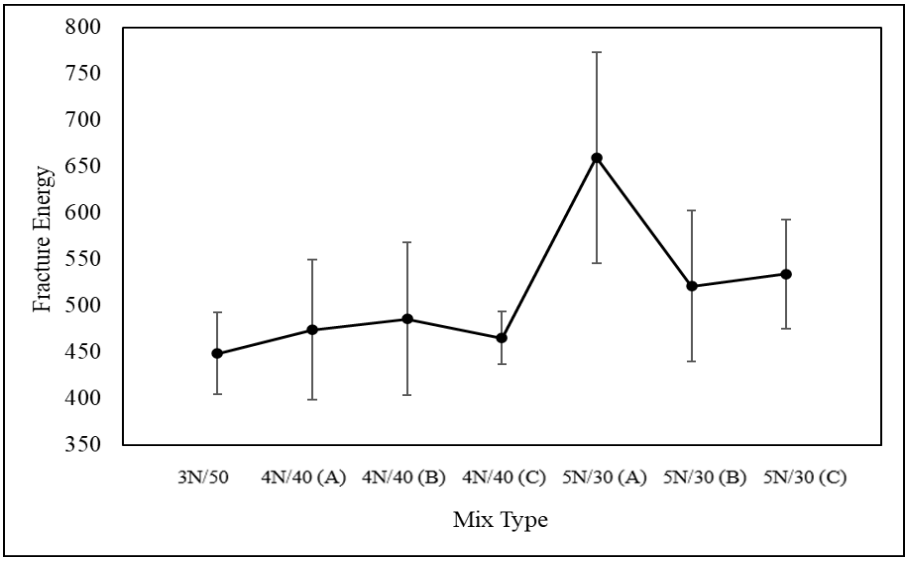

Figure 6-23 Fracture energy mean value comparison

6.4.1.2 Homogeneity Test and Check for Data Normality

The assumption check in the ANOVA is done by testing the homogeneity of variance across different samples through the Levine's test. The null hypothesis in this test claims that the different samples have the same variability, and the alternate hypothesis proves that at least one pair has different variances. It is noticed from Table 6.2 that the p-value is greater than 0.05. This implies that the different mix types have equal variance, and the difference is not significant. If the difference was significant, homogeneity corrections would have been applied.

Table 6.2 Levin's test results

F	df1	df2	p
1.371	5	28	0.265

Another assumption that needs to be satisfied for ANOVA is the normality of data by generating a normal Q-Q plot or quantile-quantile plot. The quantiles were compared against a theoretical distribution of data. It is to be expected that for a normal distribution, data points should lie on the straight line or very close. Accordingly, Figure 6-24 shows that the fracture energy data is normally distributed.

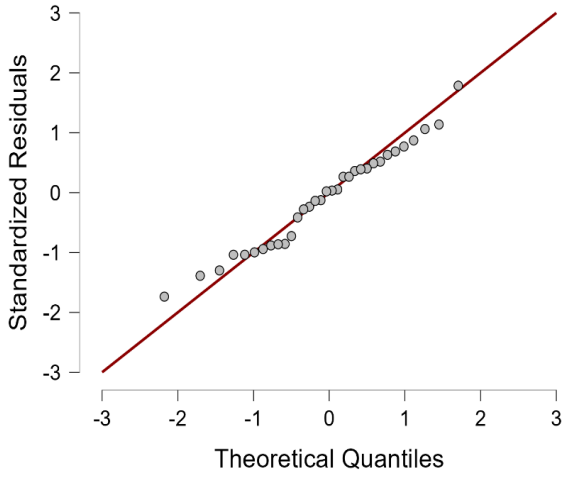

Figure 6-24 Q-Q plot to test the normality of test data

6.4.1.3 Hypothesis Testing

ANOVA tests the null hypothesis that the means of all the independent groups (different mix types in this study) are similar. However, if the one-way ANOVA generates a statistically significant result, then the alternate hypothesis that the difference between the mean values of at least one of the groups is

significant, is tested. By itself, this test does not provide any information about the independent groups which have significantly different mean values. For that purpose, further analysis is needed.

Table 6.3 ANOVA results for different mixes

Cases	Sum of Squares	df	Mean square	F	p	η^2
Mix Type	112177.947	5	22435.589	3.311	0.018	.372
Residuals	189746.479	28	6776.660			

In Table 6.3, “Mix Type” and “Residuals” represent the values for between and within the group analysis, respectively and ‘df’ represents the degrees of freedom. It is observed from the table that the p-value is less than 0.05, thereby rejecting the null hypothesis. The effect parameter, η^2 indicates that 37.2% of variance in fracture energy values is due to a change in the mix type.

6.4.1.4 Post Hoc Test (parametric analysis)

In this analysis, the significance of the difference of the independent mixes from each other is determined. This is accomplished by performing the post hoc test or multiple comparisons.

Table 6.4 Post hoc comparisons by mix type

		Mean Difference	95% CI for Mean Difference		SE	t	ρ_{bonf}
			Lower	Upper			
3N50	4N40 (A)	-25.577	-194.329	143.176	55.222	-0.463	0.999
	4N40 (B)	-37.256	-184.555	110.044	48.202	-0.773	0.987
	4N40 (C)	-16.708	-185.461	152.044	55.222	-0.303	1.000
	5N30 (A)	-211.105	-301.939	-15.115	46.930	-3.378	0.074
	5N30 (B)	-72.310	-224.638	80.018	49.848	-1.451	0.830
4N/40 (A)	4N40 (B)	-11.679	-169.353	145.995	51.597	-0.226	1.000
	4N40 (C)	8.868	-169.012	186.749	58.209	0.152	1.000
	5N30 (A)	-185.529	-286.999	21.099	50.411	-2.637	0.258
	5N30 (B)	-46.733	-209.115	115.649	53.138	-0.879	0.977
4N40 (B)	4N40 (C)	20.547	-137.127	178.222	51.597	0.398	0.999
	5N30 (A)	-173.850	-251.466	8.924	42.605	-2.846	0.187
	5N30 (B)	-35.054	-175.010	104.901	45.799	-0.765	0.988
4N40 (C)	5N30 (A)	-194.397	-295.868	12.231	50.411	-2.813	0.197
	5N30 (B)	-55.602	-217.984	106.780	53.138	-1.046	0.951
5N30 (A)	5N30 (B)	138.795	-49.642	222.075	44.458	1.939	0.592

In this analysis, the last mix 5N/30 (C) is not included, which was prepared to refine the gradation of the Superpave 5 mixes, but as this mix did not show any superior performance than the two other Superpave-5 mixes, the exclusion of this mix from the statistical analysis did not change any conclusion.

In Table 6.4, each mix type is compared to the other mixes. The mean difference, standard error of the mean, and the confidence interval values are provided in different columns. To interpret the results, it is considered that when the confidence interval (CI) values cross through 0 from lower to upper CI, the difference between groups is not significant. A Bonferroni p-value was calculated for further clarity. This correction method – although conservative in its application – was selected because it allows analysis for samples of unequal sizes. It is observed from the table that the p-value is significant only for the comparison between 3N/50 and 5N/30 (A) mixes. For the rest of the mixes, the difference is not significant.

It should be noted that generally, the DCT test has a high COV (Table 6.1). Although statistically, it is proven that 5N/30 (A) has the best performance overall, and it is only significantly different than 3N/50, a larger mean difference between mixes could have been reported with more replicates. In conclusion, while the Superpave-4 (4N/40) and Superpave-5 (5N/30) mixes have a quite similar costs of construction (no change in binder content and similar aggregate types), better performance can be achieved in the field with 5N/30 mixes with the anticipation that Superpave-5 mixes will create higher density asphalt layers, which will accumulate less damage over the years, compared to the Superpave-4 (4N/40) mixes. It is also deduced from the DCT results that 3N/50 mix design is not suitable for low-volume roads.

6.4.2 DCT Fracture Energy Results of Field Cores

Figure 6-25 illustrates the G_f values obtained from field cores from four different counties described in Chapter 4 of this report. It can be seen that most cores failed the fracture energy limit, 400 J/m^2, possibly an indication of aging in the asphalt mix. As asphalt mix ages, the material becomes more quasi-brittle and loses its fracture energy. The lowest G_f values belong to road sections with relatively low density (143.25 lb/cy CSAH 8-12 in Beltrami County and 137.61 lb/cy for CSAH 9 in Koochiching County). It is also observed that three cores from a single location in Koochiching County (CSAH 2) display very high G_f values; incidentally, this location had relatively high density (147.56 lb/cy). In addition, some cores from CSAH 18, CSAH 16 in Pope County, and CSAH 4-CR 404 in Beltrami County also show satisfactory results. These sections also display comparatively high-density values in Table 4.8 to Table 4.10 due to higher traffic volumes. It is possible that higher density values offset the detrimental impact of aging due to environmental factors. Overall, results of the field cores also indicate that an improvement in mix design for the low-volume roads may be achieved by creating high-density asphalt mixtures. This will result in better fracture energy G_f and eventually decrease the low-temperature thermal cracking. Figure 6-26 through Figure 6-28 show some pictures of the DCT samples prepared from collected asphalt cores.

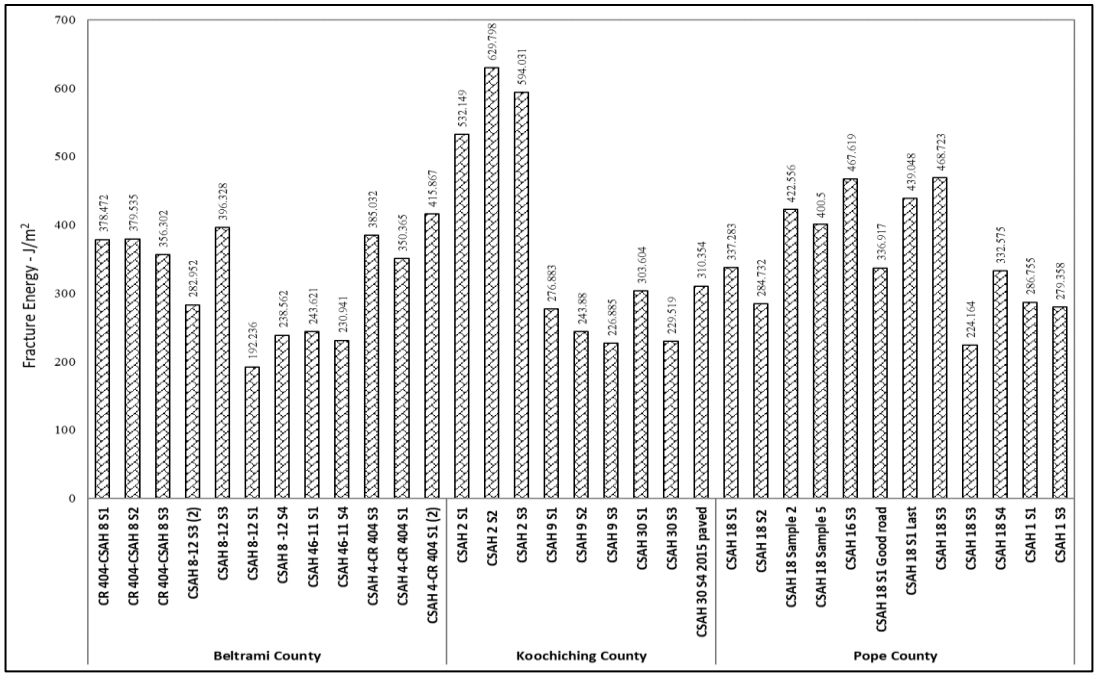

Figure 6-25 Fracture Energy values for different asphalt mixes

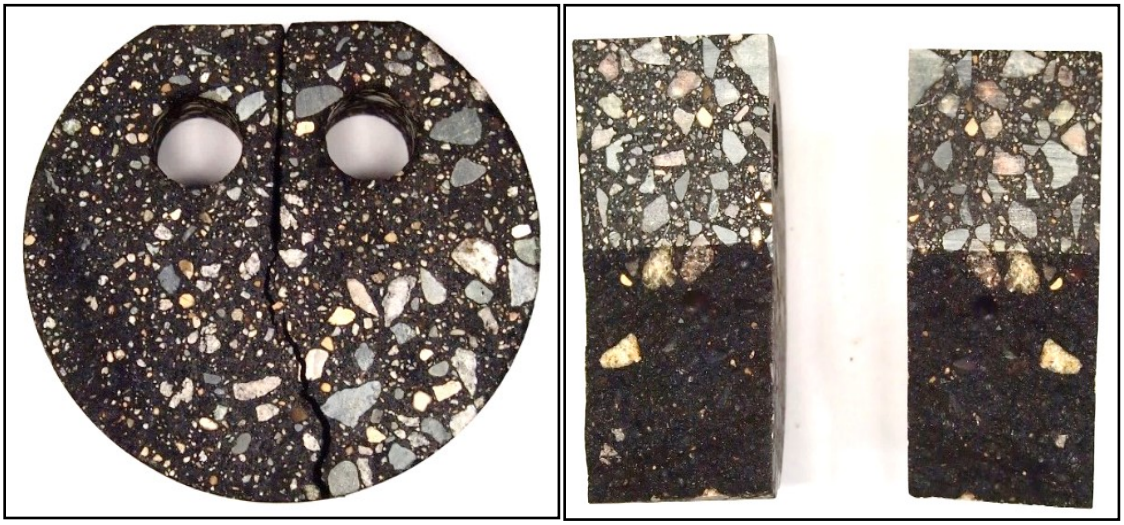

Figure 6-26 CR 404-CSAH 8 S3 DCT failed specimen

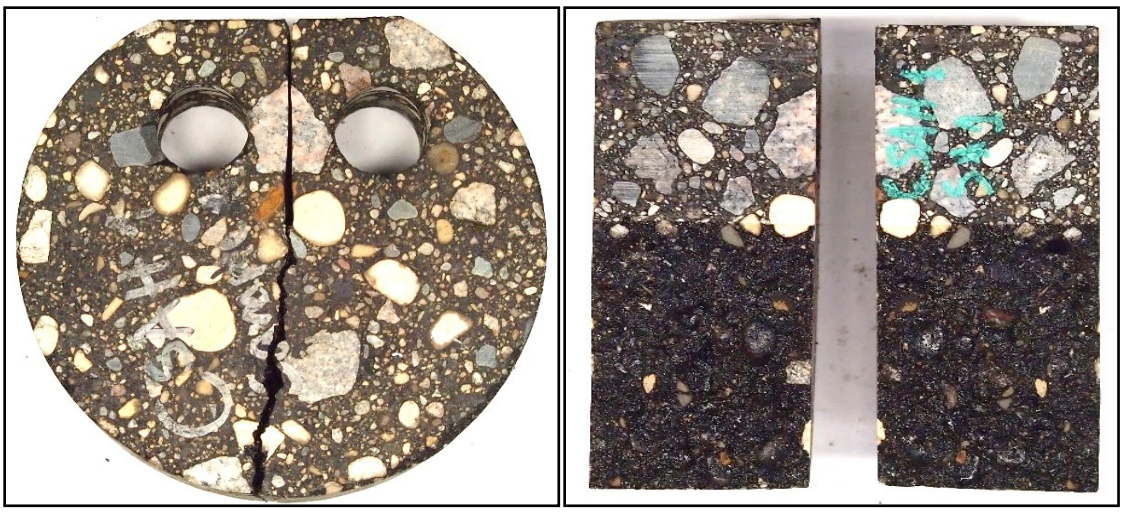

Figure 6-27 CSAH 1 S1 DCT failed specimen

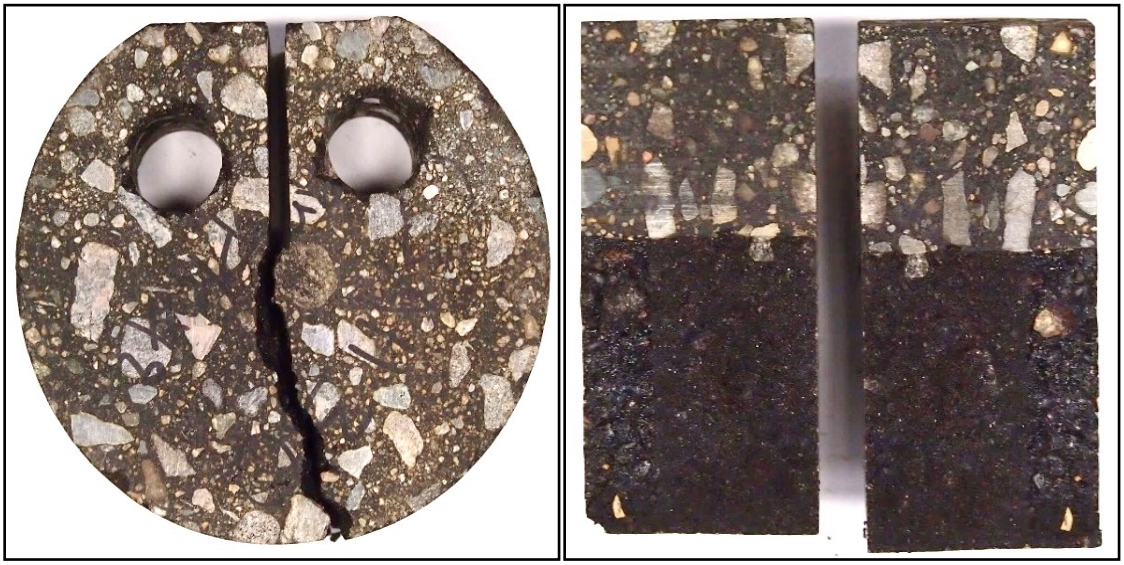

Figure 6-28 CSAH 30 S3 DCT failed specimen

A comparison of fracture energy values of laboratory prepared samples and field samples is given in Figure 6-29. The field G_f values were obtained from a previous chapter of this study. Cores were obtained from three different counties of Minnesota (see Figure 6-25). Field – I, II, and III represent the average G_f values of about 10 samples per location. It is evident that due to the impact of weather and traffic the fracture resistance of pavement decreases with time. While unaged 4N/40 mixes display better performance than the field mixes, they still perform poorly than the 5N/30 mixes. Therefore, a reduced percent of initial compacted air voids in the Superpave-5 mixes (5% for 5N/30 in comparison to 7% for 4N/40) can assure a slower rate of aging of the mix due to environmental factors.

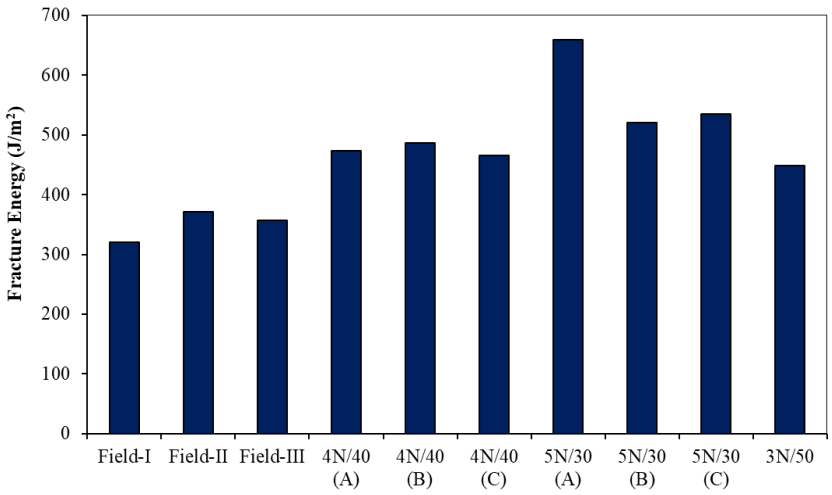

Figure 6-29 Test result comparison between laboratory and field samples

6.5 ITS Test Result Comparison

The TSR values calculated from the wet and dry strength values are compared in Figure 6-30. It shall be noted that the conditioning of the wet samples includes the application of a freeze-thaw cycle, which is not the case for the Lottman test. While the TSR value of the 4N/40C was the lowest, Superpave-5 mix 5N/30(A) had the maximum indirect tensile strength in dry condition and 5N/30(C) had the maximum indirect tensile strength in wet condition.

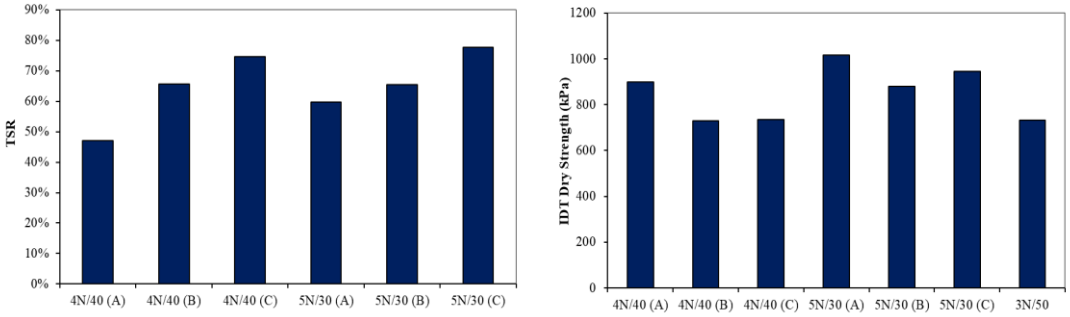

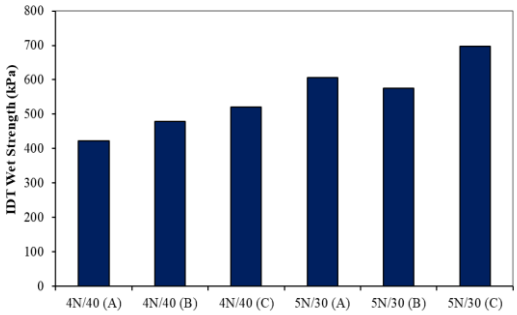

Figure 6-30 ITS test result comparison

It is noticed from the TSR test results that none of the mixes pass the minimum MnDOT TSR criterion of 80% for the Lottman test; however, as the wet-conditioned samples in this study were subjected to a freeze-thaw cycle, the TSR results were expected to be lower than that of the typical Lottman test TSR results. The presence of 18% RAP in all mixes could also be responsible for the decrease in performance after moisture conditioning. Nevertheless, the TSR values for the 5N/30 mixes were higher than the 4N/30 mixes.

6.6 DM Test Result Comparison

A comparison of dynamic modulus values of different mixes is provided in Figure 6-31. It is observed that at higher frequency values, the high-density 5N/30 mixes have the highest modulus values. In contrast, the 4N/40 mix has the lowest values. However, at high temperatures (or low frequency), the 5N/30 (B) mix performs better, and the conventional 4N/40 (C) performs the worst. This proves that Superpave-5 (5N/30) mixes have a better rut resistance than the traditional 4N/40 mixes. 5N/30 (C) had the highest modulus at all frequencies. But the 5N/30 (A) mix shows a decrease in modulus in comparison to the 5N/30 (B) mix at the lower reduced frequencies, possibly due to a slightly greater amount of fines in the former one. Due to an experimental error, similar tests could not be completed on time for the 4N/40 (B) mix. It can be noted that the gradations for the 3N/50 and 4N/40 (B) mix are the same, with a virgin binder content of 4.9% and 5.5%, respectively. On a simpler scale, it can be assumed that the 4N/40 (B) mix might have equal or even lesser modulus values than 3N/50.

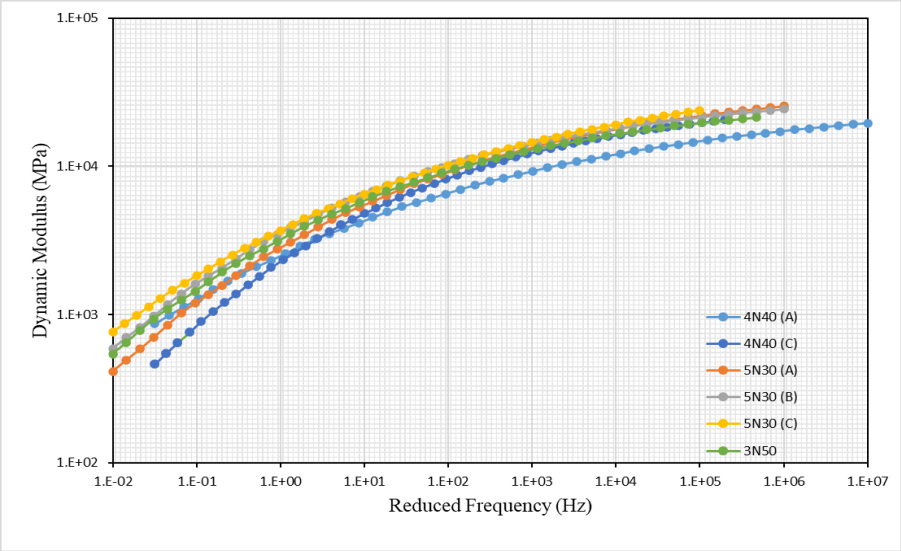

Figure 6-31 Dynamic modulus comparison for different mixes

6.7 Aggregate Gradation Comparison

Bailey method parameters were determined to study the aggregate gradation. In the Bailey Method, three sieve sizes called the Primary Control Sieve (PCS), Secondary Control Sieve (SCS), and Tertiary Control Sieve (TCS) are used to categorize the aggregates. PCS defines the difference between coarse and fine aggregates, and the coarse aggregates are designated as the size of aggregates from the largest stone to the PCS. The rest of the aggregates are further categorized with the help of SCS, which divides coarse sand and fine sand. The latter is evaluated by calculating the TCS value which is 0.22 of the SCS sieve. The level of aggregate packing in different categories is determined by calculating specific ratios, which are PCS Index (PCSI), Coarse Aggregate ratio (CA Ratio), Fine Aggregate Coarse Ratio (FA_c Ratio), and Fine Aggregate Fine Ratio (FA_f Ratio). These parameters are determined using Equations (11) and (12). To calculate CA ratio, percentage passing half sieve was calculated by interpolation.

$$\begin{cases} PCS = 0.22 \times NMAS \\ SCS = 0.22 \times PCS \\ TCS = 0.22 \times SCS \end{cases} \tag{11}$$

$$\begin{cases} PCSI = \%\ Passing\ PCS \\ CA\ Ratio = \dfrac{(\%\ Passing\ Half\ Sieve - \%\ Passing\ PCS)}{(100\% - \%Passing\ Half\ Sieve)} \\ FA_c\ Ratio = \dfrac{\%\ Passing\ SCS}{\%\ Passing\ PCS} \\ FA_f\ Ratio = \dfrac{\%\ Passing\ TCS}{\%\ Passing\ SCS} \end{cases} \tag{12}$$

Values of different Bailey method parameters for the seven different mixes evaluated in this study are given in Table 6.5.

Table 6.5 Bailey parameters for different mixes

	PCSI	CA Ratio	FA_c Ratio	FA_f Ratio
4N/40 (A)	50.87	0.89	0.36	0.20
4N/40 (B)	45.97	0.69	0.46	0.37
4N/40 (C)	53.90	1.05	0.46	0.38
5N/30 (A)	53.70	1.02	0.47	0.40
5N/30 (B)	51.80	0.91	0.46	0.37
5N/30 (C)	60.5	0.30	0.45	0.34
3N/50	45.97	0.69	0.46	0.37

According to Table 6.5, as the mix design focuses on creating dense-graded mixes, CA ratios for every mix pass the minimum value suggested for preventing segregation of the mix. Mixes 4N/40 (C) and 5N/30 (A) crossed the 1.0 mark, which indicates a higher presence of coarse aggregate fraction above the PCS sieve in comparison to gradations with a CA ratio below 1.0. However, this doesn't indicate that the mixes will be prone to segregation in the field, especially for a finer mix that experiences a wider variation of CA ratios. As far as the fine portion of the gradation for different mixes is concerned, none of the FA_c values are above 0.50 or out of the recommended range, which signifies a balanced aggregate profile. Increase in FA_c values in the rest of the mixes as compared to 4N/40 (A) indicates a looser packing of fine aggregates in 4N/40 (A). The FA_f ratio for the 4N/40 (A) is lower than the minimum recommended value. These figures for the 4N/40 (A) mix are reflected in its high VMA value in comparison to the 4N/40 (B) and 4N/40 (C) as shown in Table 5.3.

6.8 Summary

Seven different mix designs were evaluated. Three replicates of the conventional Superpave-4 (4N/40) mixes, with varying aggregate gradations, were prepared. Based on the 4N/40 mix designs, three different Superpave-5 (5N/30) mixes were developed. The design air void content, number of gyrations, binder content, and aggregate gradation varied among mixes. Thereafter, DCT ITS and Dynamic Modulus test were conducted to determine the fracture toughness and resilience of mix samples at different temperatures. The major emphasis was placed on the low-temperature performance of test specimens.

DCT and ITS testing was also conducted on moisture-conditioned samples. The following conclusions were derived from the experimental study:

i. It was concluded that aggregate gradation difference between the Superpave-5 and Superpave-4 mixes played a role in the performance of asphalt mixes. The binder content and number of gyrations were not very different from each other between various mixes prepared according to the low-volume road mix design criteria of Minnesota. Therefore, the dominant deciding factor in ranking mixes according to performance was the gradation of aggregates.
ii. For a fine dense-graded mix type, the inclusion of more fines in the mix to enable higher design air voids (from 4 to 5%) but denser compacted mixes (from 7 to 5% at N_{max}), resulted in better fracture resistance at low temperatures (comparison of 4N/40 (B) and 5N/30 (B)). However, it shall be noted that the study considered only aggregate gradation A, and this conclusion is specific to this gradation only.
iii. For a similar change in design air voids from 4 to 5% and a denser compacted mix (from 7 to 5% at N_{max}), a course 5% design air void mix with less fines performed worse at low temperature than a similar mix with more fines (comparison between 5N/30 (A) (finer) and 5N/30 (B) (with respect to the original 4N/40 (B)).
iv. For similar aggregate gradations, 5N/30 mix with 0.5% more binder performed significantly better in low temperature conditions than the conventional low-volume road 4N/40 asphalt mix (comparison between 5N/30 (A) and 4N/40 (C)).
v. Flexibility index results for the various mix designs showed that the 5N/30 mixes had a more stable and balanced mix design. Between the three different 5N/30 mix designs, the mix with more fines performed better than the mix with less fine content in this study.
vi. Overall, 5N/30 mixes had a higher indirect tensile strength than the 4N/40 mixes. While all mixes suffered a large decrease in strength after moisture conditioning, the mixes with more fines showed a bigger difference in strength before and after the wet conditioning.
vii. Aggregate gradation had a major impact on the dynamic modulus values of mixes. At high temperature, the 5N/30 mix with coarser aggregates showed a higher modulus value than the 5N/30 mix with more fines. But the overall results for the 5N/30 mixes is better or comparable to the 4/N40 mixes, which indicates that the rutting behavior of the Superpave-5 mixes will not be inferior to the 4/N40 mixes.
viii. Lastly, as the low temperature transverse cracking is the dominant distress of Minnesota's asphalt pavements, it is concluded that the use of the 5N/30 mixes over the 4N/40 mixes may provide a longer service life of the pavements.

Chapter 7: Field Compaction of Superpave-5 Mixes

7.1 Introduction

This chapter is focused on studying the mechanical properties of the plant-produced asphalt mixtures designed by the Superpave-5 mixture design method and used in pavement projects in Minnesota. Three different plant-produced/field mixes were considered in this study. Two different mechanical tests were conducted to characterize the mechanical performance of the asphalt mixes, namely, (i) DCT test, and (ii) ITS test. The mechanical performance of the Superpave-5 field mixes was compared with the lab-produced Superpave-4 and Superpave-5 mixes. Additionally, the field density of Superpave-5 mixes has been studied.

7.2 Materials

Loose plant-produced Superpave-5 asphalt mixes from three field projects were collected. These mixes were used in projects under the jurisdiction of MnDOT Districts 1 and 6. Mix collected from District 1 was used in a section of Highway-61 [TH 61 project SP 1604-45 from Grand Portage to the Canadian Border (RP 133.8-150.8)] and the other two mixes were used in asphalt pavement projects in Highway 25 (location information is not available). It may be stated that the abovementioned mixes were not used in the low-volume roads (traffic level 2) but used in highways designed for high traffic volume (traffic levels 3 and 4). Field or plant-produced mixes were not available for low-volume roads, so the mechanical performance of those three Superpave-5 mixes was studied to investigate whether the plant-produced Superpave-5 mixes provide superior mechanical properties over the Superpave-4 mixes. Also, field core density results for one of the three projects mentioned above were studied to investigate the field density of the Superpave-5 mixes in the field. This section provides the details of the three mixes used in this chapter. These mixes are named (i) Mix 1: Traffic Level 3(a), (ii) Mix 2: Traffic Level 3(b), and (iii) Mix 3: Traffic Level 4.

7.3 Asphalt Mixture Designs

7.3.1 Mix 1 (SPWEB350B): Traffic Level 3(a)

This Superpave-5 wearing course mix was designed for traffic level 3. The target air void was 5% with 30 number of gyrations. The mix was prepared with PG 58S-28 binder. The mix contained aggregates from various sources, including 30% recycled aggregate pavement (RAP). Table 7.1 shows the aggregate proportions. The aggregate gradation curve is shown in Figure 6.1 (a). Based on the gradation curve, the gradation is close to the upper bound limits especially for the coarse aggregates (>2.36 mm), indicating relatively smaller sizes of coarse aggregates.

Table 7.1 Aggregate proportions for Mix1: Traffic Level 3(a)

Aggregates and RAP	Percentage used
½" Washed Sand	19%
¾" Rock	7%
¾" Rock	24%
Manufactured Sand	20%
¾" Crushed RAP @ 4.6% AC	10%
Millings @ 5.3% AC	20%

7.3.2 Mix 2(SPWEB350C): Traffic Level 3(b)

This mix was designed for traffic level 3 as well. As per the requirement of Superpave-5, the target air void percentage was 5% air with 30 number of gyrations. The mix was prepared with polymer-modified binder grade 58H-34. The different aggregate proportions used in this mix are provided in Table 7.1. The mix had 17% RAP. The gradation curve for this mix is shown in Figure 7-1. Compared to Mix 1, the gradation curve of this mix is closer to the theoretical maximum density line.

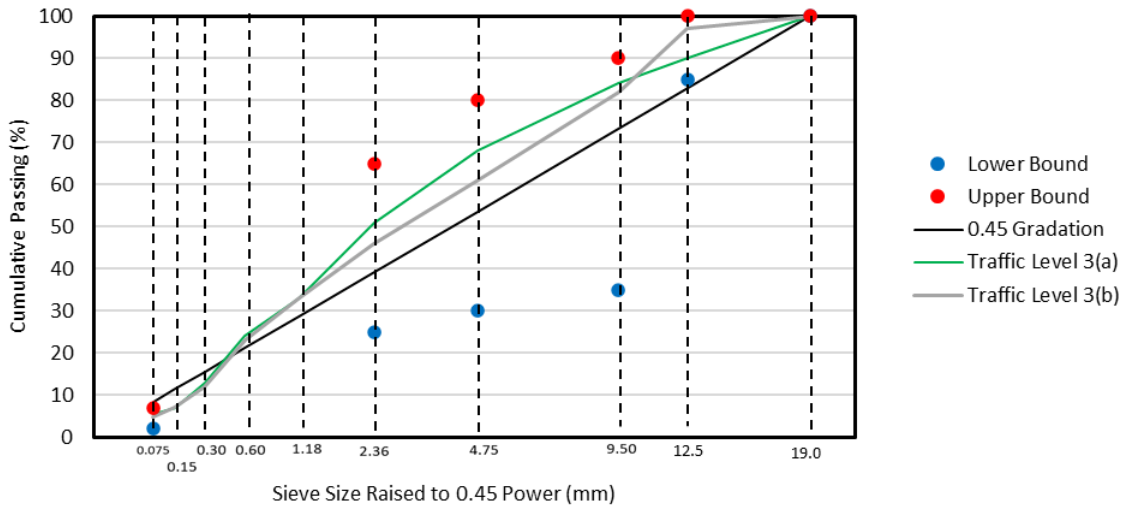

Figure 7-1 Aggregate gradation for the two Traffic level 3 mixes

Table 7.2 Aggregate proportion for Mix 2: Traffic Level 3(b)

Aggregates and RAP	Percentage used
⅝” Crushed Rock	32%
Washed Manufactured Sand	23%
Unwashed Manufactured Sand	21%
Sand	7%
RAP	17%

7.3.3 Mix 3(SPWEA450C): Traffic Level 4

The third Superpave-5 mix considered in this task was designed for traffic level 4, which was used on Highway 61 project in 2021. The target air voids percentage was 5% with 50 number of gyrations. A polymer-modified binder, PG 58H-34 grade, was used in this mix. Different aggregate proportions are provided in Table 7.3 and the gradation curve is shown in Figure 7-2. The gradation curve of the mix is approximately in the middle of the upper and lower limits. A comparison of the gradations of all three mixes is provided in Table 7.4. Table 7.5 provides a comparison of volumetric properties for the three field mixes considered. The total binder contents for Mixes 1, 2, and 3 are 5.5%, 5.2%, and 5.5%, respectively and the asphalt film thicknesses (AFT) for these mixes were 8.6, 9.7, and 8.8, respectively.

Table 7.3 Aggregate proportion for Mix 3: Traffic Level 4

Source of Material	Percentage used
½” Coarse Aggregate	23%
5/16” Fine Aggregate	20%
Crusher Fines	20%
Sand	17%
TH 61 Millings	20%

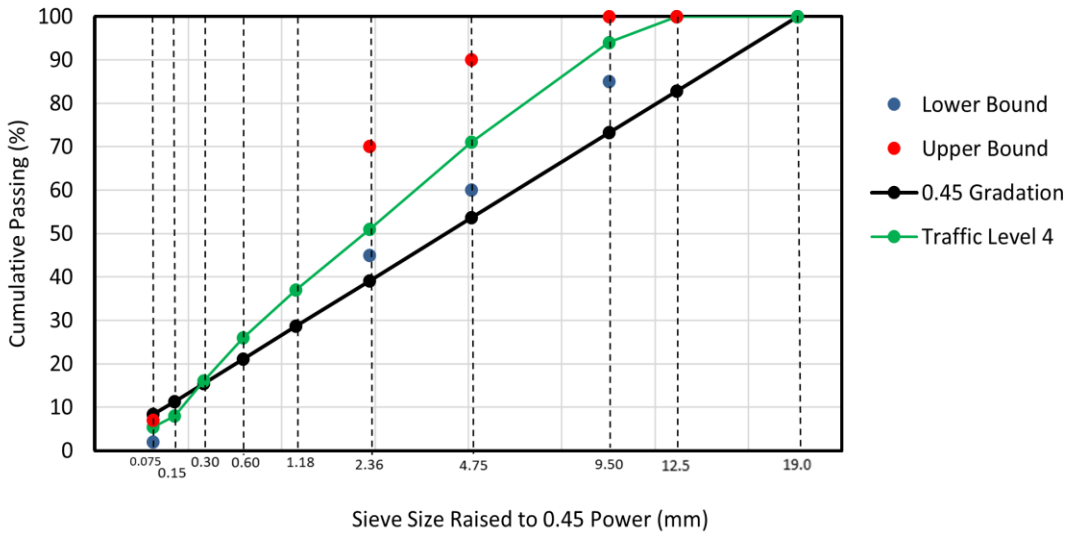

Figure 7-2 Aggregate gradation curve for Mix 3: Traffic Level 4

Table 7.4 Comparison of aggregate gradations for the three mixes

Sieve Size (mm)	Percentage Passing (%)		
	Mix 1: Traffic Level 3(a); SPWEB350B	Mix 2: Traffic Level 3(b); SPWEB350C	Mix 3: Traffic Level 4; SPWEA450C
19	100	100	100
12.5	90	97	100
9.5	84	82	94
4.75	68	61	71
2.36	51	46	51
1.18	33	33	37
0.6	24	23	26
0.3	13	12	16
0.15	7	7	8
0.075	5.4	4.7	5.4

Table 7.5 Volumetric data for different mix designs

Parameter	Mix 1: Traffic Level 3(a); SPWEB350B	Mix 2: Traffic Level 3(b); PWEB350C	Mix 3: Traffic Level 4; SPWEA450C
Gyration number	30	30	50
Total Asphalt Content (%)	5.5	5.2	5.5
Virgin Asphalt Binder (%)	4.7	5.0	5.1
Design Air Voids (%)	5.0	5.0	5.0
Gsb(mix)	2.649	2.661	2.697
Gsb(-4)	2.640	2.658	2.7
AFT	8.6	9.7	8.8

7.4 Performance Testing

The loose mixes were compacted in the laboratory to obtain cylindrical specimens of desired heights with 5+0.5% air voids to perform DCT and ITS tests.

7.5 Test Results

This section presents the DCT and ITS test results for the three mixes. A comparison of the test results among the three field mixes is provided. The results of the Superpave-5 field mixes were also compared with the Superpave-4 mixes tested in the previous chapter. The field density results of the cores collected from the Highway 61 project (Mix 3: Traffic level 4) are also included in this chapter.

7.5.1 DCT Test Results

7.5.1.1 Mix 1: Traffic Level 3(a)

Figure 7-3 shows the fracture energy of the three samples tested for the Mix 1: Traffic Level 3(a) mix. The average fracture energy of the three samples was 436 J/m^2 with a standard deviation of 30 J/m^2.

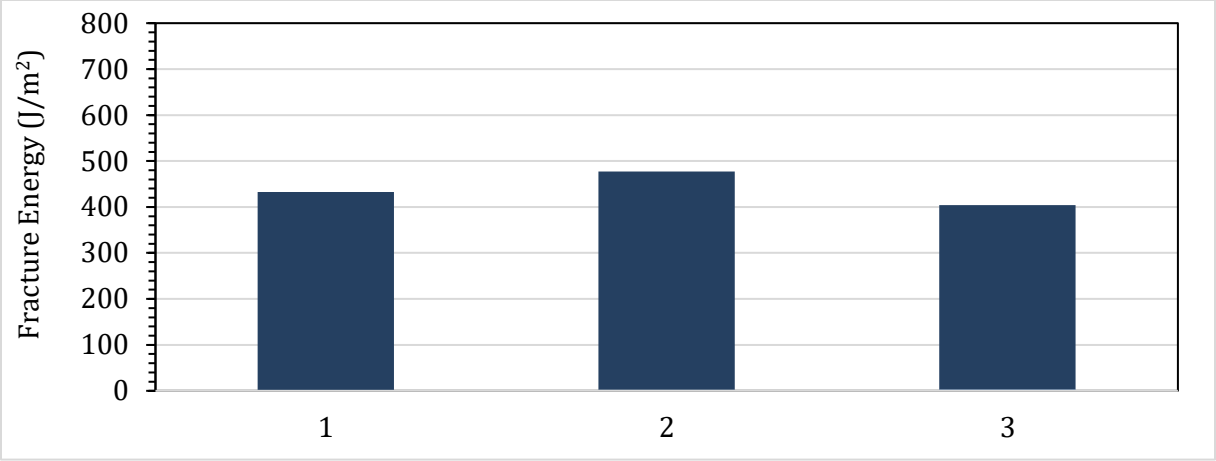

Figure 7-3 DCT test results for Mix 1: Traffic Level 3(a)

7.5.1.2 Mix 2: Traffic Level 3(b)

Figure 7-4 shows the fracture energies of the three samples tested for the Traffic Level 3(b) mix. The average fracture energy value of the three samples was 521 J/m^2 and the standard deviation was 27 J/m^2.

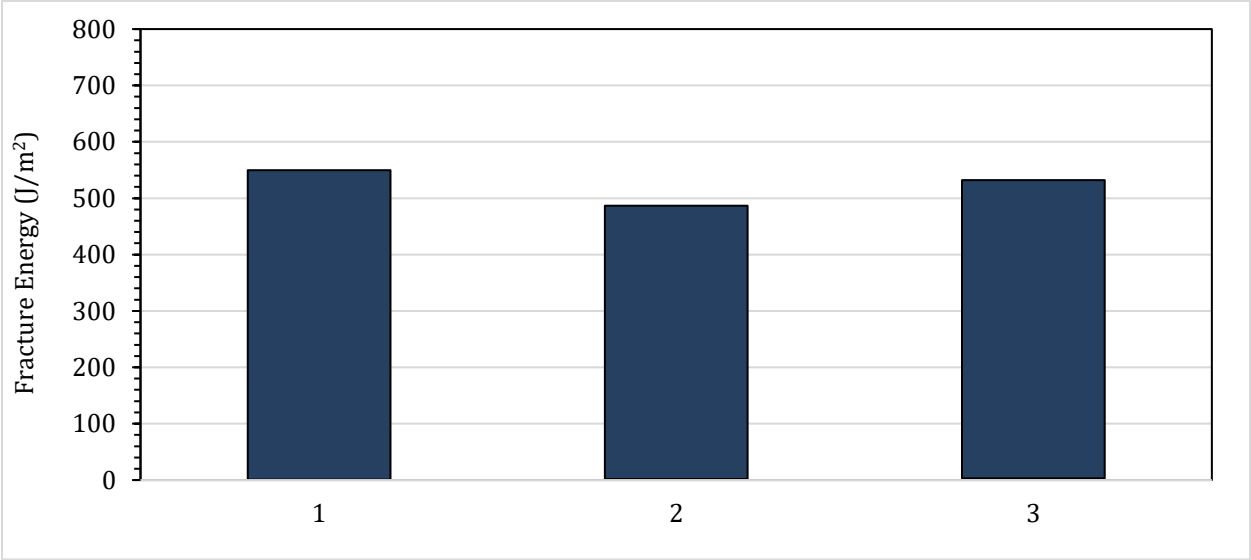

Figure 7-4 DCT test results for Mix 2: Traffic Level 3(b)

7.5.1.3 Mix 3: Traffic Level 4

Figure 7-5 shows the DCT test results of Mix 3: Traffic level 4. For this mix, a total of nine DCT samples were tested. The first seven samples were tested in the dry condition (no freeze-thaw cycle) and the last two samples were tested after conditioning with one freeze cycle (referred to as wet condition), as discussed in the previous chapter. More samples could not be tested for wet conditions because of the

scarcity of the field mixes. The average fracture energy values of dry and wet tested samples were 487 J/m^2 and 540 J/m^2, respectively, with standard deviations of 56 J/m^2 and 2 J/m^2, respectively. It should be noted that only two samples were tested for wet condition compared to seven samples for the wet condition, so the comparison between the wet condition and dry condition is not appropriate.

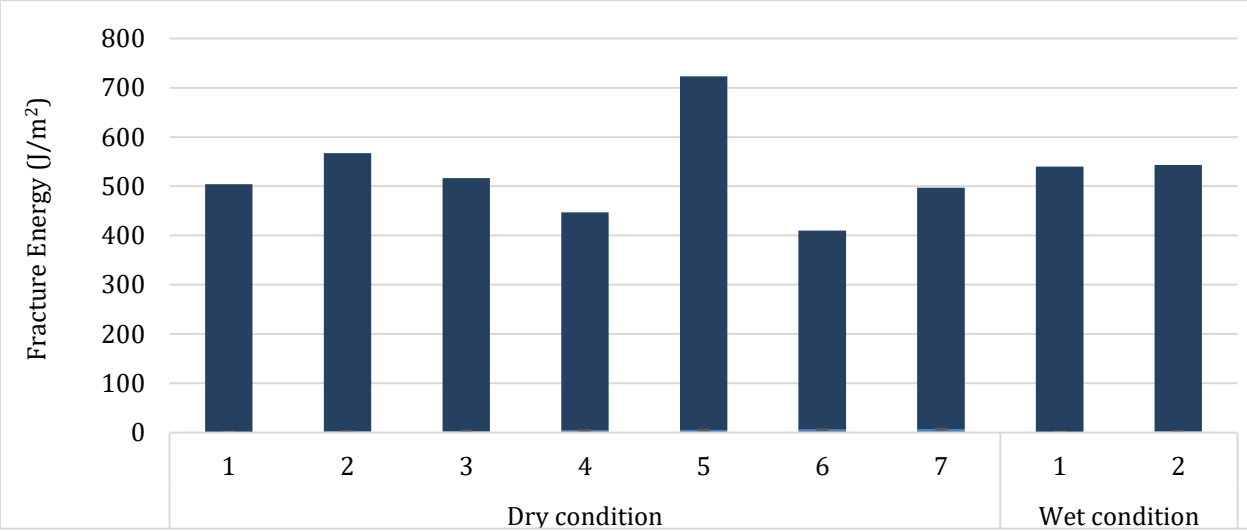

Figure 7-5 DCT test results for Mix 3: Traffic Level 4

It should be noted that fracture energy (718 J/m^2) of the DCT sample no. 5 (dry tested) was significantly higher than all other samples tested for this mix and thus considered as an outlier result. The result of this sample was omitted in the calculation of the average and standard deviation. The difference in the fracture energy between the dry and wet samples was not distinctive. Also, it should be noted that only two samples were tested for wet condition.

7.5.2 Comparison of the DCT Results

Figure 7-6 compares the fracture energies of the three mixes. Among the three mixes, mix 2: Traffic level 3(b) resulted in the highest value of fracture energy. Coincidently, the gradation of this mix was close to the theoretical maximum density line. Also, polymer-modified binder PG 58H-34 was used in this mix. Mix 1: Traffic level 3(a) resulted in the lowest fracture energy. This mix had 30% RAP and 58S-28 binder as compared to 20% and 17% RAP and polymer modified binder for the other two mixes. All three mixes nevertheless resulted in fracture energy greater than 400 J/m^2, the minimum threshold G_f value recommended in the state of Minnesota.

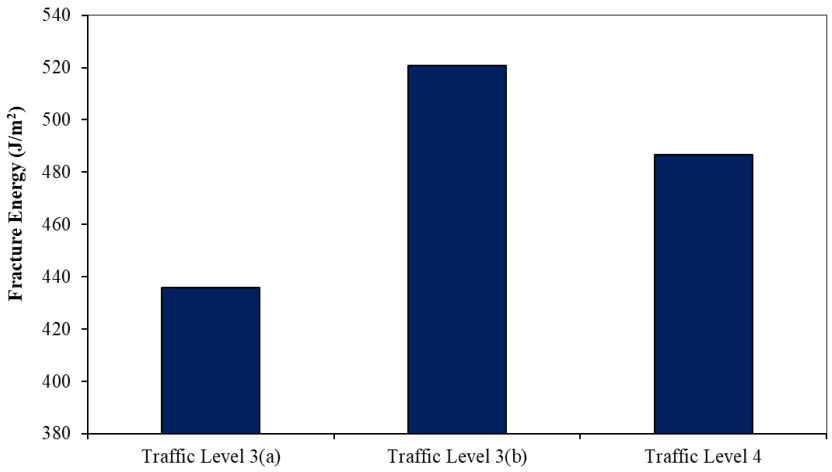

Figure 7-6 Comparison of the DCT test results between the three mixes considered in Task 5

Figure 7-7 provides a comparison of the three Superpave-5 field mixes with the laboratory-produced mixes tested in this project. The fracture energies of three Superpave -5 mixes [5N/30 (A), 5N/30 (B), 5N/30 (C)] were compared with three Superpave-4 mixes [4N/30 (A), 4N/30 (B), 4N/30 (C)] and one regressed air void mix (3N/50). It may be noted that the three Superpave-5 mixes as well as the three Superpave 4 mixes differ from each other in aggregate gradation. Among all the mixes, the lab produced Superpave mixes resulted in higher fracture energies. Despite the field-produced Superpave-5 mixes not performing as well as their lab-produced counterparts, two particular mixes - Mix 2: Traffic Level 3 (b) and Mix 3: Traffic Level 4 - showed a marginally better performance compared to the lab-produced Superpave 4 mixes. The field-produced mixes were stored in the laboratory for months after their preparation (which might have aged the mixes) and reheated for test sample preparation. Mix 1: Traffic Level 3(a), which showed lower fracture energy among all the mixes, had 30% RAP compared to 20% and 17% RAP for all other mixes. This mix was also prepared with PG 58S-28 binder, unlike the two other mixes which contained polymer-modified binder.

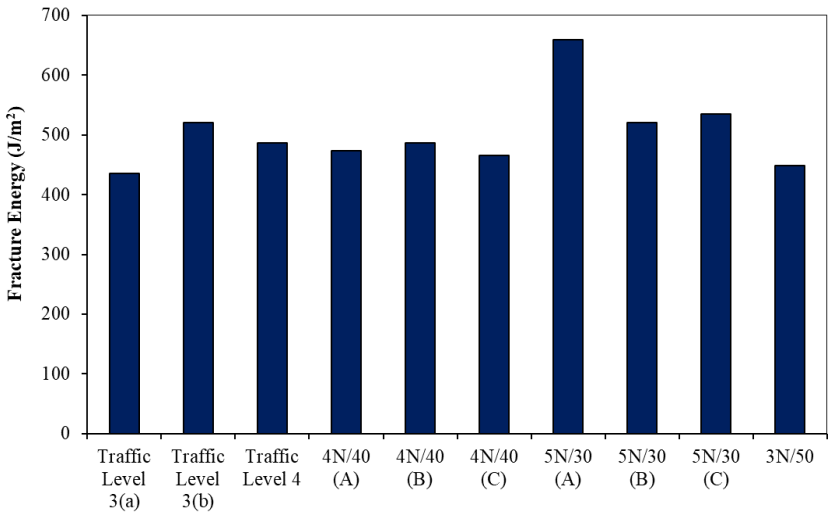

Figure 7-7 Comparison of fracture energies of Superpave 4 and Superpave-5 mixes (4N/40 mixes are Superpave-4 mixes; 3N/50 mix is regressed air void mix; others are Superpave-5 mixes)

7.5.3 ITS Test Result Comparison

Figure 7-8 presents a comparison of the indirect tensile strengths of different mixes tested in this project. As discussed before, out of the three mixes tested, loose asphalt mixtures were available for only one mix (Mix 3: Traffic Level 4) for the ITS test. A total of five samples were tested (only dry condition) for the indirect tensile strength of this mix. Previously, a total of five to seven samples were tested (in dry condition) for each of the lab-produced mixes. The indirect tensile strength of all the lab- and field-produced mixes were found to be greater than the three Superpave-4 mixes tested in the previous chapter.

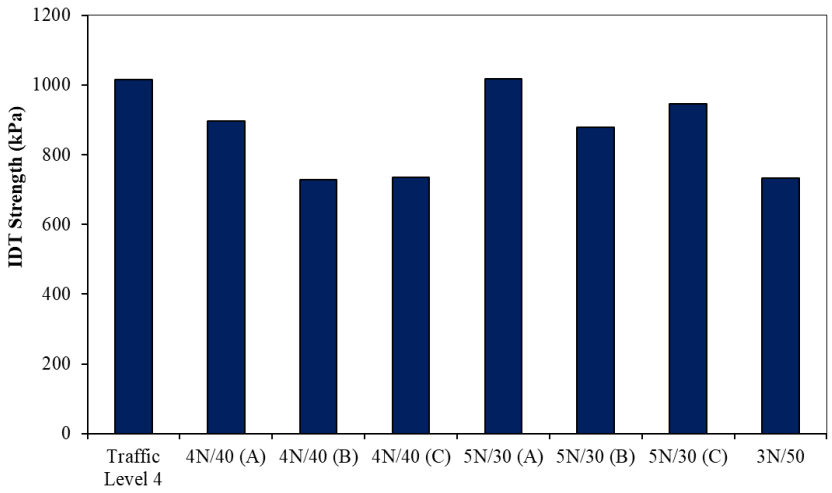

Figure 7-8 Comparison of indirect tensile strength of Superpave 4 and Superpave-5 mixes (4N/40 mixes are Superpave-4 mixes; others are Superpave-5 mixes)

7.6 Field Density Study

In this section, the field density of the Superpave-5 mixes is studied. Some asphalt core density data were collected from MnDOT District 1. The data belonged to the Highway-61 project that was constructed in the Summer of 2021. The asphalt mix tested for Mix 3: traffic level 4 in this task was collected from that project. Figure 7-9presents the core density in terms of the percentage of the maximum theoretical density (G_{mm}). The core densities of a total of 133 lots are included in Figure 7-9. In each lot, four cores were tested (two by the contractor QC and two by Agency QA). The average density of the 133 lots is 93.2% with a standard deviation of 1.18 %. It was observed that out of 133 lots that were placed, only 15 lots had their field density values in the range between 94.5% and 95.5%. While it is not prudent to make a general statement on the field density of the Superpave-5 mixes just based on the compaction data of one project site, it appears that the field density was below the target density (~95%) for most samples tested for the Highway-61 project, at least for the lots considered in Figure 6.9. The performance of this project compared to companion field sections with Superpave-4 mixes will be interesting to review to determine the benefit of the Superpave-5 mixes in the field.

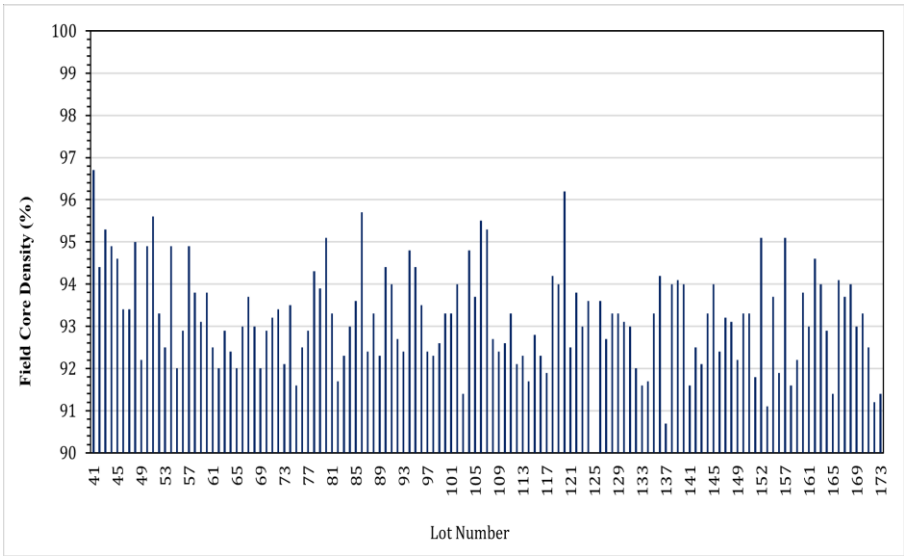

Figure 7-9 Field core density of Superpave-5 mix used in Highway-61 project

7.7 Summary

The mechanical performance of the Superpave-5 field mixes was studied and compared with the lab-produced Superpave-4 and Superpave-5 mixes. The results of the CT and ITS tests were compared. The following conclusions were derived from the test results:

1. The laboratory-produced Superpave-5 asphalt mixes yielded a slightly superior performance compared to the plant-produced Superpave-5 asphalt mixes, in terms of the DCT test results. However, it may be noted that the field-produced mixes were stored in the laboratory for months after their preparation, leading to aging. This fact and the better control of aggregate proportioning and homogeneity of the mixtures in the laboratory setup likely influenced the results. Out of three field Superpave-5 mixes, two performed better than the Superpave-4 mixes. One Superpave-5 mix that showed less fracture energy than the Superpave-4 mixes had 30% RAP in it compared to 18 to 20% RAP in the Superpave-4 mixes.
2. The ITS test results of both the lab- and field-produced Superpave-5 mixes were superior to the Superpave-4 mixes.
3. The abovementioned two observations validate that the mechanical performances of the Superpave-5 mixes are likely to be superior to their counterpart Superpave-4 mixes.
4. The density of the field cores (from 133 lots, 532 cores) collected from the Highway-61 project showed that the target field density (~95%) was not achieved in most of the project.

Chapter 8: Conclusions and Recommendations

8.1 Conclusions

Minnesota's low-volume roads primarily fail because of environmentally driven distresses rather than load-related distresses. This study investigated the common distresses of the state's low-volume roads and scopes for minimizing the distresses by changing the asphalt mixture design. The study included a comprehensive literature review and an online survey to understand the current practices of low-volume road asphalt mixture designs used in Minnesota and other states that experience wet-freeze climate. A field study was conducted to document the dominant distresses observed in the low-volume asphalt roads. Asphalt layer volumetrics and densification were studied by analyzing cores collected from 34 different roadway sections located in different parts of Minnesota. A laboratory study was conducted to determine the needed changes in the asphalt mixtures for use in low-volume roads. Mixes designed with conventional Superpave-4, Superpave-5, and regressed air voids methods were compared. The study extended to investigate the mechanical performance of the plant-produced mixes that were designed using the Superpave-5 method and verified the field compaction of the Superpave-5-based asphalt mix in a field project.

The major conclusions drawn from the study were:

<u>Literature Review and Online Survey</u>

1) The dominant distresses of the low-volume roads are not load related, rather they are developed because of environmentally driven factors. The transverse crack is the most common distress.
2) It was found that most of the compaction or densification of the asphalt layer occurs during the first three years of the service life and the field air void percentage rarely decreases to the design air voids (3% or 4%).
3) The asphalt mixtures possessing DCT test-measured fracture energy equal to 400 J/m^2 or SCB test-measured fracture energy equal to 350 J/m^2 provide good resistance against thermal cracking.
4) MnROAD's test section's performance and other key studies suggested using PG58H-34 binder is advantageous to minimize the transverse cracking, which is critical to the low-volume roads.
5) Literature review suggests that the regressed air void design and Superpave-5 mixture design concepts are promising.

<u>Field Study on the Asphalt Layer Densification and Common Distresses</u>

1) The volumetric analysis of the cores reveals that the initial air voids of the asphalt layer right after the construction range between 5.3% and 7.2% with an average value of 6.3%.

2) The air voids slightly decrease with age; traffic or the ESALs play a role in densifying the asphalt layer. But as the traffic or ESALs is less in the low-volume road, the air voids percentage was not found to decrease close to the design air voids (3 or 4%) or lower.
3) The distress survey showed that the three major distresses are longitudinal cracking, longitudinal joint cracking, and transverse cracking, which are related to environmental factors.

Mechanical Performance of the Lab Produced Asphalt Mixes and Field Cores

1) Seven different asphalt mix designs were evaluated. Three mix designs each for the conventional Superpave-4 method and Superpave-5 and one mix design for the regressed air voids method were considered in this study.
2) Among the three methods mentioned above, the Superpave-5 mixes performed better than the mixes prepared based on the two other methods in terms of the DCT fracture energy.
3) For aggregate gradation 'A', the inclusion of slightly more fines in the mix and higher design air voids (from 4 to 5%) but denser compacted mixes (from 7 to 5% at N_{max}) resulted in better fracture resistance at low temperatures.
4) For similar aggregate gradations, asphalt mix with 0.5% more binder performed better in low-temperature conditions in terms of the DCT fracture energy.
5) Superpave-5 mixes also had a higher indirect tensile strength than the conventional Superpave-4 mixes and the regressed air voids mix.
6) Aggregate gradation had an impact on the dynamic modulus values of mixes. At high temperature, the Superpave-5 mix with coarser aggregates showed a higher modulus value than the mix with more fines.
7) The dynamic modulus results for the Superpave-5 mixes are better or comparable to the conventional Superpave-4 mixes, which indicates that the rutting behavior of the Superpave-5 mixes will not be inferior to its counterpart.
8) As the low-temperature transverse cracking is the dominant distress of Minnesota's asphalt pavements, it may be concluded that the use of the Superpave-5 mixes over the conventional Superpave-4 mixes may provide a longer service life for the pavements. However, the compactibility of the Superpave-5 mixes designed for the low-volume roads (aggregate gradation A, traffic level 2) shall be verified in the field. Because of the lack of low-volume road field mixes or field sections, the same could not be performed in this project, which is a limitation of this study.

8.2 Recommendations

Based on the findings from this study, the following recommendations are made.

1) Superpave-5 asphalt mixes may be used in low-volume roads, but a field verification study is recommended.
2) It appears that using PG58H-34 binder may be beneficial to achieve higher fracture energy in the asphalt mixes.

3) An increase of the binder content by 0.5% may improve the fracture energy of mixes, which can help mitigate low-volume road distresses to some extent.
4) The Superpave-5 mix with coarse aggregate gradation close to the middle of MnDOT's Class A gradation that has 54% aggregates passing through sieve No. 8 (2.36 mm) showed the highest fracture energy. Therefore, when designing the Superpave-5 mix, the above suggestion may be followed when determining the design aggregate structure of the mix.

References

1. AASHTO R 35. (2017). *Standard practice for Superpave volumetric design for asphalt mixtures*. Washington, DC: American Association of State Highway and Transportation Officials (AASHTO).
2. Apeagyei A. K., Buttlar W. G., & B. J. Dempsey (2006). Moisture damage evaluation of asphalt mixtures Using AASHTO T283 and DC (T) fracture test. Paper presented at the 10th International Conference on Asphalt Pavements, Quebec City, Canada.
3. Apronti, D., Ksaibati, K., Gerow, K., & Hepner, J. (2016). *Estimating traffic volume on Wyoming low-volume roads using linear and logistic regression methods*. Retrieved from https://www.sciencedirect.com/science/article/pii/S209575641530670X
4. ASTM D7313-13. (2020). *Standard test method for determining fracture energy of asphalt-aggregate mixtures using the disk-shaped compact tension geometry*. West Conshohocken, PA: ASTM International.
5. ASTM D2726/D2726M-13. (2014). *Test method for bulk specific gravity and density of non-absorptive compacted bituminous mixtures.* Retrieved from doi:10.1520/d2726_d2726m-13
6. Braham, A. F., Buttlar, W. G., & Marasteanu, M. O. (2007). Effect of binder type, aggregate, and mixture composition on fracture energy of hot-mix asphalt in cold climates. *Transportation Research Record: Journal of the Transportation Research Board, 2001*(1), 102-109.
7. Chen, S., You, Z., Sharifi, N. P., Yao, H., & Gong, F. (2019). Material selections in asphalt pavement for wet-freeze climate zones: A review. *Construction and Building Materials, 201, 510-525.*
8. Curtis Turgeon. (2019). Bituminous materials. *Construction materials manual*. St. Paul, MN: MnDOT. http://www.dot.state.mn.us/materials/manuals/bituminous/Minnesota_Department_of_Transportation_Bituminous_Manual.pdf
9. Dave, E., Hoplin, C., Helmer, B., Dailey, J., Deusen, D. V., Geib, J., Dai, S., & Johanneck, L. (2016). Effects of mix design and fracture energy on transverse cracking performance of asphalt pavements in Minnesota. *Transportation Research Record: Journal of the Transportation Research Board, 2576* . 40–50. DOI: 10.3141/2576-05
10. Dave E., M. Oshone, A. Schokker, & C. E. Bennett (2019). *Disc shaped compact tension (DCT) specifications development for asphalt pavement* (Final report, MN/RC 2019-24). St. Paul, MN: Minnesota Department of Transportation.
11. D'Angelo, J. A. (2009). *Workshop summary transportation research circular: Polyphosphoric acid modification of asphalt binders: A workshop* (Vol. E-C160). Minneapolis, Minnesota: Transportation Research Board.
12. Engle, E. J. (2004). *Superpave mix designs for low-volume roads* (Final Report) Ames, IA: Iowa Highway Research Board, Project TR-414, Iowa Department of Transportation.
13. Federal Highway Administration. (2009). *Manual on uniform traffic control devices for streets and highway*s (HS-820168). Washington, DC: Federal Highway Administration.

14. Hafez, M., Ksaibati, K., & Atadero, R. (2017). Best practices to support and improve pavement management systems for low-volume paved roads. *International Journal of Pavement Engineering, 20*(5), 592-599.
15. Harmelink, D., & Aschenbrener, T. (2002). *In-place voids monitoring of hot mix asphalt pavements.* Denver: Colorado Department of Transportation.
16. Hekmatfar, A., McDaniel, R. S., Shah, A., & Haddock, J. E. (2015). *Optimizing laboratory mixture design as it relates to field compaction to improve asphalt mixture durability (Joint Transportation Research Program* (Publication No. FHWA/IN/JTRP-2015/25). West Lafayette, IN: Purdue University. http://dx.doi.org/10.5703/1288284316010
17. Huber, G., Haddock, J. E., Weilinski, J., Kriech, A., & Hekmatfar, A. (2016). Adjusting design air void levels in superpave mixtures to enhance durability. Paper presented at the E&E Congress, 6th Eurasphalt & Eurobitume Congress, Prague, Czech Republic. http://dx.doi.org/10.14311/EE.2016.348
18. Marasteanu, M., Le J., Hill K., Yan T., Man T., Turos M., Barman M., Arepalli U. M., & Munch J. (2019). *Experimental and computational investigations of high-density asphalt mixtures.* St. Paul, MN: Minnesota Department of Transportation.
19. Marasteanu, M., Buttlar, W., Bahia H., & Williams, C. (2012). *Investigation of low-temperature cracking in asphalt pavements, National Pooled Fund Study—Phase II* (Report No. MN/RC 2012-23). St. Paul, MN: Minnesota Department of Transportation.
20. MnDOT. (2020). *Standard specifications for construction.* St. Paul, MN: Minnesota Department of Transportation.
21. MnDOT. (2019a). *Centerline and Lane Mileage Reports.* St. Paul, MN: Minnesota Department of Transportation. Retrieved from http://www.dot.state.mn.us/roadway/data/reports/mlm/19_strgp.pdf
22. MnDOT. (2019b). *MnDOT bituminous manual.* St. Paul, MN: Minnesota Department of Transportation.
23. MnDOT. (2018). Standard specifications for construction, *MnDOT standard specifications for construction*. St. Paul, MN: MnDOT.
24. MnDOT. (2011). *Pavement distress identification manual*. St. Paul, MN: Minnesota Department of Transportation, St. Paul. MN. https://www.dot.state.mn.us/materials/manuals/pvmtmgmt/Distress_Manual.pdf
25. MnDOT. (n.d.). Traffic mapping application. St. Paul, MN: MnDOT. https://mndot.maps.arcgis.com/apps/webappviewer/index.html?id=7b3be07daed84e7fa170a91059ce63bb
26. Newcomb, D., & Zhou, F. (2018). *Balanced design of asphalt mixtures.* St. Paul, MN: Minnesota Department of Transportation.
27. Newcomb, D. E., Olson, R., Teig, J., & Gardiner, M. S. (1997, January). *Traffic densification of asphalt concrete pavements.* Retrieved from https://doi.org/10.3141%2F1575-01
28. Papagiannakis, A., & Masad, E. (2012). *Asphalt materials.* Retrieved from https://onlinelibrary.wiley.com/doi/pdf/10.1002/9780470259924.ch5

29. Skok, E. L., Newcomb, D. E., & Timm, D. E. (1999). *Minnesota low-volume road design 1998*. Retrieved from file:///C:/Users/Giselle%20Irankunda/AppData/Local/Packages/Microsoft.MicrosoftEdge_8wekyb3d8bbwe/TempState/Downloads/Mn_DOT1999-34%20(1).pdf http://www.dot.state.mn.us/pre-letting/spec/index.html
30. Skok, E. L., Timm, D. H., Brown, M. L., Clyne, T. R., & Johnson, E. (2003, November). *Best practices for the design and construction of low-volume roads* (2002-17REV final report best practices for the design and construction of low-volume Roads revised). St. Paul, MN: Minnesota Department of Transportation, St. Paul. MN.
31. Stroup-gardiner M., Newcomb D. E., Olson R., & Teig J. (1997). Traffic densification of asphalt concrete pavements. *Transportation Research Record: Journal of the Transportation Research Board, 1575* (1), 1-9.
32. Vitillo, N. P., Bennert, T., Smith, J., & Maher, A. (2006). Evaluation of superpave MIX design for low-volume roads in New Jersey. *Transportation Research Record: Journal of the Transportation Research Board, 1946*(1), 139-146.
33. Walker, D. (2020). Understanding asphalt pavement distresses – five distresses explained. *Asphalt, The Magazine of the Asphalt Institute*. Retrieved from http://asphaltmagazine.com/contact-us/
34. West, R., Rodezno, C., Leiva, F., & Taylor, A. (2018). *Regressing air voids for balanced HMA mix design*. Auburn, AL: National Center for Asphalt Technology at Auburn University. Https://Wisconsindot.gov/documents2/Research/0092-16-06-Final-Report.pdf
35. Williams, R., Hill, D., & Rottermond, M. (2006). Utilization of an asphalt pavement analyzer for hot mix asphalt laboratory mix design. *Performance tests for hot mix asphalt (HMA) Including fundamental and empirical procedures. Transportation Research Record: Transportation Research International Documentation 2006(1)*, 16-40.
36. Worel, B. J., Clyne, T. R., Burnham, T. R., Johnson, D. M., & Tompkins, D. M. (2007). Low-volume road lessons learned. *Transportation Research Record: Journal of the Transportation Research Board, 1989*(1), 198-207.
37. You, Z., Gilbertson, C., & Van Dam, T. (2018*). Identifying best practices in pavement* design, *materials, construction, and maintenance in wet-freeze climates like Michigan*. Lansing, MI: Michigan Department of Transportation.
38. Yuefeng, Z., Dave, E. V., Rahbar-Rastegar, R., Daniel, J. S., & Zofka ,A. (2017). Comprehensive evaluation of low-temperature fracture indices for asphalt mixtures. *Road Materials and Pavement Design*. doi: 10.1080/14680629.2017.1389085

Appendix A
Photographs of pavement distresses

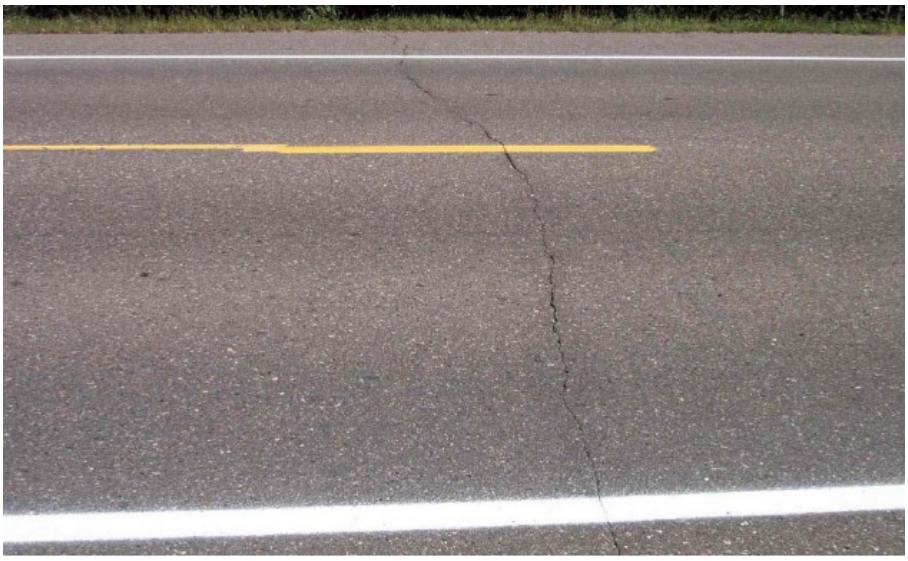

Figure A.1 Low Severity Transverse Crack (MnDOT, 2011)

Figure A.2 Medium Severity Transverse Crack (MnDOT, 2011)

Figure A.3 High Severity Transverse Crack (MnDOT, 2011)

Figure A.4 Low Severity Longitudinal Crack (MnDOT, 2011)

Figure A.5 Medium Severity Longitudinal Crack (MnDOT, 2011)

Figure A.6 High Severity Longitudinal Crack (MnDOT, 2011)

Figure A.7 High Severity Longitudinal Crack (MnDOT, 2011)

Figure A.8 High Severity Longitudinal Crack at Lane Joint (Photo Courtesy: Manik Barman)

Figure A.9 Low Severity Multiple Cracking (MnDOT, 2011)

Figure A.10 Photograph of a Pothole (Dailey et al., 2017)

Figure A.11 Medium Severity Multiple Cracking (MnDOT, 2011)

Figure A.12 High Severity Multiple Cracking (MnDOT, 2011)

Figure A.13 Alligator/fatigue Cracking, Medium Severity (MnDOT, 2011)

Figure A.14 Alligator/fatigue Cracking, High Severity (Courtesy: Joel Ulring, MnDOT)

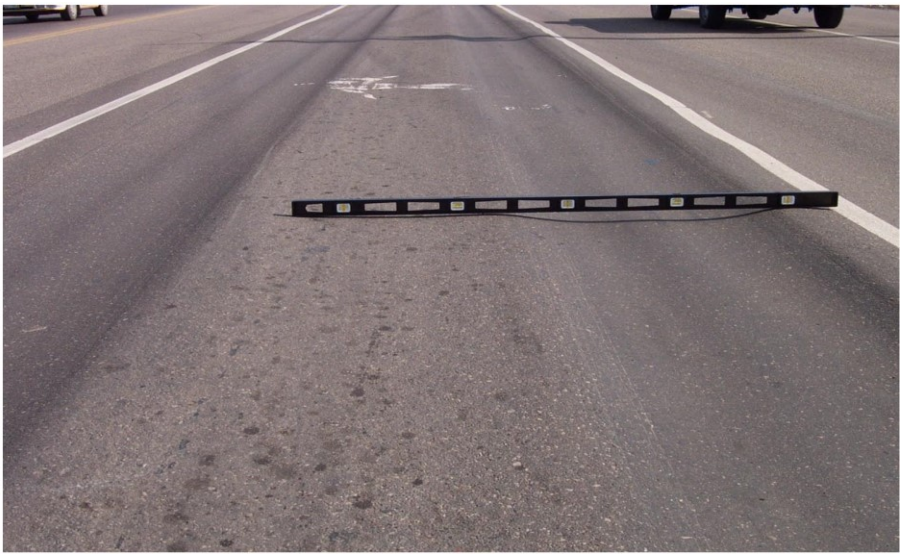

Figure A.15 Rutting, 0.50 inches Deep or Greater (MnDOT, 2011)

Figure A.16 Raveling in Asphalt Pavement (MnDOT, 2011)